
WSRC-TR-2000-00340

**Degradation and
Failure Characteristics
of NPP Containment
Protective Coating Systems (U)**

SRTC Coating System No. 2
(Phenoline 305 epoxy-phenolic topcoat,
Starglaze 2011S surfacer, concrete substrate)

Prepared by **M. E. Dupont, N. C. Iyer,
P. S. Lam, R. L. Sindelar,
T. E. Skidmore, F. R. Utsch
and P. E. Zapp**

Savannah River Technology Center
Westinghouse Savannah River Company
Aiken, SC 29808

For Division of Engineering Technology
Office of Nuclear Regulatory Research
U.S. Nuclear Regulatory Commission
Washington, DC 20555

NRC Job Code W6959

NRC Project Manager **A. W. Serkiz**

Publication Date October 2000

Westinghouse Savannah River Company
Savannah River Site
Aiken, SC 29808



DISCLAIMER

This report was prepared as an account of work sponsored by an agency of the United States Government. Neither the United States Government nor any agency thereof, nor any of their employees, makes any warranty, express or implied, or assumes any legal liability or responsibility for the accuracy, completeness, or usefulness of any information, apparatus, product, or process disclosed, or represents that its use would not infringe privately owned rights. Reference herein to any specific commercial product, process, or service by trade name, trademark, manufacturer, or otherwise does not necessarily constitute or imply its endorsement, recommendation, or favoring by the United States Government or any agency thereof. The views and opinions of authors expressed herein do not necessarily state or reflect those of the United States Government or any agency thereof.

DOCUMENT: WSRC-TR-2000-00340

TITLE: Degradation and Failure Characteristics of
NPP Containment Protective Coating Systems (U)

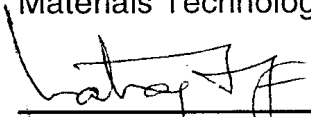
APPROVALS





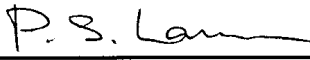
Date: 10/30/00

Mark E. Dupont, Author
Materials Applications & Process Technology Group
Materials Technology Section



Date: 10-30-00

Natraj C. Iyer, Author and Manager
Materials Technology Section



Date: 10-30-2000

Poh-Sang Lam, Author
Materials Applications & Process Technology Group
Engineering Development Section



Date: 10-30-2000

Robert L. Sindelar, Author and Manager
Materials Applications & Process Technology Group
Materials Technology Section



Date: 10-31-2000

T. Eric Skidmore, Author
Materials Consultation Group
Materials Technology Section



Date: 10-30-00

Philip E. Zapp, Author
Materials Performance & Corrosion Technology Group
Materials Technology Section

This page left blank intentionally.

Abstract

A research program to investigate the performance and potential for failure of Service Level I coating systems¹ used in nuclear power plant containment is in progress. The research activities are aligned to address phenomena important to cause failure as identified by the industry coatings expert panel. The period of interest for performance covers the time from application of the coating through 40 years of service, followed by a medium-to-large break loss-of-coolant accident scenario, which is a design basis accident (DBA) scenario.

The SRTC program consists of three major elements: Materials Properties Development, Failure Modeling Development, and DBA Performance Testing. These elements are directed at determining Service Level I coatings performance under simulated DBA conditions. The coating materials properties data (not previously available) are used in predictive coatings failure models which are then compared against coating behavior under simulated DBA conditions to obtain insights into failed coating materials characteristics and degree of failure (i.e. amount of coatings debris). The resulting data and insights are used in NRC's GSI-191, "PWR Sump Blockage"

research program. The effects of aging on coating materials properties and performance are addressed by applying an aging treatment (irradiation to 10^9 R, per ASTM D4082-95) to test specimens.

The interactive program elements are discussed in this report and the application of these elements to the SRTC System 2 coating system (Phenoline[®] 305 epoxy-phenolic topcoat, Starglaze[®] 2011S surfacer, concrete substrate) is used to evaluate performance. The SRTC System 2 coating system represents one of the predominant coating systems applied to concrete substrates in NPP containment. In order to evaluate the performance of coatings already in place, SRTC obtained original formulations of Phenoline[®] 305 for use in testing. Starglaze[®] 2011S is representative of concrete surfacer formulations which are in current use.

¹ The Service Level designation of coatings in nuclear power plants is described in ASTM Standard D5144-00

Table of Contents

	Page
Abstract	v
Table of Contents.....	vi
List of Figures.....	vii
List of Tables	ix
List of Abbreviations.....	x
Executive Summary	xi
Acknowledgments.....	xii
1.0 Background.....	1-1
2.0 SRTC Program Elements and Structure	2-1
2.1 Material Properties	2-4
2.2 Failure Modeling.....	2-6
2.3 Measured Performance Under DBA Conditions	2-7
2.4 Coating Performance	2-8
3.0 Coating System 2 Performance.....	3-1
3.1 Material Properties	3-1
3.2 Failure Modeling.....	3-14
3.3 Measured Performance Under DBA and Soak Test Conditions.....	3-25
3.4 Coating Performance	3-29
4.0 Summary and Significant Findings	4-1
4.1 Coating Research Program	4-1
4.2 Performance of System 2 Coating.....	4-1
4.3 Summary of Major Findings for System 2 Performance	4-3
5.0 Future Activities.....	5-1
5.1 General Conclusions.....	5-1
5.2 Factors Affecting Potential for Debris Formation in NPP Containment Coating.....	5-1
5.3 Additional Consideration of Factors Affecting NPP Containment Coating Performance.....	5-2
Appendix A Mechanical Testing Description.....	A-1
Appendix B Irradiation Aging of Protective Coatings	B-1
Appendix C Application of Finite Element and Fracture Mechanics Analyses in Predicting Failure of NPP Coatings.....	C-1
Appendix D Test Apparatus Descriptions	D-1
Appendix E Performance Test Descriptions.....	E-1
Appendix F Characterization Facilities Description.....	F-1
Appendix G Phenomena Identification and Ranking Table Process	G-1

List of Figures

	Page
2-1	Task Logic Diagram for SRTC Project 2-1
2-2	Type 1 Defect in Coating System 2-6
2-3	Type 2 Defect in Coating System 2-6
2-4	Laboratory Plate Specimens Coated with Phenoline [®] 305 before (left) and after (right) before and after Exposure to 10 ⁹ Rad per ASTM D4082-95..... 2-7
2-5	“Full DBA” Profile for PWR per ASTM D3911-95 2-8
2-6	Blister Formation in Near-Surface Region of Phenoline [®] 305 Following Irradiation to 10 ⁹ Rad and a Water Soak 2-9
3-1	Free-film tensile test results for Phenoline [®] 305 in the dry condition 3-8
3-2	Free-film tensile test results for Phenoline [®] 305 in the wet condition 3-8
3-3	Free-film tensile test results for Starglaze [®] 2011S in the dry condition 3-9
3-4	Free-film tensile test results for Starglaze [®] 2011S in the wet condition 3-9
3-5	Tensile test data for Phenoline [®] 305 at 200°F obtained in the dry condition 3-10
3-6	Adhesion pull test results for System 2..... 3-11
3-7	Adhesion G-value test results for non-irradiated System 2..... 3-12
3-8	Adhesion G-value test results for irradiated System 2..... 3-12
3-9	Non-irradiated System 2 specimen block and pullers from the G-value tests 3-13
3-10	Photograph of puller from a 100°F non-irradiated, wet condition G-value test 3-13
3-11	Mode 1 Analysis model 3-14
3-12	Mode 2 Analysis model 3-15
3-13	Oblique view of cross-section of non-aged System 2 specimen illustrating minor cracking which occurred during DBA-LOCA testing 3-15
3-14	Applied G-Values at the Edge of a dry Defect (Diameter 12 mm) during DBA Test..... 3-16
3-15	Applied G-Values at the Edge of a Vapor Pressurized Defect (Diameter 12 mm) during DBA Test..... 3-17
3-16	Applied G-Values at the Edge of a Vapor Pressurized Defect (Diameter 12 mm) during Cooling Phase in DBA Test 3-18
3-17	Failure of Mode 1 Defects based on Peak Tensile Stress Criterion 3-18
3-18	Failure of Mode 1 Defects based on Peak Tensile Stress Criterion 3-19
3-19	Failure of Mode 1 Defects based on Failure Strain Criterion 3-19
3-20	Failure of Mode 1 Defects based on Failure Strain Criterion 3-20
3-21	Applied G-Values at the Edge of a Vapor Pressurized Defect (Diameter 1/8 in.) during DBA Test..... 3-21
3-22	Applied G-Values at the Edge of a Vapor Pressurized Defect (Diameter 1/8 in.) during Cool-down Phase in DBA Test 3-21
3-23	Failure of a Vapor Pressurized Mode 1 Defects (Diameter 1/8 in.) based on Peak Tensile Stress Criterion 3-22
3-24	Failure of a Vapor Pressurized Mode 1 Defects (Diameter 1/8 in.) based on Peak Tensile Stress Criterion. 3-22
3-25	Failure of a Vapor Pressurized Mode 1 Defects (Diameter 1/8 in.) based on Failure Strain Criterion 3-23

List of Figures

3-26	Failure of a Vapor Pressurized Mode 1 Defects (Diameter 1/8 in.) based on Failure Strain Criterion	3-23
3-27	System 2 specimen, non-aged, following DBA testing	3-24
3-28	Cross-section of circumferential crack in System 2 specimen (Fig. 3-26) illustrating the location of coating failure at the edge of the glass disk used to create the Type 1 defect	3-25
3-29	Typical Pressurized Water Reactor Design Basis Accident (DBA) Testing Parameters (from ASTM D3911-95).....	3-26
3-30	Typical Temperature-pressure Profile from SRTC System 2 D3911 DBA-LOCA Test	3-27
3-31	Temperature-Pressure Curves from Plant-specific LOCA Test	3-28
3-32	System 2 specimens before (left) and after (right) irradiation to 10^9 rad	3-29
3-33	Cross-section of System 2 coating, irradiated to 10^9 rad, original magnification 30X	3-29
3-34	Micrograph of blistering formed on Phenoline [®] 305 free-film specimen following irradiation and heating to 200°F, dry.....	3-30
3-35	Sloughing of surface of irradiated specimen following water soak at 200°F	3-30
3-36	SEM micrographs illustrating the appearance of the outermost layer (left) and the bulk Phenoline [®] 305 coating (right) of irradiated System 2	3-31
3-37	Overall views of nonaged System 2 specimens before (left) and after DBA testing	3-32
3-38	Overall views of irradiation-aged System 2 specimens before (left) and after DBA testing	3-32
3-39	Detail of the surface of the non-aged specimen after DBA testing	3-33
3-40	Detail of the surface of the irradiation aged specimen after DBA testing	3-33
3-41	Cross-section of the surface of the irradiation aged specimen after DBA testing	3-34
3-42	System 2 non-aged (left) and irradiation aged (right) specimens following DBA pulse-test	3-34
3-43	Detail of irradiation-aged specimen in Figure 3-42, taken above the water immersion level, illustrating extensive blister formation	3-34
3-44	Detail of irradiation-aged specimen in Figure 3-42 taken below the water immersion level	3-35
3-45	Cross-section of irradiation-aged specimen in Figure 3-42, taken from above the water immersion line.....	3-35
3-46	Overall view of non-irradiated System 2 specimen, submerged overnight in 200° F water.....	3-35
3-47	Overall view of irradiated System 2 specimen, submerged overnight in 200° F water	3-35
3-48	Irradiated and non-irradiated System 2 specimens, soaking in 200° F water	3-36
3-49	Coating debris remaining in the vessel following removal of the System 2 specimens	3-36
3-50	Overall view of some of the debris removed from the vessel used to soak the specimens	3-37
3-51	Detail of debris, 7X	3-37
3-52	Single debris blister, 20X	3-37
3-53	Detail of the surface of the irradiation-aged immersion test specimen illustrating the extent of blister formation and detachment	3-38
3-54	Cross-section of the surface of the irradiation-aged soak test specimen	3-38
3-55	Effect of Temperature on Blister Development for Non-irradiated and Irradiated Phenoline [®] 305 and Starglaze [®] 2011S in Water Immersion	3-39
3-56	Frequency Histogram of Debris Size Distribution	3-40

List of Tables

		Page
2-1	Cross-Reference Table for Coating Systems Presently Investigated by the SRTC Project and Those Evaluated by the Industry Coatings PIRT	2-2
2-2	Project Alignment with Industry PIRT System f (SRTC System 2: Concrete Substrate, Surfacer, Epoxy Phenolic Topcoat).....	2-3
2-3	Material Property Parameters Used in Analyzing Coating Performance	2-5
3-1	Material Properties for Coating Failure Analysis Using Modes 1 and 2 Failure Models.....	3-3
3-2	Free-Film Tensile Test Results for Phenoline [®] 305	3-4
3-3	Free-Film Tensile Test Results for Starglaze [®] 2011S	3-4
3-4	Densities	3-4
3-5	Thermal Conductivity.....	3-5
3-6	Coefficients of Thermal Expansion	3-6
3-7	Specific Heats	3-7
3-8	Adhesion Pull Test Results for System 2	3-10
3-9	Adhesion G-Value Test Results for System 2	3-11

List of Abbreviations

AE	Acoustic Emission	NACE	National Association of Corrosion Engineers
ASTM	American Society for Testing and Materials	NMRS	Nuclear Magnetic Resonance Spectroscopy
BWR	Boiling Water Reactor	NPP	Nuclear Power Plant
CSS	Containment Spray System	NRC	(U.S.) Nuclear Regulatory Commission
DBA	Design Basis Accident	PIRT	Phenomena Identification and Ranking Table
DFT	Dry Film Thickness	PTFE	Polytetrafluorethylene
DSC	Differential Scanning Calorimetry	PWR	Pressurized Water Reactor
ECCS	Emergency Core Cooling System	SEM	Scanning Electron Microscopy
EDS	Energy Dispersive Spectroscopy	SIMS	Secondary Ion Mass Spectroscopy
EIS	Electrochemical Impedance Spectroscopy	SRTC	Savannah River Technology Center
EPRI	Electric Power Research Institute	SSC	Structure, System, and Component
ETC	Environmental Test Chamber	SSPC	Steel Structures Painting Council
FT-IR	Fourier Transform-Infrared Spectroscopy	TEM	Transmission Electron Microscopy
IOZ	Inorganic Zinc	TGA	Thermogravimetric Analysis
LOCA	Loss of Coolant Accident	XRD	X-ray Diffraction

Executive Summary

The U. S. Nuclear Regulatory Commission (NRC) has identified the potential for degradation and failure of “qualified” protective coatings applied to exposed surfaces within nuclear power plant primary containment during the design life of such plants, and has communicated such concerns to license holders in NRC Generic Letter 98-04 dated July 14, 1990. As a consequence of this letter, the NRC commissioned the Savannah River Technology Center (SRTC) to investigate the potential for degradation and failure of such coating systems when subjected to DBA conditions, and to characterize failed coating debris. The formation and transport of some types of coating debris to a PWR ECCS sump debris screen was judged to have an undesirable safety impact during the post-LOCA period.

An investigative approach was previously established in the SRTC coatings research program (ref. WSRC-TR-2000-00079) and applied to a reference coating system. The approach is a combination of:

- a) Measurement of critical coating materials’ properties at conditions representative of a post-LOCA period,
- b) The development of a predictive coating system failure model,
- c) Subjecting such coating systems to DBA conditions,
- d) Comparing model and test results to judge predictive capability,
- e) Documenting the degree of failure, and
- f) The characterization of failed coating debris, which will be integrated into the PWR sump blockage research program (GSI-191).

This approach was applied to investigate a Service Level I protective coating system and the results are contained in this report. The coating system is a predominant system (epoxy-phenolic topcoat over an epoxy surfacer) that was applied to concrete within PWR containments in the early to mid-1970s. The specific formulation is Phenoline[®] 305 and Starglaze[®] 2011S over concrete prepared in accordance with ASTM D5139-90. The effects of an accumulated gamma dose of a 40-year service plus DBA on the coating performance were simulated by irradiating the coating to 10⁹ rads at 1x10⁶ rads/hour in accordance with ASTM D4082-95. Laboratory specimens were exposed to DBA conditions specified in the ASTM D3911-95 steam temperature profile for PWR containment, and other relevant DBA conditions, including a “pulse” steam temperature profile and a high temperature (up to 200°F) water immersion.

The research results reported in this interim report for the subject coating system arrive at the following conclusions:

1. Properly applied coatings that would contain only minor defects and that have not been subjected to irradiation of 10⁹ rads, can be expected to remain fully adhered and intact on a concrete substrate, following exposure to simulated DBA conditions.
2. Non-bond embedded defects, if greater than approximately 1/8” in diameter, are subject to cracking during DBA exposure; the disbonding of the cracked coating to subsequently create a debris source term was not observed.
3. Properly applied coatings that have been subjected to irradiation of 10⁹ rads (a gamma radiation exposure as defined in ASTM Standard D4082-95) exhibited profound blistering, leading to disbondment of a near-surface coating layer (1-2 mils of the 10 mils thickness) when exposed to elevated temperatures and moisture conditions within the range of DBA conditions. This failure of the coating produced a coating debris source term.

The research approach described in this interim project report will be extended to investigate a second predominant Service Level I protective coating system consisting of an epoxy-phenolic topcoat over an inorganic zinc primer with a steel substrate. During the course of that investigation, the following topics will be investigated, in an effort to better understand the observations which have been made to-date:

- The combined effects of aging conditions on coating performance (dose, dose rate, oxidation, and temperature).
- The combined effects of simulated LOCA exposure on coating performance (temperature/pressure profile, water immersion, etc.)
- The debris formation mechanism (gas generation, blister pressurization, time-to-fail, etc.)
- The debris characteristics (size distribution, “stickiness,” etc.)

Acknowledgments

The following individuals have made contributions to the success of the SRTC Coatings Evaluation Program:

Nuclear Regulatory Commission:

Aleck Serkiz

Savannah River Technology Center:

Chris Beam

Glen Chapman

Mark Dupont

Dr. Natraj Iyer

Dr. Poh-Sang Lam

Doug Leader

Dr. McIntyre Louthan

Tommy McCoy

Bridget Miller

Dr. Michael Morgan

Tracy Murphy

Harold Peacock

Curt Sexton

David Silver

Dr. Robert Sindelar

Eric Skidmore

Tina Stefek

Craig Stripling

Karthik Subramanian

Frank Utsch

Dr. Philip Zapp

Principal investigators in **bold**.

Bechtel Savannah River Company

Bobby Hill

PIRT Panel Members:

Jon Cavallo, Chm.

Tim Andreycheck

Jan Bostelman

Dr. Brent Boyack

Garth Dolderer

David Long

Yuly Korobov

Corrosion Control, Consultants
and Labs, Inc.

Westinghouse Electric Corp.,
Pittsburgh, PA

ITS Corporation

Los Alamos National
Laboratory

Florida Power and Light

Keeler and Long (now retired).

Carboline Company

1.0 Background

Nuclear power plants (NPPs) must ensure that the emergency core cooling system (ECCS) or safety-related containment spray system (CSS) remains capable of performing its design safety function throughout the life of the plant. This requires ensuring that long-term core cooling can be maintained following a postulated loss-of-coolant accident (LOCA). Adequate safety operation can be impaired if the protective coatings which have been applied to the concrete and steel structures within the primary containment fail, producing transportable debris which could then accumulate on BWR ECCS suction strainers or PWR ECCS sump debris screens located within the containment.

Service Level I coatings were used on the interior containment steel shells, concrete walls and floors, and other structures, thereby providing environmental protection to these substrates and facilitating decontamination, as necessary. The coatings, which were applied during plant construction, were expected to last throughout the 40-year license period or design life of the plant, except for minor local damage due to mechanical impact or cleaning chemicals. These coatings were selected based on demonstrated adequate survivability under simulated DBA-LOCA conditions as described in ASTM Standard D3911-95, or earlier ANSI standards. The assumption was that qualified coatings that were properly selected and applied at time-of-construction would not fail during normal plant operation or during a LOCA. Coating condition monitoring and maintenance were considered unnecessary.

There is clear evidence for failure of qualified coatings during plant design life. Such failures are described in attachments to NRC GL 98-04, "Potential for Degradation of Emergency Core Cooling System and Containment Spray System after a Loss-of-Coolant Accident Because of Construction and Protective Coating Deficiencies and Foreign Material in Containment," July 14, 1998. This evidence resulted in NRC's Office of Nuclear Reactor Regulation requesting that research (NRR 6/2/97) be directed at debris generation testing of protective coatings that are likely to fail during an accident. The research would determine the timing of the coating failure during an accident (e.g., minutes, hours, days) and the characteristics of the failed coating debris (e.g., chips, large strips, particulate materials). This research need was the basis for NRC's Office of Nuclear Regulatory Research, Division of Engineering Technology, initiating a program through the Savannah River Technology Center to research the performance of aged containment coatings under simulated LOCA conditions.

SRTC's program is designed to investigate NPP containment coatings through a better understanding of coating materials' properties (e.g., property changes introduced by elevated temperature and irradiation effects), development of a predictive coating failure model, and DBA performance testing of coating samples representative of coatings applied in NPPs. The ultimate goal is to establish a coating debris database that characterizes and quantifies the failed material. The SRTC program elements and interactive approach are described in Sections 2 and 3, and the results for a specific concrete coating system (concrete substrate, surfacer, and epoxy-phenolic topcoat) are described in Section 3.

This Interim Report highlights research findings that have been reported in monthly letter status reports to the NRC since project initiation in July 1998. Research results on various other coating systems have been reported also in public meetings, held on November 5, 1998, April 15, 1999, and November 22, 1999, at NRC Headquarters. A topical report on SRTC's coating System 5, epoxy polyamide topcoat over epoxy polyamide primer on steel, was issued in March 2000 ["Degradation and Failure Characteristics of NPP Containment Protective Coating Systems (U) Interim Report", WSRC-TR-2000-00079, March 2000]. That report established the experimental and analytical approach used in this Interim Report. Licensees, industry NPP coatings groups, and individual NPP coatings specialists have shown considerable interest and offered assistance to the program. Similar public interaction will be continued throughout the research project, which is scheduled for completion in December 2000. The data obtained are to be integrated into NRC's Generic Safety Issue (GSI) 191, PWR Sump Blockage project. In addition, the research findings from this study will be used in evaluating a potential need for review and revision of ASTM Standards D3911-95, "Standard Test Method for Evaluating Coatings Used in Light-Water Nuclear Power Plants at Simulated Design Basis Accident (DBA) Conditions, and D4082-95, "Standard Method for Effects of Gamma Radiation on Coatings for Use in Light-Water Nuclear Power Plants", which are currently used by licensees in the qualification of Service Level I coatings.

This page left blank intentionally.

2.0 SRTC Program Elements and Structure

The Savannah River Technology Center coatings research program is designed to investigate the potential degradation and failure of Service Level I protective coatings under postulated LOCA conditions. The key program elements and interactive paths are shown in Figure 2-1. The program goal is to obtain insights into the performance of “qualified” coating systems. Coating behavior could range from no failure to disbonding accompanied by the

production of debris that could degrade the performance of PWR ECCS sumps. The assumption has been that properly selected and applied “qualified” coatings will not fail during the normal plant design life (i.e., 40 years) nor following a LOCA. Minor blistering and cracking are not considered to be failures, whereas coating disbondment is considered a failure and the accompanying “free” material constitutes a debris source term.

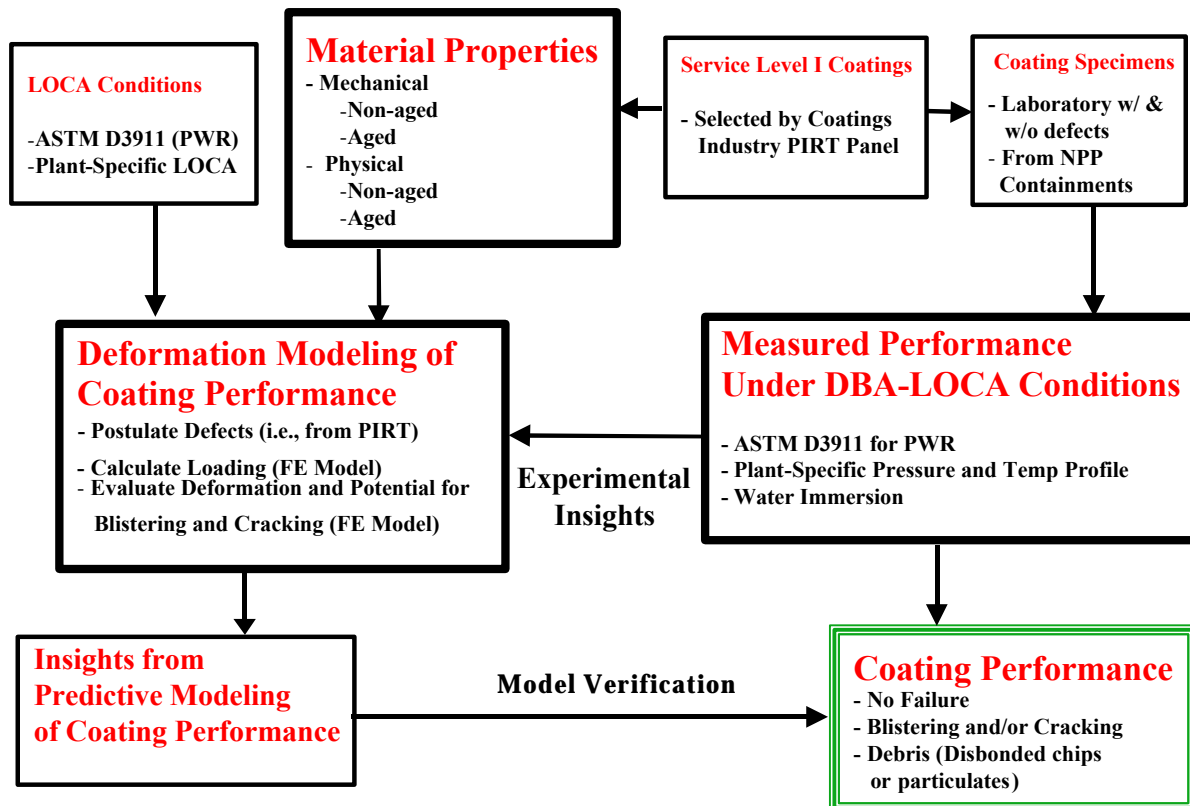


Figure 2-1. Task Logic Diagram for SRTC Project

The four principal program elements are:

1. Measuring key coating materials' properties,
2. Developing a predictive coatings failure model,
3. Subjecting selected coatings to design basis accident conditions, or simulated LOCA conditions, and measuring performance, and

4. Providing insights into the performance of Service Level I coatings and, if failures occur, identifying debris source characteristics which include size, shape, and amount (per unit exposed area).

Protective coating materials applied in NPPs were identified from the EPRI “Coatings Handbook for Nuclear Power Plants,” EPRI TR-106160, June 1996 [2.1], from plant specific responses, from surveys performed by several industry groups, and from the industry PIRT panel. Although EPRI TR-106160 lists data collected from 29 nuclear industry respondents and represents over 200

unique coating products in over 1000 different plant-specific applications, the data set does not lend itself to identification of a limited set of generic coating systems on which to focus the research effort. This identification of generic coating systems that represent widespread use in NPPs was facilitated by formation of an industry Phenomena Identification and Ranking Table panel. A

detailed description of a generic PIRT process is described in reference 2.2. The specific PIRT process, panel members and the PIRT relevant to this Interim Report [2.3] are discussed in Appendix G. Table 2.1 identifies the available coating products reviewed in this project, and also cross-references such materials with the PIRT panel’s generic descriptions.

Table 2-1. Cross-Reference Table for Coating Systems Presently Investigated by the SRTC Project and Those Evaluated by the Industry Coatings PIRT Panel

Substrate	Generic Description	Coating Products Tested at SRTC	SRTC System No.	PIRT System Letter
Steel	Epoxy-phenolic over inorganic zinc	Phenoline® 305 over Carbozinc® 11	1	a (1)
Concrete	Epoxy-phenolic over surfacer	Phenoline® 305 over Starglaze® 2011S surfacer	2	e (5)
Steel	Phenolic-modified epoxy over inorganic zinc	Amercoat® 90HS over Dimetcote® 9	3	
Steel	Phenolic-modified epoxy over epoxy-polyamide	Amercoat® 90HS over Amercoat® 370	4	
Steel	Epoxy-polyamide over epoxy-polyamide	Amercoat® 370 over Amercoat® 370	5	d (4)
Steel	Inorganic zinc	Dimetcote® 9	6	(9)
Steel	Epoxy-phenolic over epoxy-phenolic			b (2)
Steel	Epoxy over inorganic zinc			c (3)
Concrete	Epoxy over surfacer			f (6)
Concrete	Epoxy-phenolic over epoxy-phenolic			g (7)
Concrete	Epoxy over epoxy			h (8)

These generic coating systems encompass NPP Service Level I protective coatings that date back to the early 1970s. Coating systems applied to PWR containment internal steel surfaces and to concrete walls and floors are to be investigated in this project. PIRT System “a” was identified to be of primary interest due to an instance of significant “area of detachment” of the topcoat from the IOZ primer in a NPP and also based on insights from the PIRT completed for that system. The PIRT system “f” was identified as the primary concrete coating system since this is the most widely used system. A previous Interim Report addressed the PIRT panel coating system d (SRTC designation System 5). System 5 was used to benchmark the adequacy and success of the technical

approach of the project. The present Interim Report discusses the investigation of the concrete coating system “e”. System “e” was selected in lieu of system “f” to expedite the project schedule. System “e” shares the same topcoat as system “a”, which is the other principal system that is to be investigated. Use of system “e” was endorsed by the industry PIRT panel, as was the use of the system “f” PIRT to guide the investigation of the system “e” coatings. System “e” will hereafter be referred to as System 2, in accordance with the project’s nomenclature.

The ASTM standards accepted by the nuclear industry for preparation of coating test samples (ASTM D5139-90)[2.4], irradiation of test samples (ASTM D4082-95)[2.5], and simulation of DBA testing (ASTM D3911-95)[2.6] are an integral part of this research program. These standards form the basis for test sample procurement and testing. Thus, the procurement of coating materials and preparation of “qualified” test samples becomes a path-limiting activity. An example is the procurement of coating formulation materials needed for System “a”, which became very difficult and protracted because a particular type of asbestos was a principal constituent of the CZ11 primer used in NPPs in the 1970s. Delays were encountered also in the acquisition of coated concrete samples.

The integration of PIRT panel evaluations (which are derived from identification of phenomena and processes that could lead to coating failure, and the ranking thereof) is illustrated in Table 2.2. The linking of project activities and PIRT phenomena/process elements is represented by the central column identifying physical properties and phenomena of importance. Project resources were directed at PIRT phenomena/processes ranked high and to a lesser degree to the PIRT phenomena/processes of medium rank.

Section 3 of this report details results to date for material property testing, predictive failure modeling, DBA test findings and coating performance following a DBA test for SRTC System 2. Significant insights are provided in Section 4, and Section 5 discusses near-term and planned concluding activities for this project.

Table 2-2. Project Alignment with Industry PIRT System f (Concrete Substrate, Surfacer, Epoxy Topcoat)
(analog for SRTC System 2: Concrete Substrate, Surfacer, Epoxy Phenolic Topcoat)

High-Ranked Industry PIRT Phenomena/Processes	Time Phase	Related Inputs and Physical Properties	Related Project Activities
Coating Anomalies in Surfacer or in Topcoat	1,2,3	Surface Cleanliness	Adhesion and DBA Testing with Defect 1 Coupons
Environmental Exposure to Topcoat	1	Total Radiation Dose, Temperature/Humidity History, Decontamination Chemicals, Corrosion, Erosion, Abrasion	Radiation Aging and Thermal Aging of Laboratory Specimens, Characterization and Testing of Plant Specimens
Pressure Gradients from ILRTs at Substrate	2,3	Adhesive Strength	Adhesion Testing
Expansion/Contraction at Substrate/Surfacer Interface	2,3,5	Coefficient of Thermal Expansion	DBA Testing and Modeling of Stresses
Expansion/Contraction at Surfacer/Topcoat Interface	2,3,5	Coefficient of Thermal Expansion	DBA Testing and Modeling of Stresses
Outgassing/Vapor Expansion from Substrate	1,2,3	Permeation	DBA Testing
Blistering/Delamination at Substrate/Surfacer Interface or at Surfacer/Topcoat Interface	1,2,3,4	Adhesive and Tensile Strength, Ductility	Adhesion Testing, Tensile Testing, DBA Testing, Modeling of Stresses
Vapor Build-up at Substrate/Surfacer Interface or at Surfacer/Topcoat Interface	1,2,3	Adhesive and Tensile Strength, Ductility, Permeation	Adhesion Testing, Tensile Testing, DBA Testing, Modeling of Stresses
Environmental Exposure to Topcoat	1	Total Radiation Dose, Temperature/Humidity History, Decontamination Chemicals, Corrosion, Erosion, Abrasion	Radiation Aging and Thermal Aging of Laboratory Specimens, Characterization and Testing of Plant Specimens

Table 2-2. Project Alignment with Industry PIRT System f (Concrete Substrate, Surfacer, Epoxy Topcoat) (Cont'd)
 (analog for SRTC System 2: Concrete Substrate, Surfacer, Epoxy Phenolic Topcoat)

Medium-Ranked Industry PIRT Phenomena/Processes	Time Phase	Related Inputs and Physical Properties	Related Project Activities
Calcium Carbonate Build-up at Substrate/Surfacer Interface	1,5	Surface Cleanliness	Adhesion and DBA Testing with Defect 1 Coupons
Environmental Exposure to Surfacer or Topcoat	1,5	Total Radiation Dose, Temperature/Humidity History, Decontamination Chemicals, Corrosion, Erosion, Abrasion	Radiation Aging and Thermal Aging of Laboratory Specimens, Characterization and Testing of Plant Specimens
Pressure Gradients from ILRTs at Substrate	1	Adhesive Strength	Adhesion Testing
Expansion/Contraction at Substrate/Surfacer Interface	2,3,5	Coefficient of Thermal Expansion	DBA Testing and Modeling of Stresses
Expansion/Contraction at Surfacer/Topcoat Interface	2,3,5	Coefficient of Thermal Expansion	DBA Testing and Modeling of Stresses
Outgassing/Vapor Expansion from Substrate	4,5	Permeation	DBA Testing
Blistering/Delamination at Substrate/Surfacer Interface or at Surfacer/Topcoat Interface	5	Adhesive and Tensile Strength, Ductility	Adhesion Testing, Tensile Testing, DBA Testing, Modeling of Stresses
Vapor Build-up at Substrate/Surfacer Interface or at Surfacer/Topcoat Interface	4	Adhesive and Tensile Strength, Ductility, Permeation	Adhesion Testing, Tensile Testing, DBA Testing, Modeling of Stresses
Coating Anomalies in Surfacer and Topcoat	4,5	Surface Cleanliness	Adhesion and DBA Testing with Defect 1 Coupons
Water Intrusion or Immersion of Surfacer of Topcoat at Pool	5	Water Permeation and Water Chemistry	DBA Testing

Phase 1: Normal service to 40 years.

Phase 2: 0 to 40 seconds into loss-of-coolant accident.

Phase 3: 40 seconds to 30 minutes after LOCA.

Phase 4: 30 minutes to 2 hours after LOCA.

Phase 5: Beyond 2 hours after LOCA.

2.1 Material Properties

The coating system materials' properties being assembled in the coatings research program are a fundamental set of properties that are used to analyze coating performance and potential for coating failure. The properties may be dependent on temperature and wetness, and may be changed by aging mechanisms (e.g., oxidation, irradiation-induced scissioning, and thermal-induced

cross-linking or scissioning) active during the service period and/or the design basis accident (DBA) scenario.

Materials' properties are required input to analytical models of coating deformation and failure (see Figure 2-1). The input parameters used for coating System 2 are contained in Table 2-3. The table also includes several property parameters, not used directly as inputs to modeling, that provide a quantitative measure of the

effects of aging and DBA exposure conditions on the potential for coating failure. One such parameter being measured in the research program is the adhesion strength. It is a simple measurement with sensitivity to detect differences in specimens tested at various conditions of temperature, wetness, and irradiation exposure. A reduction in the adhesion strength indicates an increase in potential for failure. The properties have

been categorized as either “properties for loading” or “properties for mechanical response.” The properties for loading are those used to calculate the stress distribution in the coating system; the properties for mechanical response are those used to calculate deformation of the coating system. The steps in analytical modeling are outlined in section 2.2.

Table 2-3. Material Property Parameters Used in Analyzing Coating Performance*

Material Property Parameter	Topcoat	Surfacer	Substrate
Properties for Mechanical Response			
Ultimate Tensile Strength (σ_u)	Applicable	Applicable	Not Applicable
Ductility (Total Strain at Failure, ϵ_f)	Applicable	Applicable	Not Applicable
Young’s Modulus (E)	Applicable	Applicable	Applicable
Poisson’s Ratio (ν)	Applicable	Applicable	Applicable
Adhesion Strength to Under Layer	Applicable	Applicable	Not Applicable
Adhesion Energy to Under Layer (G_{material})	Applicable	Applicable	Not Applicable
Cohesion Energy	Applicable	Applicable	Not Applicable
Properties for Loading			
Coefficient of Thermal Expansion (α_T)	Applicable	Applicable	Applicable
Glass Transition Temperature	Applicable	Applicable	Not Applicable
Thermal Conductivity	Applicable	Applicable	Applicable
Specific Heat	Applicable	Applicable	Applicable
Density (ρ)	Applicable	Applicable	Applicable

*Parameters listed as “not applicable” are those that either have no meaning for the coating component or are not significant to coating performance.

Most of these parameters are not available either in the open literature or from the coatings vendors. The properties that are available are either not at specific environmental conditions of interest (e.g., temperature and wetness of a DBA) or may not be accurate for the specific formulation of a coating of interest (e.g., Phenoline® 305).

Therefore, the coating-specific properties are being measured at DBA-relevant conditions in the coatings research program. The temperature range (100-300°F) and wetness (dry and wet) at which the properties are being measured span the conditions of the ASTM DBA profile for a PWR [2.6]. Section 3.1 describes the properties that

have been measured for Phenoline® 305 and Starglaze® 2011S. These properties are collected in embedded look-up tables as described in section 3.1.

The testing methods to measure the properties for loading are ASTM standard methods. The testing methods for the mechanical response have been developed in the research program. The mechanical test methods are described in detail in Appendix A of this report.

An irradiation exposure to 1×10^9 Rad at 120°F in a cobalt-60 gamma source, in accordance with ASTM standard D4082-95 [2.5], has been applied to the mechanical test specimens as an aging treatment. Properties for the parameters in Table 2-3 are collected for coatings in both the “non-aged” condition, to represent a properly formulated, properly cured coating in its initial condition, and the “aged” condition, represented by a coating subjected to treatment according to ASTM D4082-95. Appendix B describes the aging treatment in detail. Section 3.1 contains the properties for the non-aged and aged Phenoline® 305 and Starglaze® 2011S coatings.

2.2 Failure Modeling

Analytical modeling is used to predict coating performance under the environmental conditions of the DBA. These conditions include elevated temperatures and pressures from steam, including expected transient and steady-state conditions. Environmental conditions can create stresses in the coating that, if high enough, can cause cracking in the coating, or delamination of the coating, or both. Either cracking or delamination events are precursors in the production of a debris source (e.g., free chip). It is the production of debris that constitutes failure of the coating.

The analytical modeling is capable of predicting cracking and delamination events. The approach is to build finite element analysis models of the topcoat/primer/substrate system and input the conditions of interest to analyze the system response. There are three fundamental categories of inputs to the models:

1. Configuration – includes an initial defect postulate, location of the defect in the coating system, number of coatings and coating thickness, and the type of substrate onto which the coating is applied.
2. Materials Properties – includes mechanical and physical properties of the coating layers and substrate materials.
3. Loading – includes both direct loads (e.g. impingement of water) and environmental conditions that lead to coating stresses.

There are several parts in the analysis of coating performance. The first part is the determination of the stress distribution in a non-defected coating system at a time period of interest in the DBA cycle and a check of the following criterion for cracking:

$$\sigma_{\text{material failure}} \leq \sigma_{\text{applied}} \text{ or } \epsilon_{\text{material failure}} \leq \epsilon_{\text{applied}}$$

The second part is the consideration of a so-called Type 1 defect, defined as a local delaminated region beneath the surface of the coating, as shown in Figure 2-2. This type of defect may be subject to “Mode 1 deformation” that is the formation of a blister dome, followed by delamination, and cracking. As described in Appendix A, the resistance to separation of a coating along an interface may be quantified through the property G_{material} . G_{material} is the adhesion energy to separate a coating layer from an under layer or substrate at a defect of specified size. G_{applied} is the calculated adhesion energy developed by external forces acting on a coating layer at the defect. The stress-strain and G_{applied} distributions are determined at a time period of interest in the DBA profile. Separation of a coating layer will proceed if the criteria expressed by these inequalities are satisfied:

$$G_{\text{material}} \leq G_{\text{applied}} \text{ and}$$

$$\sigma_{\text{material failure}} \leq \sigma_{\text{applied}} \text{ or } \epsilon_{\text{material failure}} \leq \epsilon_{\text{applied}}$$



Figure 2-2. Type 1 Defect in Coating System

The third part is the consideration of a Type 2 defect, defined as a local hole through the coating, as shown in Figure 2-3. This type of defect may be subject to “Mode 2 deformation” that is a separation or peel-back of the coating, followed by cracking. As in the evaluation of Mode 1 deformation, the stress-strain and G_{applied} distributions are determined for the external loads at the Mode 2 defect, and the two criteria for delamination and cracking are checked. The material properties are the same for both modes.

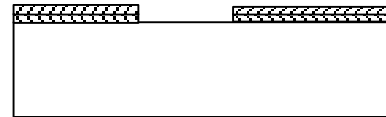


Figure 2-3. Type 2 Defect in Coating System

The details of analytical modeling are outlined in Appendix C of this report. Section 3.2 provides the results of the analyses of coating System 2 for various specific Type 1 and Type 2 defect postulates and DBA profiles using the measured properties for Phenoline® 305 and Starglaze® 2011S as listed in section 3.1.

2.3 Measured Performance Under DBA Conditions

Direct measurement of coating systems performance is achieved by exposing laboratory specimens, with and

without initial design defects and in as-applied and irradiation-aged conditions, to DBA profiles. The specimens are characterized with standard metallurgical practices to quantify blistering, cracking, and debris. The performance tests completed on the SRTC System 2 coating system were:

Test Performed	Test Description	Test Conditions
ASTM D3911 DBA-LOCA Test	7 day test per ASTM D3911-95	Included immersion of a portion of the specimens
Plant-Specific Pressure/Temperature Test	Pulse test incorporating rapid heating and rapid cooling of specimen	Included immersion of a portion of the specimens
Coating System Immersion Test	Immersion test of complete coating system (concrete substrate, surfacer, topcoat)	Testing performed from room temperature to 200°F and with 200°F initial condition
Free-film Immersion Test	Immersion of free-film specimens of surfacer and topcoat, in aged and non-aged conditions	Testing performed from room temperature to 200°F

Concrete blocks are coated and used as laboratory specimens for both the mechanical tests (adhesion strength tests (i.e., pull tests) and adhesion energy tests (i.e., G-value tests)) and for DBA testing. Figure 2.4 shows sections of block specimens with the System 2 coating before and after the irradiation aging treatment.

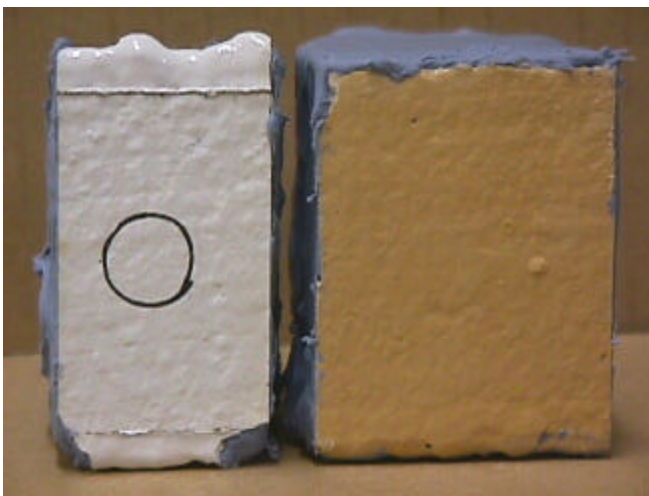


Figure 2-4. Laboratory Specimens Topcoated with Phenoline[®] 305 before (left) and after (right) exposure to 10⁹ Rad per ASTM D4082-95

The block specimens also are fabricated to contain a Type 1 (delamination under the coating) or a Type 2 (hole through coating) defect. Type 1 defects were created by weakly affixing 0.472-in.-(12 mm) diameter, 0.005-in.-thick glass discs to the concrete; Type 2 defects were created by drilling through the coating to the glass discs with a Dremel[®] tool.

There are two DBA profiles investigated in this study: the pressurized water DBA profile specified in ASTM standard D3911-95 [2.6], termed the “full DBA profile” in this report, and a plant-specific rapid pressure/temperature pulse test. Figure 2-5 below shows the ASTM profile, which is run for a total exposure period of approximately one week.

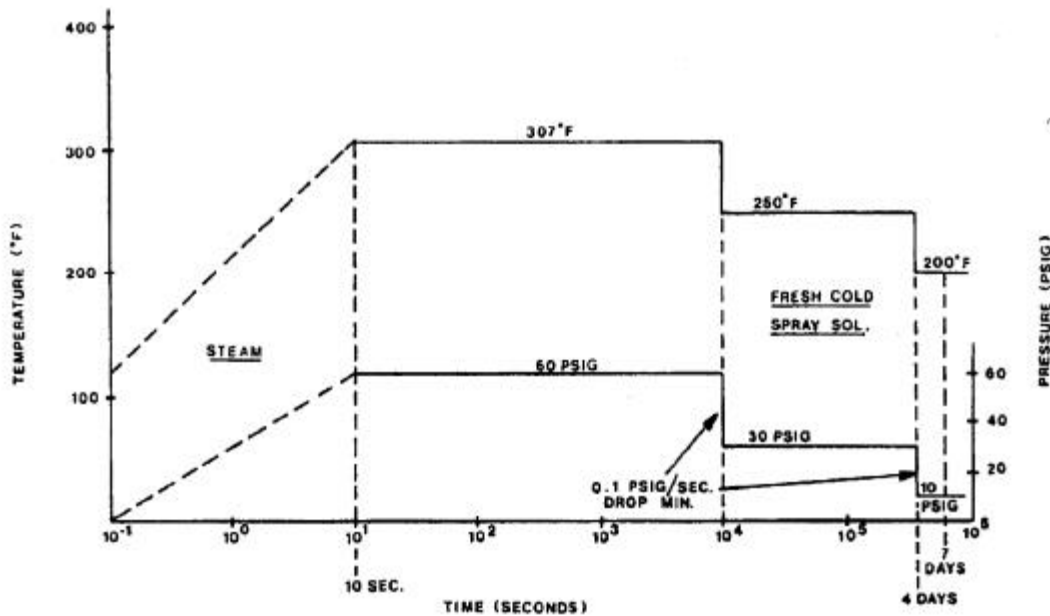


Figure 2-5. DBA Profile for PWR per ASTM D3911-95

The SRTC Monitored Environmental Test Chamber has been designed to duplicate, as closely as possible, the conditions specified in the ASTM profile. A description of this unique facility, which is fully equipped for video monitoring and recording and data logging, is provided in Appendix D of this report. A “plant-specific” DBA was used in the program to investigate the performance of a coating under a severe heat-up and cool-down pulse. Calculations of plant-specific temperature/pressure profiles typically contain this transient, which is not incorporated in the D3911-95 DBA profile.

The industry PIRT panel identified in their PIRTs the potential for coating degradation during immersion, following a LOCA event. The significance of this observation was reinforced during the course of testing, when SRTC observed a propensity for blistering of irradiated coatings when subjected to a water soak at elevated temperature. Therefore, SRTC modified the standard ASTM DBA test sequence to include water immersion for a portion of the test specimens. To study this blistering phenomenon in greater detail, SRTC developed an apparatus for videotaping the performance of coating test specimens while immersed in water at a range of temperatures. Descriptions of the DBA and soak testing of coatings are contained in Appendices D and E of this report.

2.4 Coating Performance

Measurement of coating performance following combinations of irradiation aging and DBA exposure is performed by a variety of standard metallurgical and analytical techniques. Chemical information is obtained using SEM/EDS (energy dispersive spectroscopy). Optical and scanning electron microscopy are used to provide details on the structure and debris source term geometric characteristics. Appendix F contains a description of the techniques applied to the coating specimens in the coatings research program at SRTC. Section 3.4 of this report provides the results of characterization of System 2 following irradiation, DBA exposure, and irradiation plus DBA exposure. Figure 2-6 below shows an example of blistering that has occurred in the irradiation-aged System 2 coating following a water soak exposure at 200° F and atmospheric pressure. This blistering emphasizes the role moisture or wetness can play in the development of coating failure.

The coatings research program also includes characterization and DBA testing of NPP plant specimens. The intent is to investigate and compare the performance of plant specimens with aged laboratory specimens.



Figure 2-6. Blister Formation in Near-Surface Region of Phenoline[®] 305 Following Irradiation to 10^9 Rad and a Water Soak

References for Section 2

- | | |
|---|--|
| <p>2.1 “Coatings Handbook for Nuclear Power Plants,” EPRI TR-106160, June 1996.</p> <p>2.2 G. E. Wilson and B. E. Boyack, <i>Nuclear Engineering and Design</i> 186, 23-37, 1998.</p> <p>2.3 Industry Coatings PIRT Report No. IC99-02, June 16, 2000, “PWR Containment Coatings Research Program Phenomena Identification and Ranking Tables (PIRTs),” by Jon R. Cavallo, Tim Andreychek, Jan Bostelman, Brent Boyack, Garth Dolderer, and David Long.</p> | <p>2.4 STM D5139-90, “Standard Specification for Sample Preparation for Qualification Testing of Coatings to be Used in Nuclear Power Plants.”</p> <p>2.5 ASTM D4082-95, “Standard Test Method for Effects of Gamma Radiation on Coatings for Use in Light-Water Nuclear Power Plants.”</p> <p>2.6 ASTM D3911-95, “Standard Test Method for Evaluating Coatings Used in Light-Water Nuclear Power Plants at Simulated Design Basis Accident (DBA) Conditions.”</p> |
|---|--|

This page left blank intentionally.

3.0 Coating System 2 Performance

3.1 Material Properties

This section reports the values of the physical and mechanical properties used for analyzing the performance of coating System 2, epoxy-phenolic topcoat and epoxy surfacer on concrete. The properties of specific coating products, epoxy-phenolic Phenoline[®] 305 and epoxy surfacer Starglaze[®] 2011S used in coating System 2 tests, are reported.

As discussed in section 2.1, the properties are functions of temperature, aging condition, and wetness or moisture content. The limits of these variables were enumerated in a statistical design developed for the coatings program. The temperature range was 100, 200, and 300°F; the aging condition was non-aged (no irradiation) and aged (irradiation to 10⁹ rad at 120°F); and either wet (by soaking in water for 16 hours) or dry (no soak). The effect of moisture on mechanical properties was evaluated at 100 and 200°F. Physical properties, including thermal conductivity, coefficient of thermal expansion, specific heat, and glass transition temperature, were measured by program subcontractors using standard laboratory techniques. Mechanical properties were measured at SRTC, with techniques developed specifically for this program. Appendix A describes the mechanical property testing techniques.

The measured data for coating System 2, along with literature data for the concrete substrate, are organized in Table 3-1 with data from the non-aged condition and the aged condition. The connections of the data in Table 3-1 to the failure model are emphasized through the grouping of (1) those properties that govern the mechanical response of the coating and (2) those properties that govern the loading on the coating induced by the DBA environment. Entries in these tables either are data values themselves or are references to subsequent tables (“embedded tables”) which then list the values of the specific property under all the measurement conditions. The tabulated data for adhesion, adhesion G_{material} , and free-film tensile strength are supplemented with load/extension or stress/strain curves at selected conditions. The mechanical properties are discussed in the order of their appearance in Table 3-1 in the following sections.

3.1.1 Tensile Properties: Tensile Strength, Ductility (strain at failure), and Modulus

Tensile properties were measured on free-film specimens, prepared with methods described in Appendix A. The Phenoline[®] 305 specimens were from 0.009 to 0.016 inch in thickness with a gage length of 1.4 inches and a gage width of 0.25 inch. The Starglaze[®] 2011S specimens varied in thickness from 0.033 to 0.080 inch; gage length was 1 to 2.5 inches, and width 0.52 to 0.58 inch. The tensile specimens were pulled to failure in an Instron universal testing machine. The extension rate was 0.02 to 0.05 inch/minute. Figure 3-1 shows the engineering stress-engineering strain curves for Phenoline[®] 305 in the dry condition calculated from the load-displacement data, and Figure 3-2 the curves for Phenoline[®] 305 in the wet condition. Figures 3-3 and 3-4 show the curves obtained for Starglaze[®] 2011S in the dry and wet conditions respectively. The stress-strain curves were subsequently adjusted for toe compensation according to ASTM D882-97 “Standard Test Method for Tensile Properties of Thin Plastic Sheeting.” The parameters calculated from the adjusted curves are the elastic modulus and percent strain at failure; ultimate stress was measured from the raw data. Tables 3-2 and 3-3 report these parameters for Phenoline[®] 305 and Starglaze[®] 2011S, respectively.

The Phenoline[®] 305 data show that temperature and radiation are significant factors affecting tensile properties. Increasing temperature and irradiation to 10⁹ rad markedly reduces the ultimate strength and the modulus. Irradiation to a total dose of 10⁹ rad reduces strength especially at the higher test temperatures of 200 and 300°F. At 300°F in the dry condition, the ultimate strength falls from 460 psi in the non-irradiated specimens to 30 psi in the irradiated one. Strain at failure does not change monotonically with irradiation. It decreases with irradiation at 100°F, increases at 200°F, and is little changed at 300°F, compared with measurements on non-irradiated specimens. Phenoline[®] 305 was tested at a lower total gamma radiation dose of 10⁷ in the 200°F dry condition (Figure 3-5). The 10⁷-rad specimens showed a slight strengthening and similar ductility compared with the unirradiated specimen. The wetness condition (dry versus overnight immersion in tap water at the test temperature) affects the coating differently depending on temperature. It has a high impact on the 100°F data, but a low impact on the 200°F data. This may result from the unavoidable drying of the wet 200°F test specimen during equilibration in the oven just before testing.

Starglaze® 2011S is generally a weaker material in tensile testing than is Phenoline® 305, and it is far less ductile, with failure strains of a few percent compared to tens of percent for Phenoline® 305. Ultimate strength decreases with radiation and increasing test temperature, while strain at failure increases somewhat. Wetness condition tended to lower ultimate strength and modulus and had a small impact on strain at failure. In replicate tests, variations of 50% have been seen in measured properties. For example, the three Starglaze® 2011S tests at 200°F in the dry, non-irradiated condition had ultimate strengths of 170, 210, and 340 psi.

3.1.2 Adhesion (Adhesion Strength to Under Layer)

The adhesion test, also referred to as the adhesion pull test to distinguish it better from the adhesion G-value test below, measures the adhesion strength of the coating to its under layer(s). The adhesion strength is calculated by dividing the peak load from the load-extension curve by the area of the puller. Separation of the puller (that is, the failure location) can occur within the topcoat, the surfacer, and even the concrete substrate, as well as at interfaces between adjacent layers. The measured adhesion strength is therefore a sort of lower bound on the strength of the various interfaces and layers.

The adhesion strengths measured for System 2 are listed in Table 3-8. Only non-irradiated specimens were tested, due to limited gamma cell volume and availability. The load-extension curves are plotted in Figure 3-6. The data show the significant effect of increasing test temperature in reducing the adhesion strength.

3.1.3 Adhesion G-Value (Adhesion Energy to Under Layer)

The adhesion G_{material} test measures the adhesion energy between layers of a coating, or in other words the resistance to separation of layers. This novel method of coating performance measurement is adapted from fracture

mechanics concepts, as discussed above. A comparison of the coating material's intrinsic G_{material} with a calculated G_{applied} that represents the environmental loading on the coating permits one to predict whether a coating defect will grow. As described in Appendix A, the G_{material} test is an adhesion test with the puller affixed to the coating directly over a zero-adhesion defect. The defect was created on System 2 specimens with a 12-mm-diameter, 0.13-mm thick glass disk affixed to the concrete surface. A successful test requires the defect to be the site of the failure or separation of the puller from the specimen.

Table 3-9 lists the test conditions, peak loads, G_{material} in J/m^2 , and failure location for coating System 2. G-values were determined only for those tests in which the failure location met the criterion above. The notation 'nd' for 'not determined' indicates that the test failed the criterion, and so a G-value could not be calculated. The load-extension curves are shown in Figure 3-7 for the non-irradiated specimens and in Figure 3-8 for the irradiated specimens. Figure 3-9 is a photograph of a System 2 specimen that had been immersed in water and tested at 100°F and 200°F. The location of failure was at the glass defect-concrete interface in these tests. In one of the 200°F tests, the failure occurred partly at the glass-concrete interface and partly within concrete beneath the glass defect, due to the strength of the concrete-surfacer bond. Figure 3-10 depicts a close-up of the puller used in one of the 100°F wet tests.

3.1.4 Cohesion Energy

Cohesion energy is a test of tearing resistance in free-film specimens subjected to a tensile test. The test specimen is similar to the 'dog-bone' used to determine tensile strength, but contains a defect in the form of an edge notch in the middle of the gage length. Cohesion tests were run only on Phenoline® 305 at the sole condition of dry, non-irradiated, 200°F.

Table 3-1. Material Properties for Coating Failure Analysis Using Mode 1 and 2 Failure Models^{a,b}

Material Property	Non-Aged Condition			Aged Condition Representing 40 Years of Service including 10 ⁹ rad Exposure		
	Epoxy Phenolic	Surfacer	Concrete	Epoxy Phenolic	Surfacer	Concrete
Properties for Mechanical Response						
Tensile Strength (psi)	See Table 3-2	See Table 3-3	275 [2]	See Table 3-2	See Table 3-3	275 [2]
Ductility (Total Strain at Failure) (%)	See Table 3-2	See Table 3-3	<0.02% [6]	See Table 3-2	See Table 3-3	<0.02% [6]
Modulus (ksi)	See Table 3-2	See Table 3-3	4540 [5]	See Table 3-2	See Table 3-3	4540 [5]
Poisson's Ratio	0.35 [8]		~0 [4]	0.35 [8]		~0 [4]
Adhesion Strength (psi) to Under Layer	See Table 3-8			See Table 3-8		
Adhesion Energy (J/m ²) to Under Layer (G _{material})	See Table 3-9			See Table 3-9		
Cohesion Energy (in-lb/in ²)						
Properties for Mechanical Response						
Coefficient of Thermal Expansion (m/m/°C)	See Table 3-6	See Table 3-6	0.4 – 1.4x10 ⁻⁵ [4]	See Table 3-6	See Table 3-6	0.4 – 1.4x10 ⁻⁵ [4]
Glass Transition Temperature (°F)	74.8	N/A	N/A	76.6	N/A	N/A
Thermal Conductivity (W/m/K)	See Table 3-5	See Table 3-5	0.87 – 1.3 [1]	See Table 3-5	See Table 3-5	0.87 – 1.3 [1]
Specific Heat (J/kg/K)	See Table 3-7	See Table 3-7	836 – 1170 [7]	See Table 3-7	See Table 3-7	836 – 1170 [7]
Density (kg/m ³)	See Table 3-4	See Table 3-4	2277 [3]	See Table 3-4	See Table 3-4	2277 [3]

^aListed properties are a function of moisture content and temperature and are for dry films near room temperature

^bTable values without [] are measured values

Table 3-2. Free-Film Tensile Test Results for Phenoline[®] 305

Temp. °F	Aging	Wetness Condition	Ultimate Strength (psi)	Modulus (psi)	% Strain at Failure
100	Non-irradiated	Dry	1700	43000	16
100	Non-irradiated	Dry	2000	110000	10
200	Non-irradiated	Dry	480	2000	2.3
300	Non-irradiated	Dry	460	3100	15
100	Non-irradiated	Wet	1200	26000	16
200	Non-irradiated	Wet	740	3200	26
100	Irradiated	Dry	300	80000	0.4
100	Irradiated	Dry	1000	51000	2.5
200	Irradiated	Dry	180	280	63
300	Irradiated	Dry	30	190	11
100	Irradiated	Wet	290	35000	1.4
200	Irradiated	Wet	220	290	68

Table 3-3. Free-Film Tensile Test Results for Starglaze[®] 2011S

Temp. °F	Aging	Wetness Condition	Ultimate Strength (psi)	Modulus (psi)	% Strain at Failure
100	Non-irradiated	Dry	390	42000	nd
100	Non-irradiated	Dry	390	66000	1.8
200	Non-irradiated	Dry	340	26000	1.0
200	Non-irradiated	Dry	210	22000	1.3
200	Non-irradiated	Dry	170	32000	nd
300	Non-irradiated	Dry	120	17000	0.6
100	Non-irradiated	Wet	290	27000	1.9
200	Non-irradiated	Wet	230	11000	2.8
100	Irradiated	Dry	340	30000	1.0
200	Irradiated	Dry	120	6200	2.5
300	Irradiated	Dry	50	3400	1.7
100	Irradiated	Wet	160	50000	2.2
200	Irradiated	Wet	140	13000	1.8

nd = not determined

Table 3-4. Densities

	Non-Irradiated (kg/m ³)	Irradiated (kg/m ³)
Phenoline [®] 305	1423	1497
Starglaze [®] 2011S	2252	2058

Table 3-5. Thermal Conductivity

Temperature (°F)	Phenoline [®] 305	Starglaze [®] 2011S	
	Non-irradiated (W/m•K)	Non-irradiated (W/m•K)	Irradiated (W/m•K)
100	1.591	1.799	1.737
200	1.640	1.805	1.807
300	1.717	1.942	1.852

Note: Insufficient irradiated Phenoline[®] 305 was available for testing.

Table 3-6. Coefficients of Thermal Expansion[†]

Temperature (°C)	Phenoline [®] 305		Starglaze [®] 2011S	
	Non-irradiated (m/m•K)	Irradiated (m/m•K)	Non-irradiated (m/m•K)	Irradiated (m/m•K)
-20	6.0 x10 ⁻⁵	5.9 x10 ⁻⁵	4.3 x10 ⁻⁵	4.2 x10 ⁻⁵
-10	5.6 x10 ⁻⁵	6.0 x10 ⁻⁵	4.0 x10 ⁻⁵	4.1 x10 ⁻⁵
0	5.4 x10 ⁻⁵	5.9 x10 ⁻⁵	3.8 x10 ⁻⁵	4.0 x10 ⁻⁵
10	5.6 x10 ⁻⁵	5.8 x10 ⁻⁵	3.6 x10 ⁻⁵	4.0 x10 ⁻⁵
20	5.9 x10 ⁻⁵	5.6 x10 ⁻⁵	3.3 x10 ⁻⁵	4.2 x10 ⁻⁵
30	6.3 x10 ⁻⁵	5.6 x10 ⁻⁵	3.3 x10 ⁻⁵	4.2 x10 ⁻⁵
40	6.8 x10 ⁻⁵	5.8 x10 ⁻⁵	3.4 x10 ⁻⁵	4.1 x10 ⁻⁵
50	7.4 x10 ⁻⁵	6.1 x10 ⁻⁵	3.3 x10 ⁻⁵	4.0 x10 ⁻⁵
60	8.0 x10 ⁻⁵	6.4 x10 ⁻⁵	3.2 x10 ⁻⁵	3.7 x10 ⁻⁵
70	8.5 x10 ⁻⁵	6.7 x10 ⁻⁵	3.0 x10 ⁻⁵	3.6 x10 ⁻⁵
80	9.1 x10 ⁻⁵	7.2 x10 ⁻⁵	2.9 x10 ⁻⁵	3.5 x10 ⁻⁵
90	9.7 x10 ⁻⁵	7.9 x10 ⁻⁵	2.9 x10 ⁻⁵	3.6 x10 ⁻⁵
100	10.1 x10 ⁻⁵	8.7 x10 ⁻⁵	2.8 x10 ⁻⁵	3.6 x10 ⁻⁵
110	10.6 x10 ⁻⁵	9.4 x10 ⁻⁵	2.8 x10 ⁻⁵	3.7 x10 ⁻⁵
120	11.3 x10 ⁻⁵	10.2 x10 ⁻⁵	2.7 x10 ⁻⁵	3.8 x10 ⁻⁵
130	12.2 x10 ⁻⁵	11.1 x10 ⁻⁵	2.7 x10 ⁻⁵	3.9 x10 ⁻⁵
140	13.5 x10 ⁻⁵	12.3 x10 ⁻⁵	2.7 x10 ⁻⁵	4.1 x10 ⁻⁵

[†] Total thermal expansion from reference temperature at -30°C.

Table 3-7. Specific Heats

Temperature (°C)	Phenoline [®] 305		Starglaze [®] 2011S	
	Non-irradiated (J/kg•K)	Irradiated (J/kg•K)	Non-irradiated (J/kg•K)	Irradiated (J/kg•K)
-20	954.95	855.1	676.75	677.65
-10	1013.95	896.05	701.65	700.1
0	1051.55	926.05	720.05	717.7
10	1086	957.8	738.75	736.4
20	1122.5	994.45	760.45	755.05
30	1163	1033.25	783.25	775
40	1207	1080.4	809.8	797.5
50	1271	1171	846.1	817.35
60	1395	1248.5	856.15	839.35
70	1450.5	1302.5	882.2	862.35
80	1525	1371	910.3	885.7
90	1575	1424.5	927.35	904.05
100	1594.5	1451	939.85	918.15
110	1606	1467.5	951.4	929.8
120	1616.5	1482	961.45	940.5
130	1627.5	1496	970.35	949.95
140	1633	1505	978.6	958.2
150	1636	1511	985.05	966
160	1643.5	1519.5	993.7	974.95
170	1648.5	1528.5	999.95	983.45

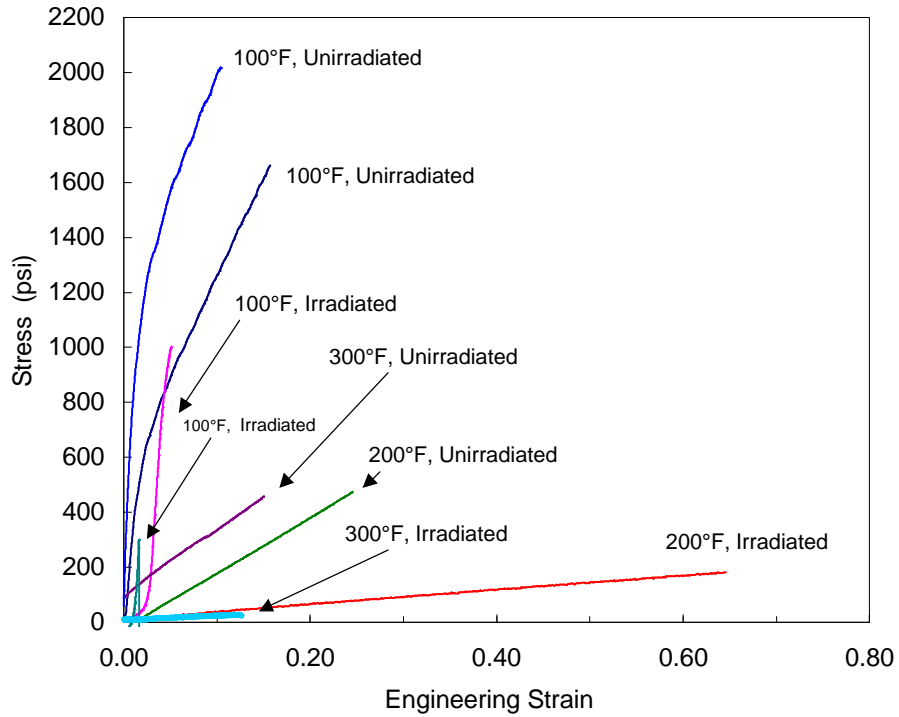


Figure 3-1. Free-film tensile test results for Phenoline[®] 305 in the dry condition

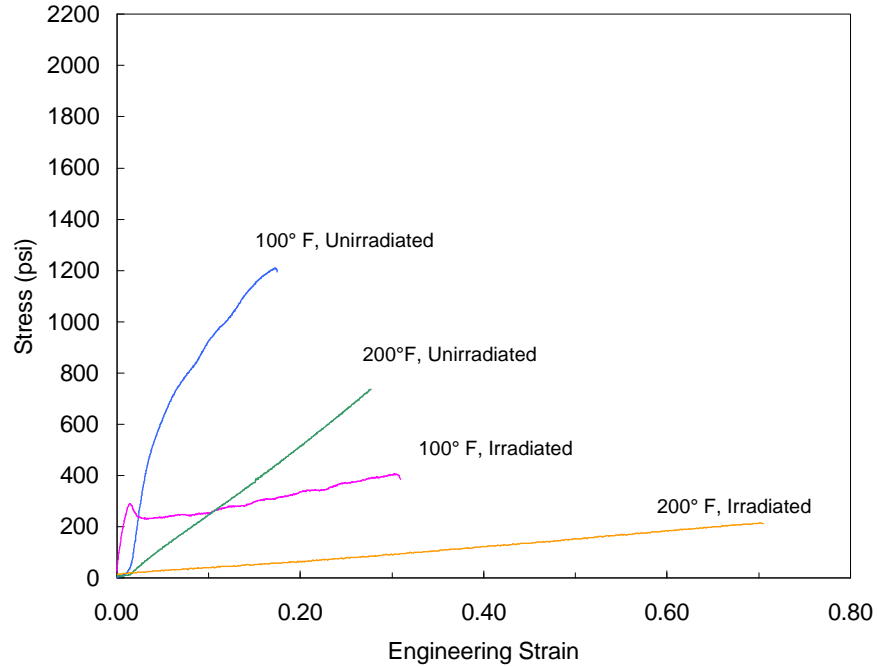


Figure 3-2. Free-film tensile test results for Phenoline[®] 305 in the wet condition

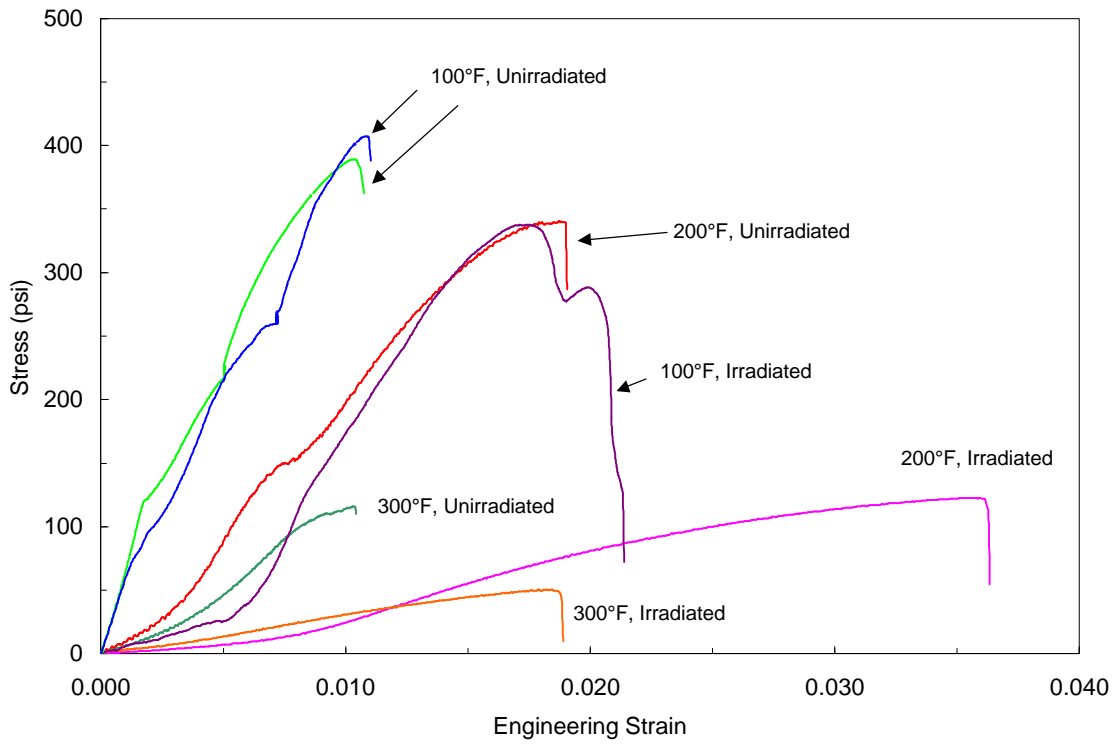


Figure 3-3 . Free-film tensile test results for Starglaze[®] 2011S in the dry condition

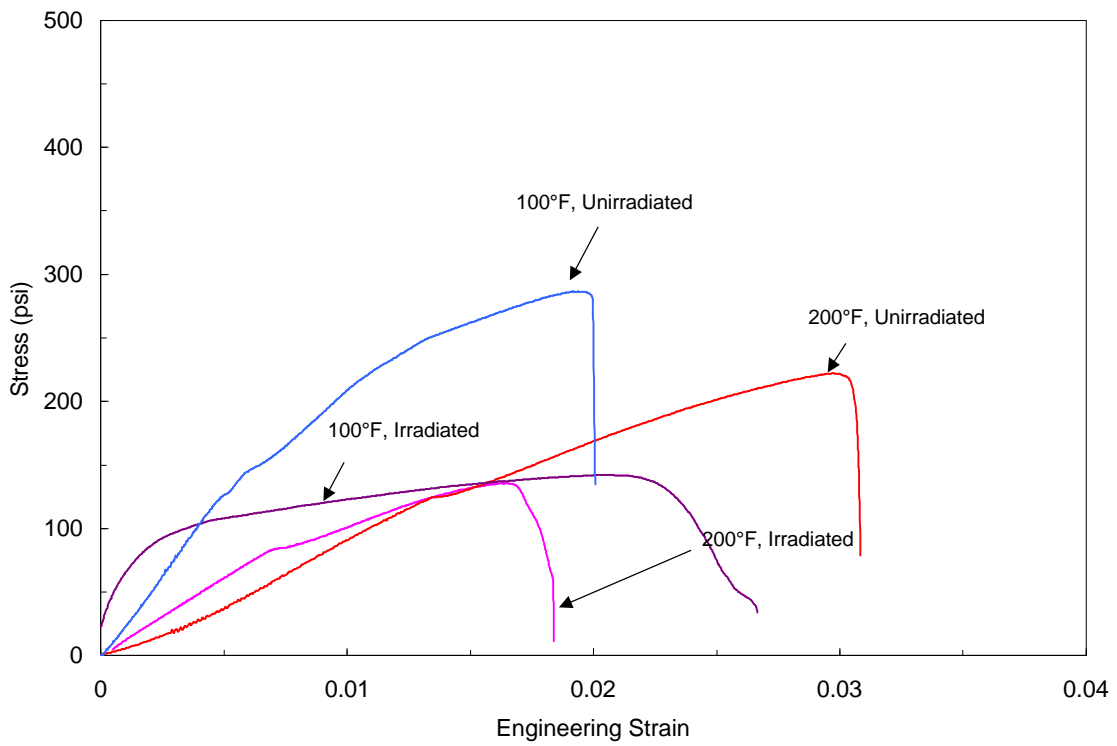


Figure 3-4 . Free-film tensile test results for Starglaze[®] 2011S in the wet condition

Phenoline 305 Tensile Data, 200°F Dry Condition

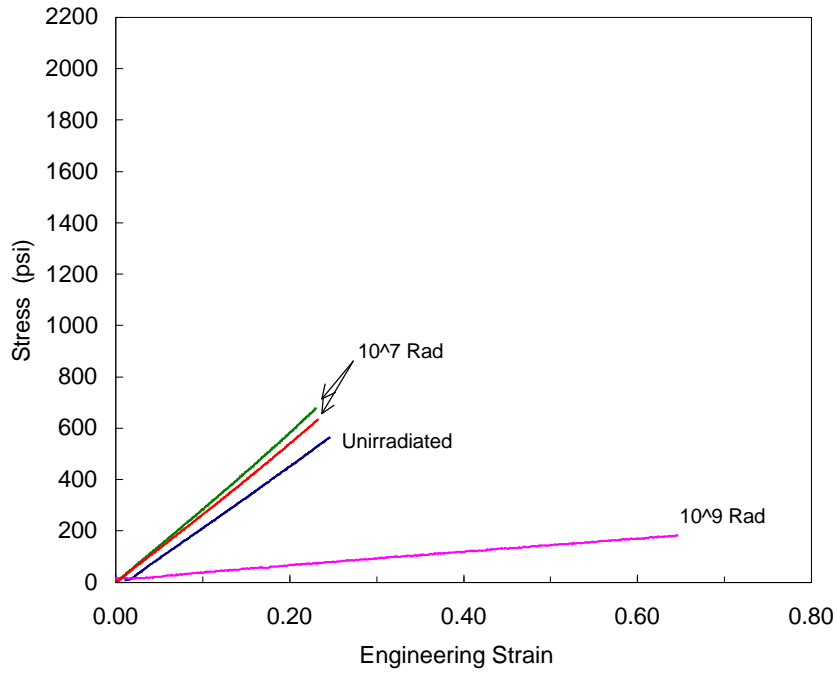


Figure 3-5. Tensile test data for Phenoline[®] 305 at 200°F obtained in the dry condition

Table 3-8. Adhesion Pull Test Results for System 2

Temperature °F	Aging	Wetness Condition	Adhesion Strength (psi)
100	Non-irradiated	Dry	770
200	Non-irradiated	Dry	310
300	Non-irradiated	Dry	150
100	Non-irradiated	Wet	630
200	Non-irradiated	Wet	280

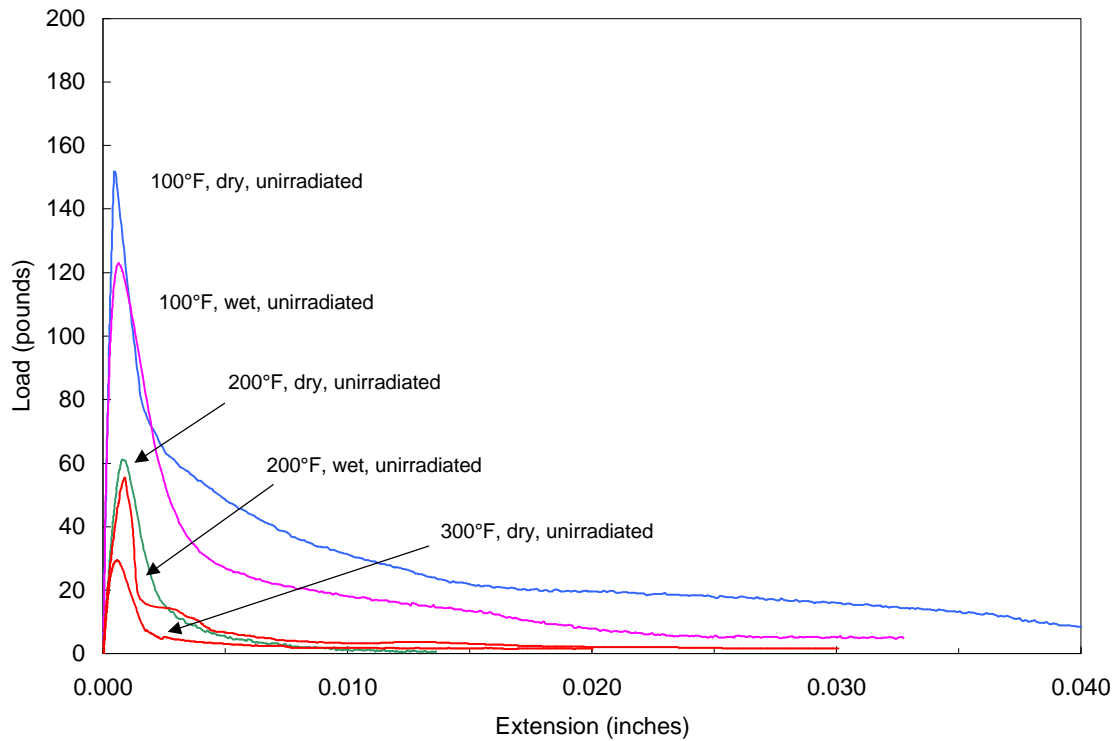


Figure 3-6. Adhesion pull test results for System 2

Table 3-9. Adhesion G-Value Test Results for System 2

Temperature °F	Aging	Condition	Peak Load (lb)	Material G-Value (J/m ²)	Failure Location
100	Non-irradiated	Dry	120	420	glass/concrete interface
100	Non-irradiated	Wet	110	570	glass/concrete interface
200	Non-irradiated	Dry	35	180	glass/concrete interface
200	Non-irradiated	Wet	12	19	glass/concrete interface
300	Non-irradiated	Dry	13	nd	Within surfacer
100	Irradiated	Dry	74	nd	Within topcoat
100	Irradiated	Wet	57	nd	Within topcoat & surfacer
200	Irradiated	Dry	7.3	nd	Within topcoat
300	Irradiated	Dry	0.50	nd	Within topcoat

nd = not determined

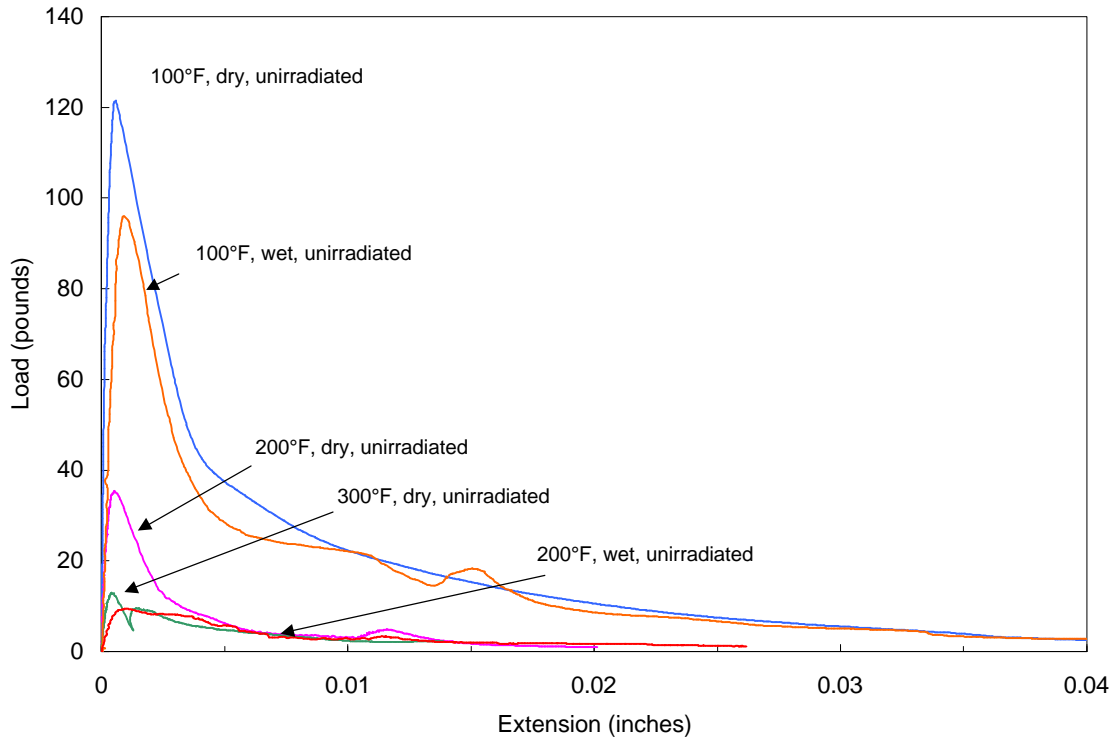


Figure 3-7. Adhesion G-value test results for non-irradiated System 2

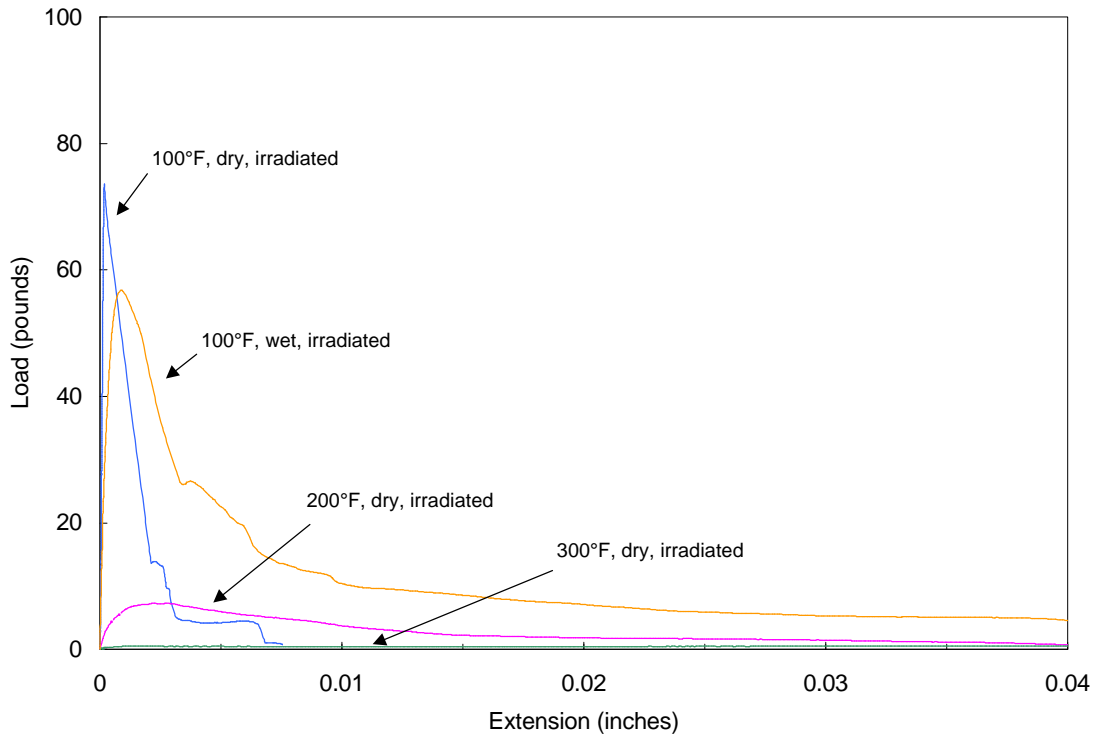


Figure 3-8. Adhesion G-value test results for irradiated System 2



Figure 3-9. Non-irradiated System 2 specimen block and pullers from the G-value tests. The two left pullers were tested at 100°F, and the two on the right at 200°F. Broken glass discs (type 1 defect) reflect light on pullers. Second from right puller has concrete fragment from beneath level of the type 1 defect.



Figure 3-10. Photograph of puller from a 100°F non-irradiated, wet condition G-value test

3.2 Failure Modeling

Analytical modeling is used to predict the performance of coating System 2 under the temperature and pressure conditions of the DBA. The temperature and pressure conditions include both transient and steady state. Coating stresses and deformations are calculated using finite element analysis. The resulting coating conditions are evaluated with respect to: 1) stress/strain overloads; and 2) fracture instabilities in order to determine the onset of coating failure. The analytical modeling does not extend beyond cracking and blistering of the coating to predict the total disbondment to create chip or particulate debris that would fall from the surface. Appendix C provides the details of the finite element method to calculate temperature profiles and coating deformations to analyze coating performance.

Two separate analytical models (Mode 1 and Mode 2) were established to analyze the coating deformation where either a blister first forms (Mode 1 deformation) or a crack first forms (Mode 2 deformation). Figure 3-11 is a schematic of the Mode 1 deformation model. For Mode 1 analysis, it is assumed that the defect may exist in the coating materials (topcoat or primer) or on the material interfaces (between topcoat and primer or between primer and the substrate). Mode 1 deformation would cause a blister to grow in size or crack or both under DBA conditions. The second type of defect model, Figure 3-12, is a coating defect emanating from the end of surface scratch or a through-coating crack. Mode 2 deformation would cause an initial cracked and delaminated region to extend in size or “peel back”.

Analytical models are built for the configurations of the non-defected and defected laboratory specimens used in the experimental DBA testing. The materials properties used in this analysis are listed in Tables 3-1 to 3-7. The coating thicknesses were measured from a sectioned block. As a result, the topcoat (Phenoline® 305) thickness input to the finite element model is 10 mils and the surfacer (Starglaze® 2011S) thickness input is 40 mils.

The defected laboratory specimens are those with Type 1 internal defects (Figure 2-2) and Type 2 through-coating hole defects (Figure 2-3). The Type 1 laboratory defect is similar to the Mode 1 model in the analysis; that is, a specimen contains a circular non-bond area between the coating and the substrate. The Type 2 laboratory specimen contains a circular region in which the coating material is removed, exposing the bare substrate. In addition, two lines are scribed through the coating, tangent to the circle, to create an initial defect that would be subject to the Mode 2 or “peel-back” deformation. Both Type 1 and Type 2 specimens are subjected to DBA testing as described in section 3.3.

This section provides the results of the analysis of the coating System 2 for the following general cases under the transient conditions of the DBA:

- Non-irradiated, non-defected
- Non-irradiated, Type 1 defect, no trapped water
- Non-irradiated, Type 1 defect, trapped water
- Non-irradiated, Type 2 defect

The objective of the analytical modeling is to predict coating performance under the ASTM D3911-95 DBA-LOCA exposure using the temperature-dependent and wetness-dependent material properties. The most severe events of the ASTM DBA-LOCA exposure in terms of thermal excursion are 1) heating during the first 10 seconds and 2) the cool-down after long-term (10,000 seconds) steady state exposure. Therefore, a 10-second rise time from 120°F to 307°F and a 5-second fall from 307°F to 250°F were evaluated as the first two transients in the profile. The predicted performance is summarized in section 3.2.5.

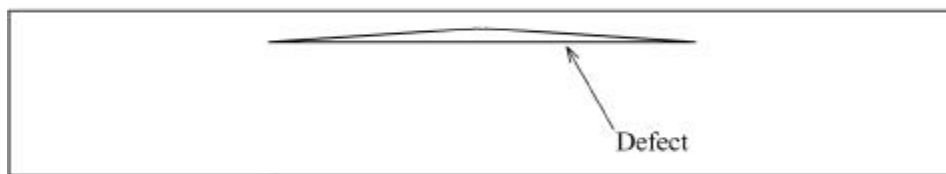


Figure 3-11. Mode 1 Analysis Model

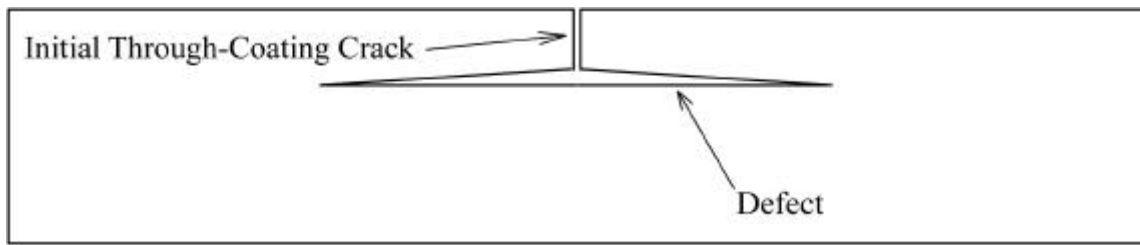


Figure 3-12. Mode 2 Analysis Model

3.2.1 Thermal-Stress Analysis for Coating System 2

The coating systems with or without defects under DBA temperature were calculated with the temperature dependent Young's moduli (Tables 3-2 and 3-3). For this analysis it was assumed that the deformation of the coating system would not affect the heat transfer characteristics of the model. Therefore, the temperature distributions in the coating-substrate system were first calculated with a thermal transient finite element analysis. These temperature distributions were then input to the stress analysis using the same finite element mesh but with continuum type of elements. The Young's modulus determined at 200°F was used for the temperatures above 200°F where the data are not available.

3.2.2 Failure Prediction for Coating System 2 – Non-Defected Coating

The stress level in the coatings was calculated for an idealized system in which the topcoat (Phenoline[®] 305) is uniformly 10 mils and the surfacer (Starglaze[®] 2011S) is uniformly 40 mils. The stresses in the non-defected topcoat and the surfacer are always under compression during the DBA exposure. Therefore, no major cracking in either the topcoat or the surfacer is predicted.

As discussed in Section 3.3, cracking was observed in the topcoat, with the cracks through the topcoat thickness to the surfacer (see Figures 3-13 and 3-39). This would be expected if local stress intensifiers (e.g., thin spots and/or micro-cracks in the topcoat/surfacer interface) were present in the topcoat. Minor cracks in the topcoat were observed from both the full DBA and “plant-specific” DBA exposures.

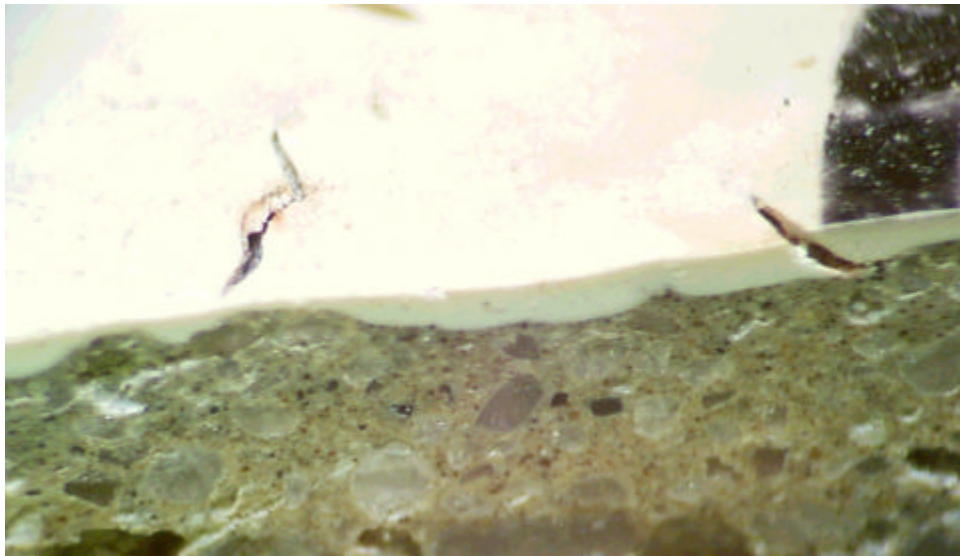


Figure 3-13. Oblique view of cross-section of non-aged System 2 specimen illustrating minor cracking which occurred during DBA-LOCA testing. The cracks appear in the topcoat only, and extend to the underlying surfacer. Magnification is approximately 15X.

3.2.3 Failure Prediction for Coating System 2 – Type 1 Defect Coating

The following analysis and results reported in this section show that a Type 1 defect in the System 2 coating at the surfacer/concrete interface will not propagate as a large blister or crack during DBA exposure, unless water is trapped within the defect. In the case where water is trapped with a 12 mm diameter Type 1 defect, the defect would exhibit cracking at the base of the defect rather than first propagating as a large blister. Furthermore, a Type 1 defect less than 1/8" in diameter is not subject to cracking even if it contains trapped water.

Thermo-mechanical analysis was performed to characterize the response of a System 2 coating with a Type 1 defect (12 mm in diameter). The front surface of the specimen was assumed to be subjected to the ASTM D3911-95 DBA temperature-pressure profile: The temperature rises from 122 °F to 307 °F in 10 seconds; remains at 307 °F for 10,000 seconds, and then drops from 307 °F to 250 °F in five seconds. The calculation continued for an additional 10 seconds to show the post-spray effects.

The calculated temperature profile was input to the mechanical analyses. Two cases were considered: 1) The defect is traction free (no moisture), and 2) The defect is loaded by the net pressure defined as the difference between the vapor pressure inside the defect and the ambient pressure of the test chamber.

Both the thermal and mechanical properties of the concrete substrate were obtained from the properties compiled in section 3.1. The Young's modulus is 31300 MPa, coefficient of thermal expansion is 0.9×10^{-5} m/m•K (averaged), thermal conductivity is 1.0 W/m•K (averaged), specific heat is 1000 J/kg•K (averaged), and density is 2277 kg/m³. The physical and thermal properties for the coating materials can be found in Tables 3-4 to 3-7.

The selected tensile data input for the topcoat and surfacer were those at 100 and 200 °F under wet condition, as listed in Tables 3-2 and 3-3. (The load-deflection curves were converted to the stress-strain curves by procedures suggested in the ASTM D882-97). The Poisson's ratios for these coating materials were set to be 0.4 (Table 3.1).

A Type 1 defect with diameter 12 mm was placed between the surfacer and the concrete substrate. The J-integral option in the finite element code (ABAQUS) was used to evaluate the applied G-values for this defect with and without vapor pressure due to trapped water in the defect. When there is no vapor pressure present inside the defect, the applied G-value is mainly due to the thermal expansion mismatch. The maximum applied G-value (0.03 J/m^2) occurs about a second after the initial heating is complete (10 seconds and at 307 °F), as shown in Figure 3-14. It can be seen that the peak value of the applied G-value is insignificant compared to the material G-values in Table 3-9, and thus no delamination would occur. It can be concluded that this defect will not grow under the condition in which there is no trapped water in the defect.

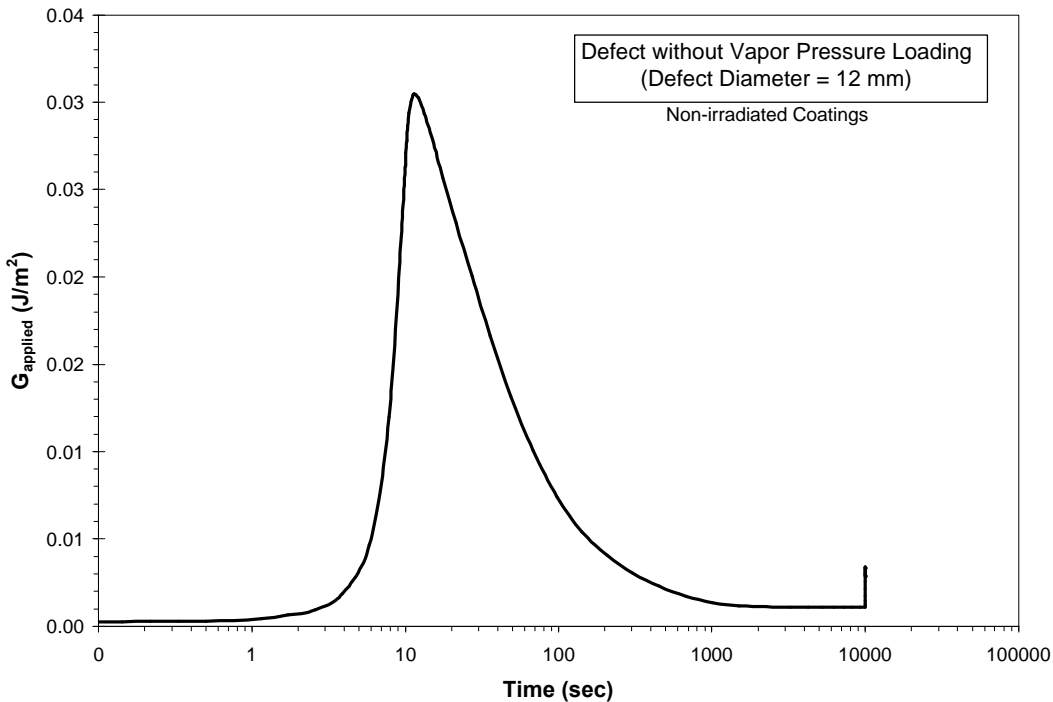


Figure 3-14. Applied G-Values at the Edge of a dry Defect (Diameter 12 mm) during DBA Test (Logarithmic Time Scale)

During the application of cooling water spray, the DBA temperature and the associated pressure will decrease. However, the defect temperature, dominated by the concrete underneath the defect, remains high due to the insulation of the topcoat and the surfacer. If moisture is present inside the defect, the vapor pressure inside the defect would surpass the ambient pressure in the DBA. The net pressure will cause the defect to form a blister. The applied G-value is thus increased dramatically during the cool-down stage. The highest applied G-value achieved is 141 J/m^2 (Figures 3-15 and 3-16), which exceeds the material G-value tested at 200°F and under wet condition (19 J/m^2) in Table 3-9. Therefore, this defect under vapor pressure loading is predicted to grow at 1.8 seconds after the DBA cooling stage begins (Figure 3-16). When the cooling spray is completed, the defect temperature gradually equilibrates with the ambient, and the net pressure eventually returns to zero.

As the defect forms a blister under the pressure loading, the material would be stretched under tensile stress and strain (parallel to the layers). Figure 3-17 shows the maximum tensile stress (in the surfacer layer) during the first 10025 seconds of the DBA testing time. It can be seen that the

tensile stress in the Starglaze[®] surfacer would exceed the ultimate stress (Table 3-3) in the cool-down phase. The time of failure is predicted to be 0.5 seconds after the spray begins (Figure 3-18).

Similarly, the time history of the maximum tensile strain in the highly stressed area is plotted in Figures 3-19 and 3-20, along with the evolution of the failure strain which is a function of temperature. Based on the failure strain criterion, the coating would fail initially in the Starglaze[®] layer near the edge of the defect at 2 seconds after the spray begins, as shown in Figures 3-20 and 3-26.

The DBA test results (Figures 3-27 and 3-28) are consistent with the prediction, if it is assumed that water becomes trapped within the defect, either from the release from concrete or because water permeates the coating during the hold at 307°F and then is trapped during the rapid cool-down to 250°F .

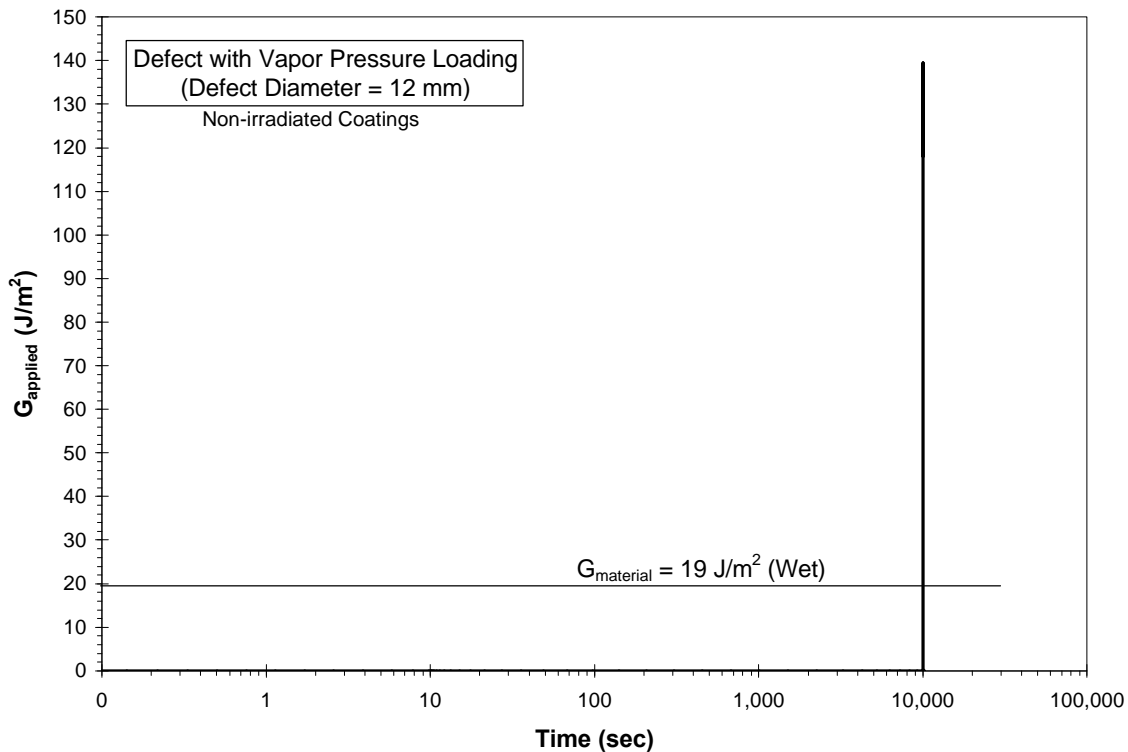


Figure 3-15. Applied G-Values at the Edge of a Vapor Pressurized Defect (Diameter 12 mm) during DBA Test (Logarithmic Time Scale)

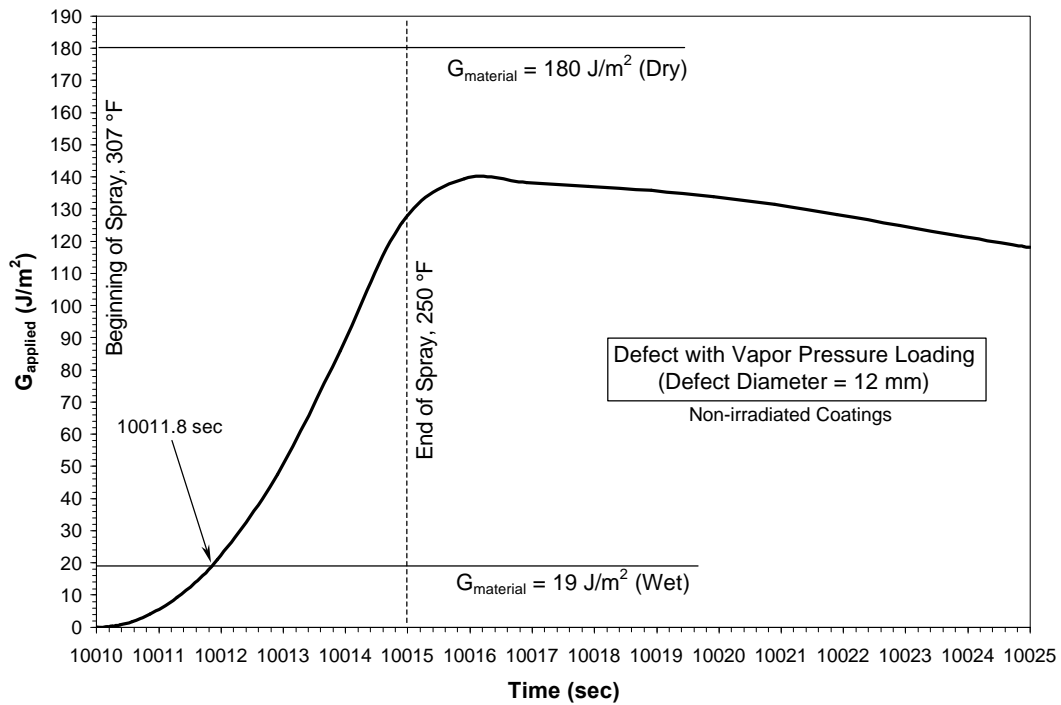


Figure 3-16. Applied G-Values at the Edge of a Vapor Pressurized Defect (Diameter 12 mm) during Cooling Phase in DBA Test (Linear Time Scale)

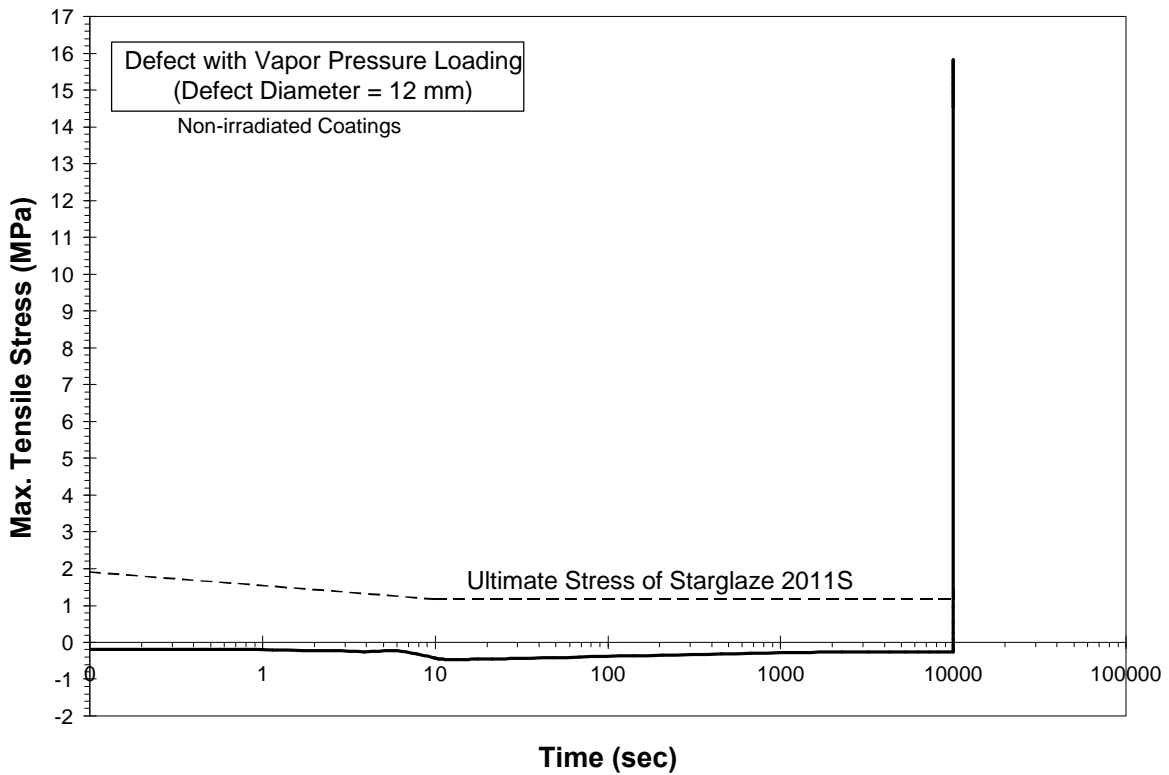


Figure 3-17. Failure of Mode 1 Defects based on Peak Tensile Stress Criterion (Entire Time History with Logarithmic Time Scale)

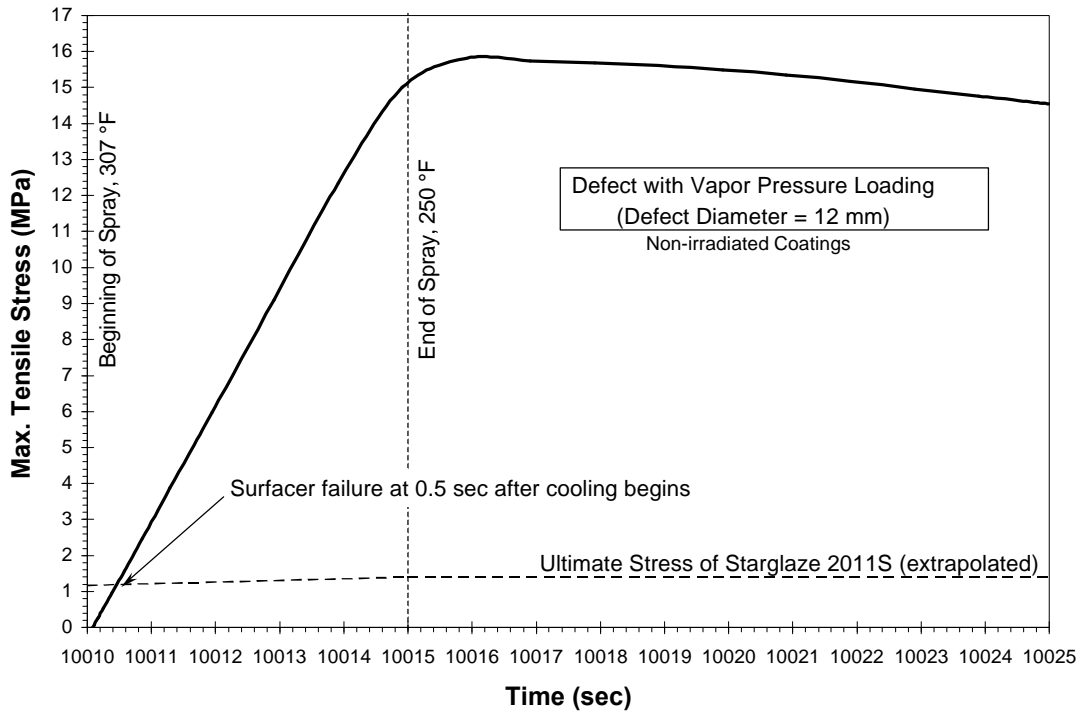


Figure 3-18. Failure of Mode 1 Defects based on Peak Tensile Stress Criterion (Cool-down Phase with Linear Time Scale)

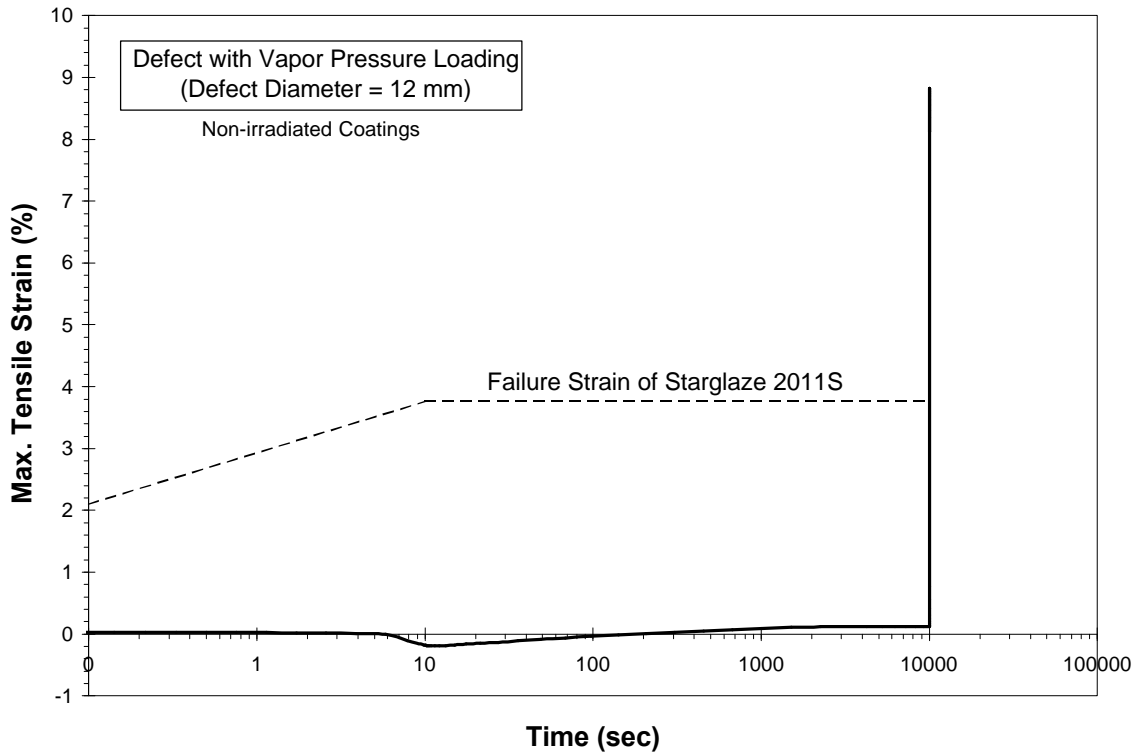


Figure 3-19. Failure of Mode 1 Defects based on Failure Strain Criterion (Entire Time History with Logarithmic Time Scale)

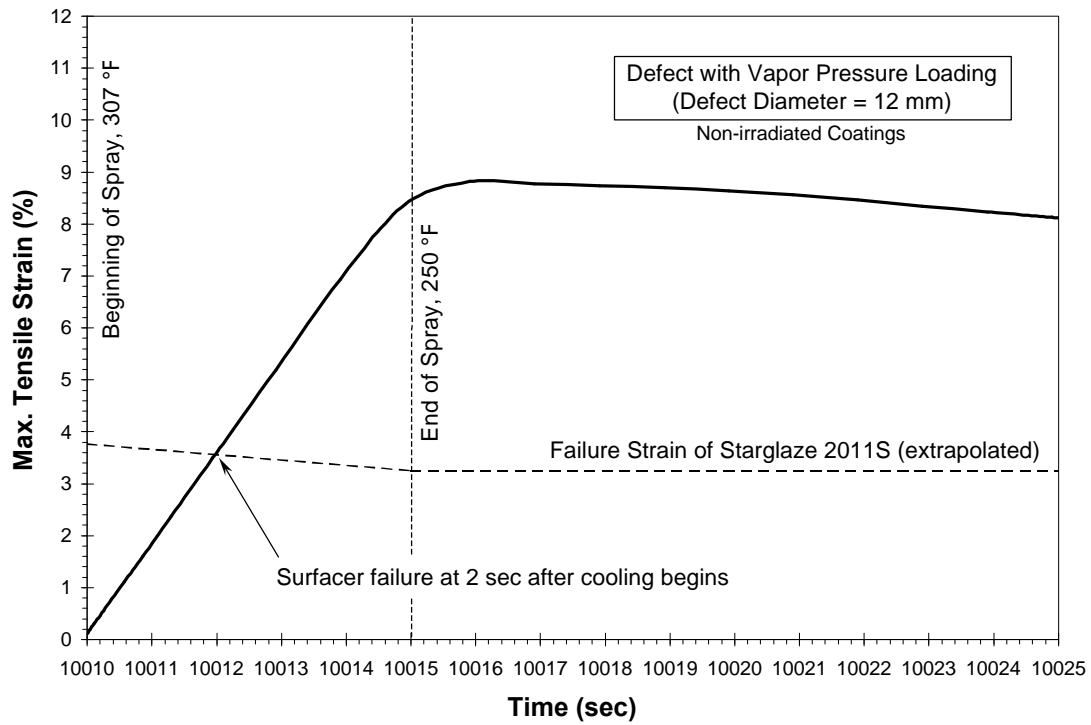


Figure 3-20. Failure of Mode 1 Defects based on Failure Strain Criterion (Cool-down Phase with Linear Time Scale)

The same analysis was performed with a smaller defect (diameter 1/8 in.) which is subject to water vapor pressure loading. Figures 3-21 to 3-26 show that this defect remains

stable during DBA testing, regardless which failure criterion is applied (material G value, ultimate stress, or failure strain criterion).

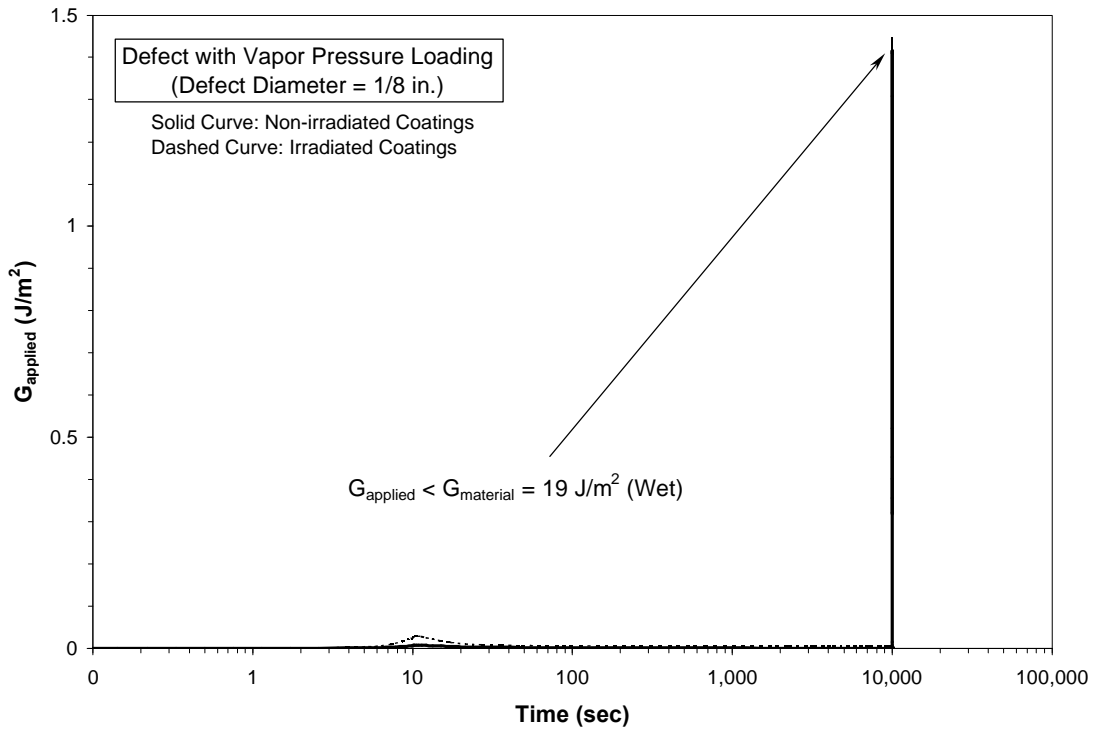


Figure 3-21. Applied G-Values at the Edge of a Vapor Pressurized Defect (Diameter 1/8 in.) during DBA Test (Logarithmic Time Scale)

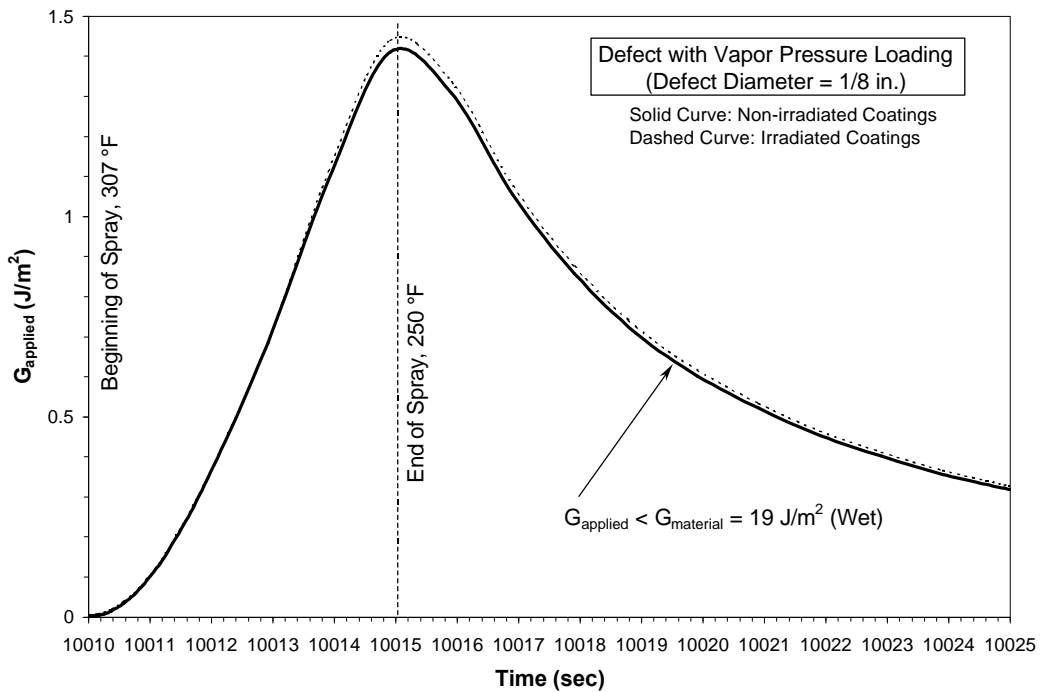


Figure 3-22. Applied G-Values at the Edge of a Vapor Pressurized Defect (Diameter 1/8 in.) during Cool-down Phase in DBA Test (Linear Time Scale)

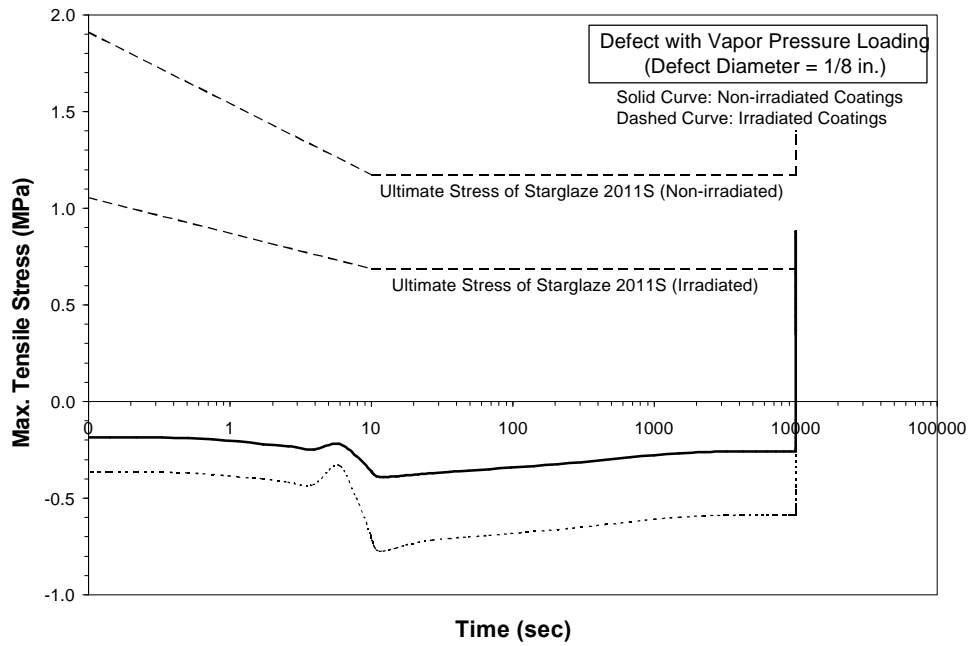


Figure 3-23. Failure of a Vapor Pressurized Mode 1 Defects (Diameter 1/8 in.) based on Peak Tensile Stress Criterion (Entire Time History with Logarithmic Time Scale)

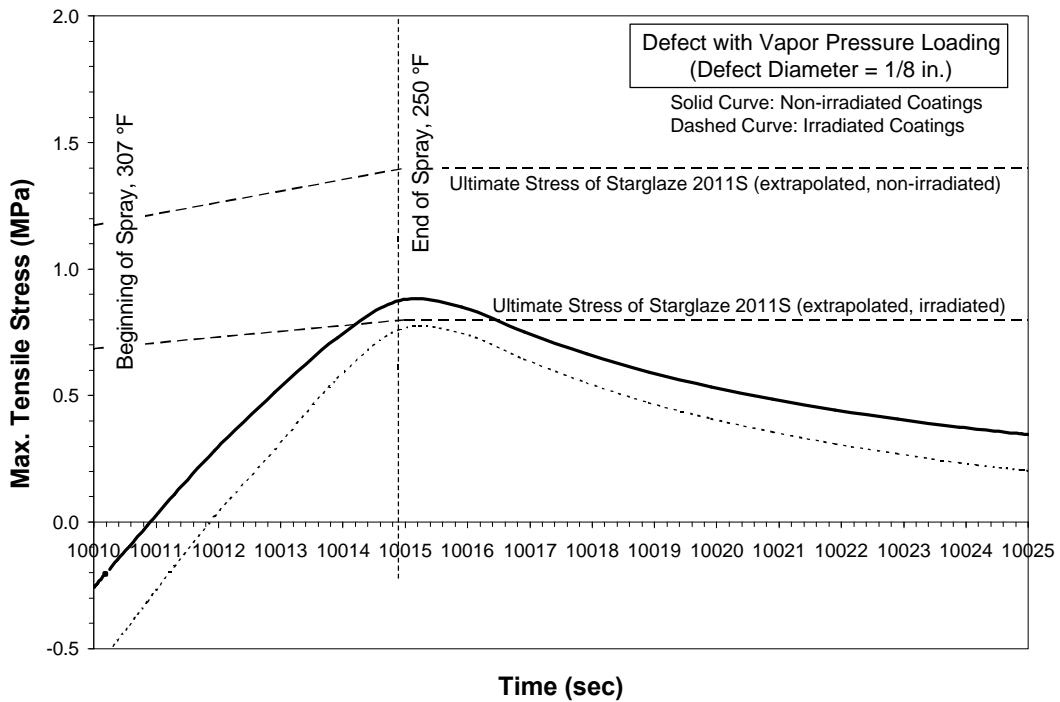


Figure 3-24. Failure of a Vapor Pressurized Mode 1 Defects (Diameter 1/8 in.) based on Peak Tensile Stress Criterion (Cool-down Phase with Linear Time Scale)

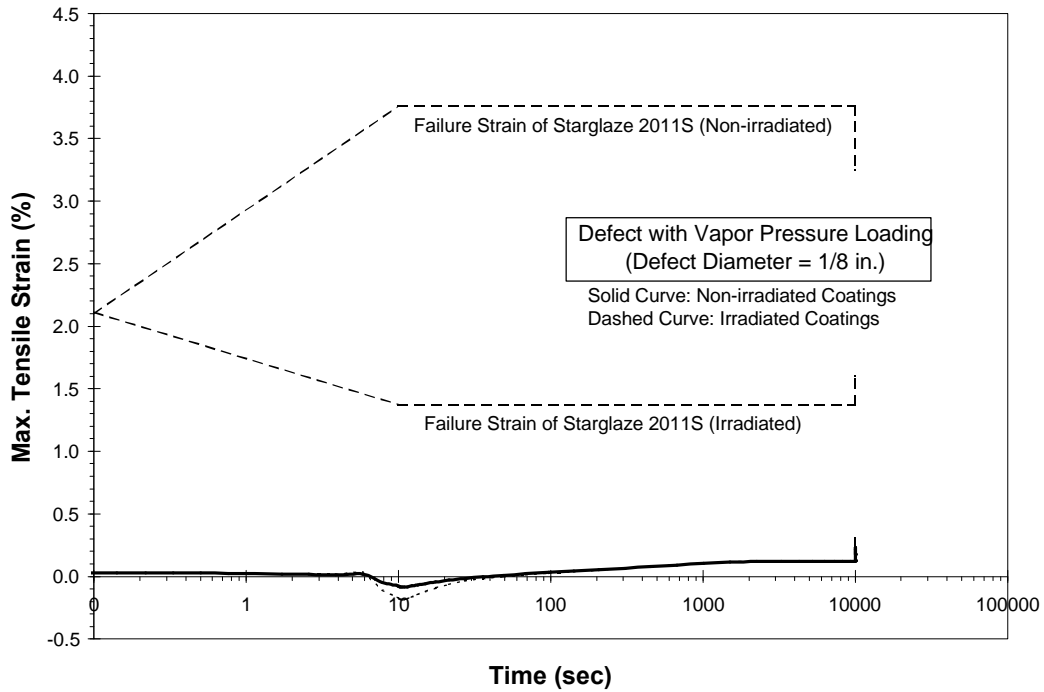


Figure 3-25. Failure of a Vapor Pressurized Mode 1 Defects (Diameter 1/8 in.) based on Failure Strain Criterion (Entire Time History with Logarithmic Time Scale)

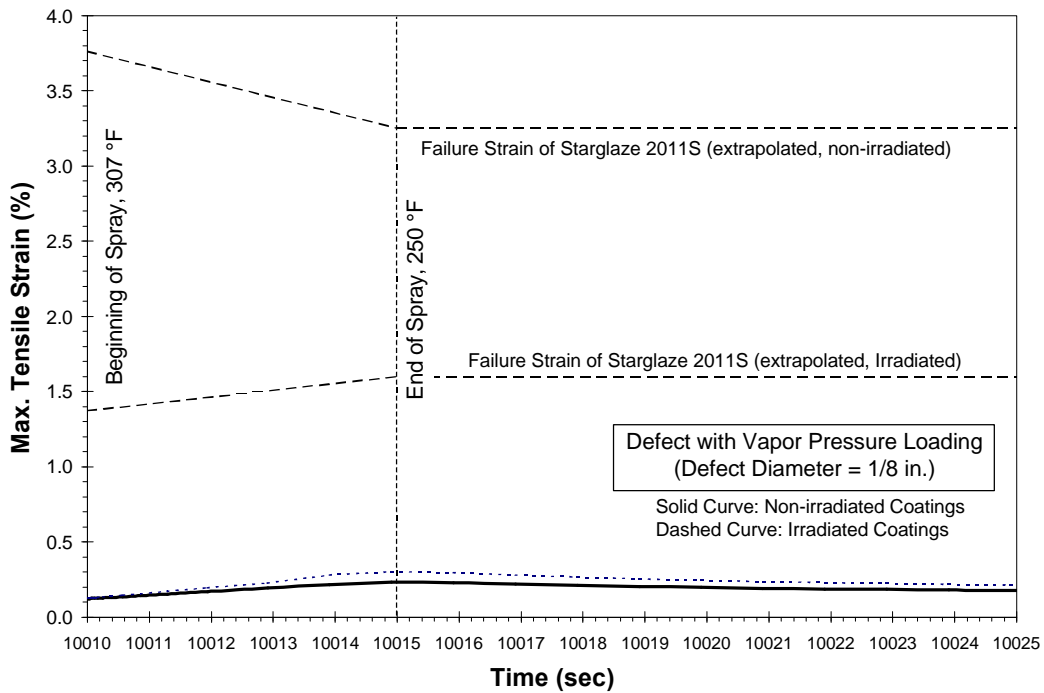


Figure 3-26. Failure of a Vapor Pressurized Mode 1 Defects (Diameter 1/8 in.) based on Failure Strain Criterion (Cool-down Phase with Linear Time Scale)

3.2.4 Failure Prediction for Coating System 2 – Type 2 Defect Coating

A Type 2 defect is not subject to peel-back deformation (Mode 2) during the DBA for a non-irradiated or irradiated coating system. This occurs for the general cases where the thermal expansion of the coating material is higher than that of the substrate, as it is for Phenoline® 305. Therefore, it can be concluded that the intact Phenoline® 305 will not fail under these conditions.

3.2.5 Predictions

Analytical modeling of coating deformation using finite element analysis can predict deformations that precede failure (disbondment); that is, “incipient failure” (blister formation & growth, cracking, peel-back of cracked films) can be predicted.

The intact (non-defected), non-irradiated coating System 2 using Phenoline® 305 topcoat and Starglaze® 2011S surfacer is not predicted to undergo major cracking under DBA conditions because a compressive stress exists in the coating throughout the time period. For the same reason, a coating containing Type 2 defects will not result in peel-back (Mode 2) deformation, as shown by SRTC testing (Figure 3-27).

Incipient failure would be predicted for the coating if it contains large (> 1/8” diameter) Type 1 defects with entrapped water. This was demonstrated by testing and shown in Figure 3-27. The timing of the significant events (cracking of the blister) for a Mode 1 deformation depends on the delamination and cracking criteria (see Section 2.2). With the assumption that the DBA temperature (and corresponding pressure) drop from 307 to 250°F is completed in 5 seconds, it can be concluded:

(i) G-value criterion

The 1/8” diameter defect remains adhered to the substrate, whereas the 12 mm diameter defect would start to propagate at 1.8 seconds after the cooling and pressure drop begins.

(ii) Peak stress criterion; failure strain criterion

Stress: A Type 1 defect 12 mm in diameter would cause a through-coating crack at 0.6 seconds after the cooling and pressure drop begins. A Type 1 defect 1/8” in diameter would not cause a coating crack.

Strain: A Type 1 defect 12 mm in diameter would cause a through-coating crack at 1.95 seconds after the cooling and pressure drop begins. A Type 1 defect 1/8” in diameter would not cause a coating crack.

As a result, the cracking failure due to the peak stress criterion appears to occur first. The Type 1 specimen was predicted to fail by cracking in the defect edge when moisture is present. This is consistent with the laboratory observations shown in Figures 3-27 and 3-28.

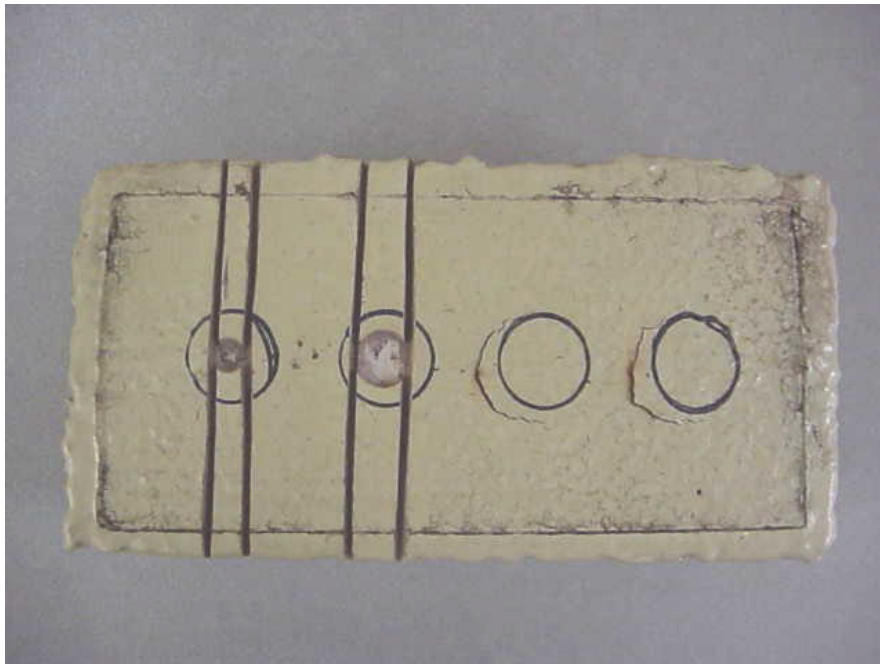


Figure 3-27. System 2 specimen, non-aged, following DBA testing. Note the circumferential cracks in the coating adjacent to the two Type 1 defects on the right. No evidence of coating peel-back was observed in the Type 2 defects on the left.



Figure 3-28. Cross-section of circumferential crack in System 2 specimen (Fig. 3-26) illustrating the location of coating failure at the edge of the glass disk used to create the Type 1 defect.

3.3 Measured Performance Under DBA and Soak Test Conditions

Two DBA profiles are used in this study: a full DBA test per ASTM D3911-95, and a rapid transient DBA

pressure/temperature pulse test to simulate a “plant-specific” DBA. In addition, soak tests (water immersion) were performed at elevated temperatures to simulate submergence of coatings following a DBA. Details of the construction and operation of the SRTC coating performance test systems are available in appendices D and E.

Test Performed	Test Description	Test Conditions
ASTM D3911 DBA-LOCA Test	7 day test per ASTM D3911-95	Included immersion of a portion of the specimens
Plant-Specific Pressure/Temperature Test	Pulse test incorporating rapid heating and rapid cooling of specimen	Included immersion of a portion of the specimens
Coating System Immersion Test	Immersion test of complete coating system (concrete substrate, surfacer, topcoat)	Testing performed from room temperature to 200°F and with 200°F initial condition
Free-film Immersion Test	Immersion of free-film specimens of surfacer and topcoat, in aged and non-aged conditions	Testing performed from room temperature to 200°F

The standard DBA temperature and pressure profile for qualification of coating systems is given in ASTM standard D3911-95 and is termed the “full DBA profile” in this report. Figure 3-29 shows this profile, which is run for a total exposure period of approximately 1 week. A

typical temperature-pressure profile from a DBA test performed in the SRTC Monitored Environmental Test Chamber is shown in Figure 3-30. The temperature/pressure profile is given in two parts, due to software restrictions.

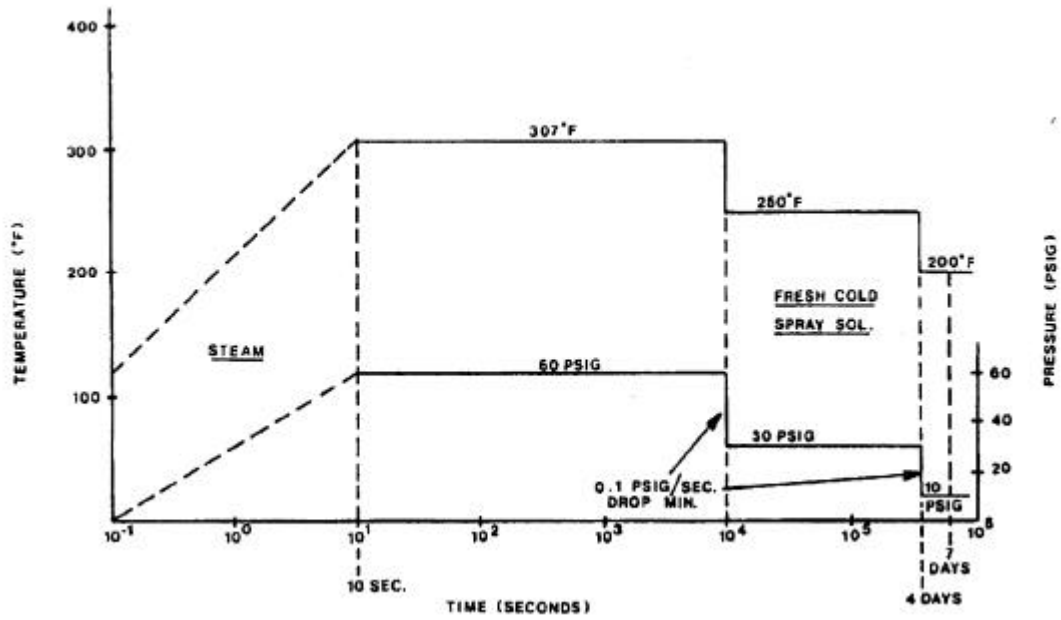


Figure 3-29. Typical Pressurized Water Reactor Design Basis Accident (DBA) Testing Parameters (from ASTM D3911-95). (Note: The ASTM figure contains an error: 30 psig should be 15 psig, which is equivalent to 30 psia).

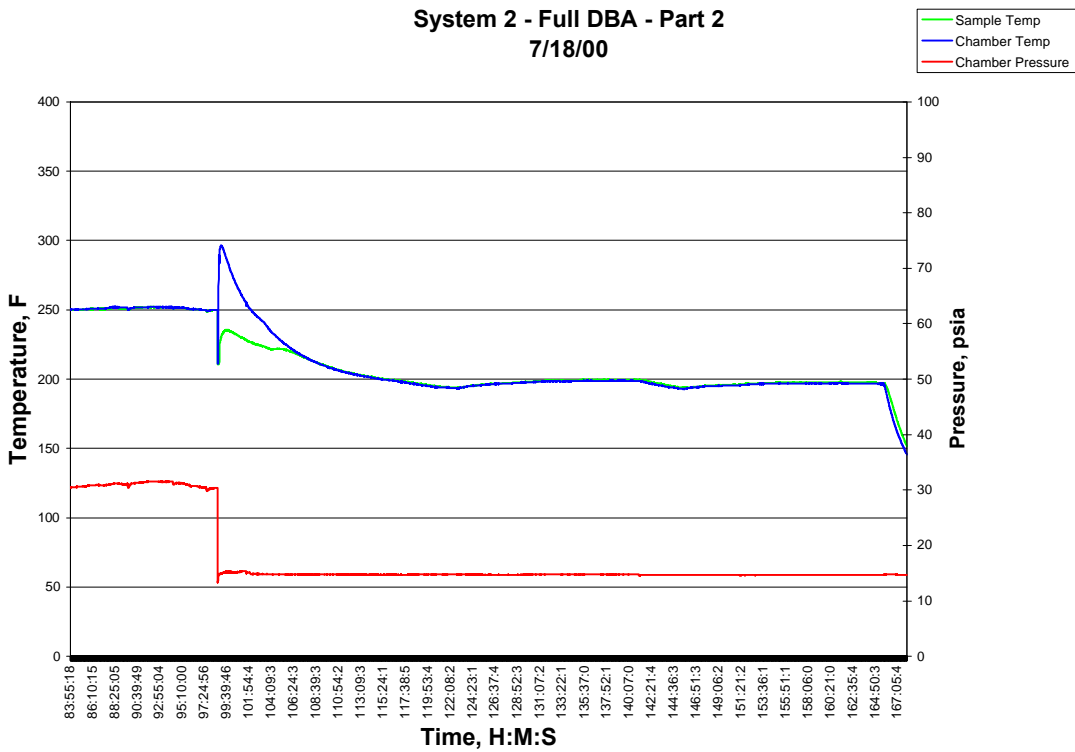
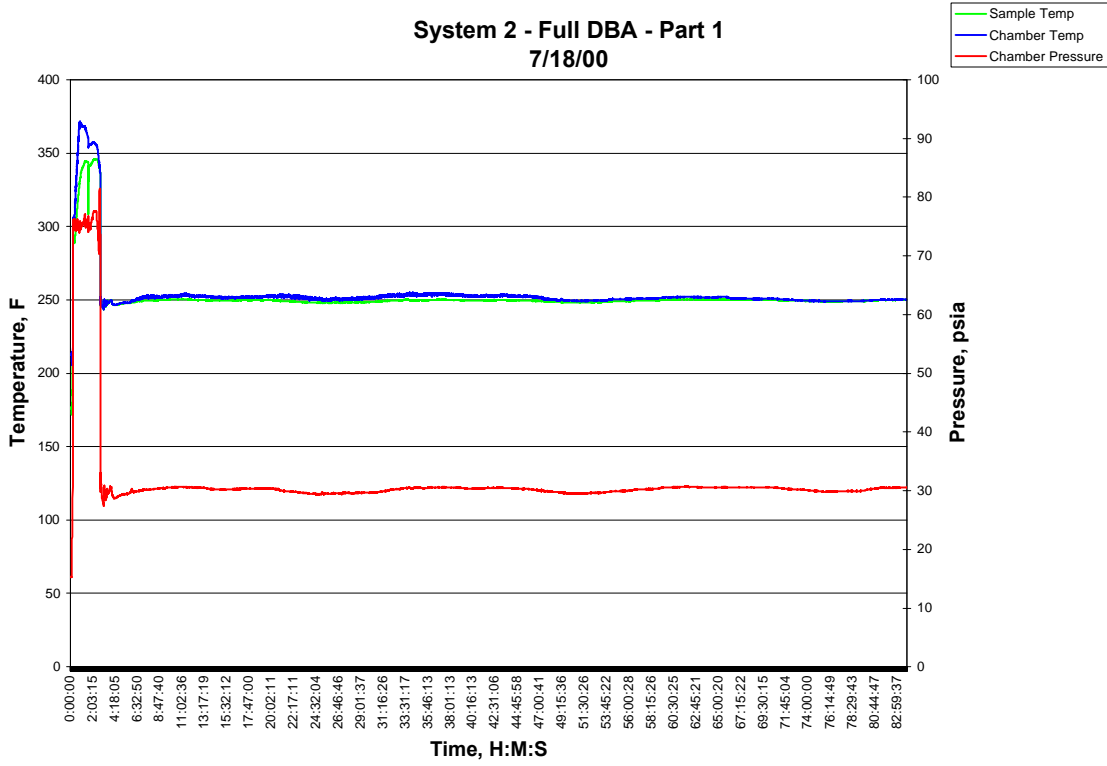


Figure 3-30. Typical Temperature-pressure Profile from SRTC System 2 D3911 DBA-LOCA Test

Coating System 2 Performance

Computer modeling indicated a susceptibility to failure of an epoxy coating during a rapid pulse transient, if water were present beneath the coating (see Section 3.2). A similar rapid transient has been calculated for nuclear power plants using the MELCOR computer model. To examine System 2 coating performance in this type of plant-specific LOCA event, the SRTC coatings

performance evaluation system was used to subject aged and non-aged System 2 specimens to a rapid temperature-pressure pulse (Figure 3-31). Evidence of blister and debris formation was observed in the irradiation-aged specimen (Figure 3-32). No evidence of failure was observed in the non-aged specimen.

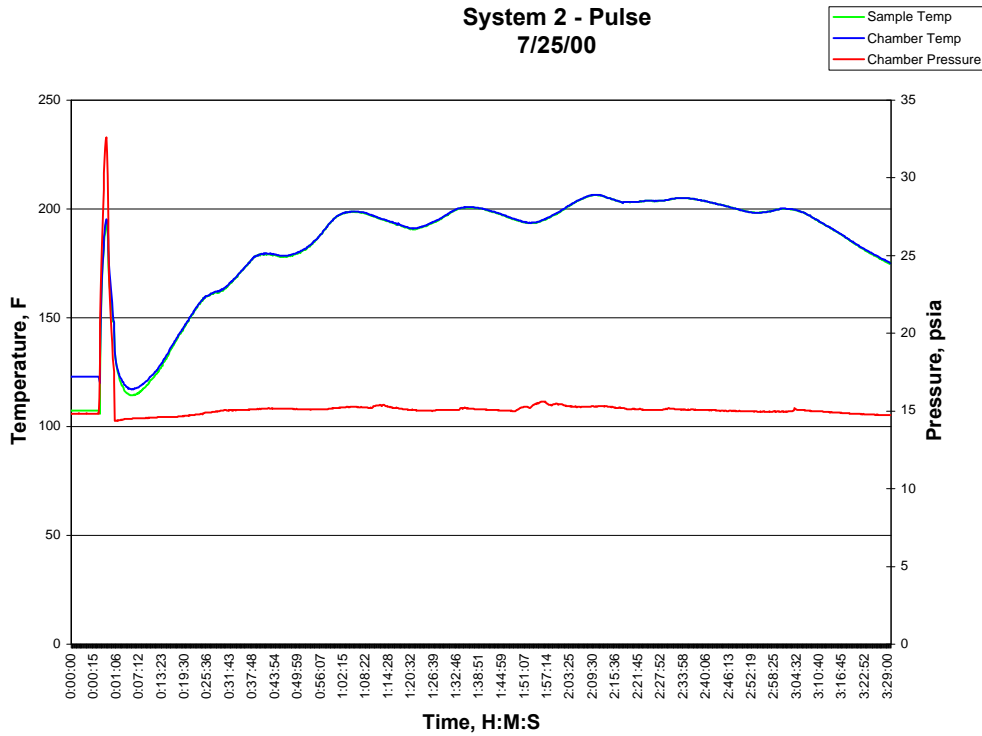


Figure 3-31. Temperature-Pressure Curves from Plant-specific LOCA Test

3.4 Coating Performance

Characterization of the performance of Phenoline® 305 following irradiation aging, DBA exposure, and irradiation plus DBA exposure was performed by a variety of standard metallurgical and analytical techniques. Chemical and compound information were obtained using SEM/EDS. Optical and SEM microscopy were used to provide details on the structure and debris source term geometric characteristics. Appendix F contains a description of the techniques applied to the coating specimens in the coatings research program at SRTC. The principal findings are 1) the resistance of the non-aged coating to any significant degradation and, 2) the development of blistering and the creation of a debris source in the aged (irradiated) coating. The debris source term forms in the top 1-2 mils of the topcoat, and is formed only under certain temperature and wetness conditions.

Significant changes appear to occur in the near-surface layer of the aged (irradiated in air) System 2 coating. A surface color change from the unirradiated material (Figure 3-32) was observed. The color change extends a few thousandths of an inch into the topcoat, as seen in Figure 3-33.

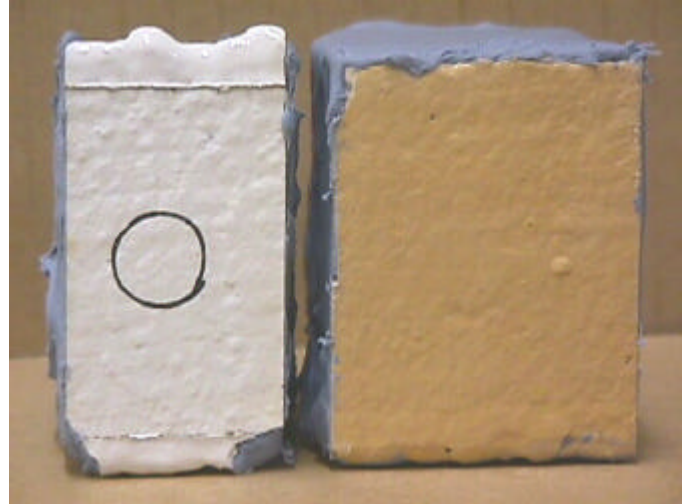


Figure 3-32. System 2 specimens before (left) and after (right) irradiation to 10^9 rad.

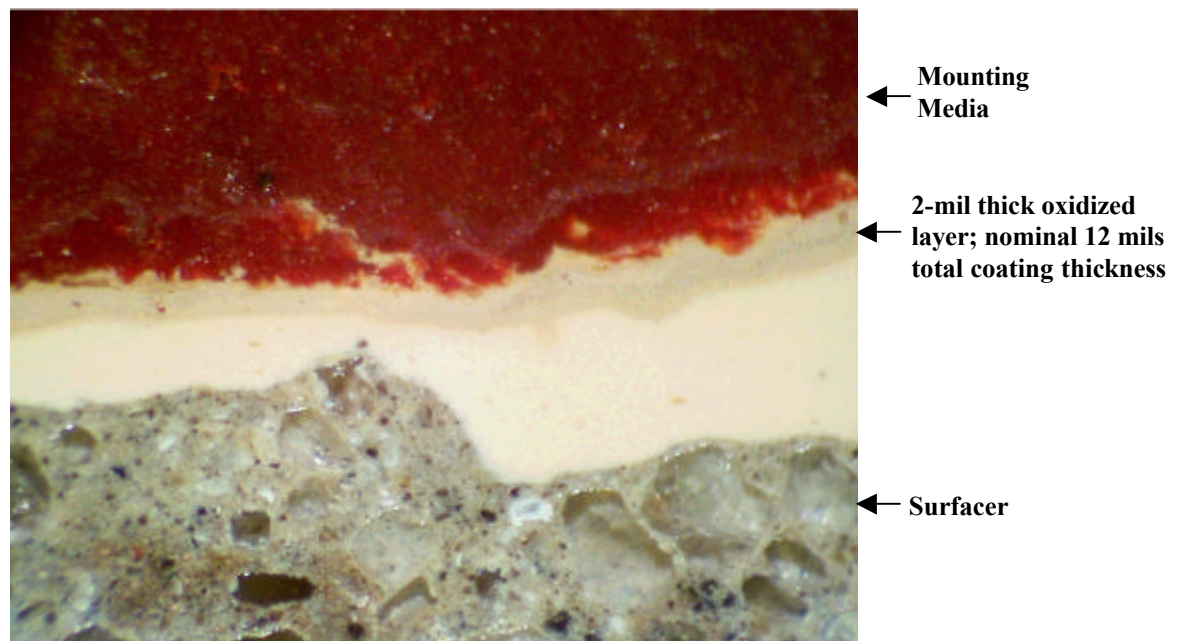


Figure 3-33. Cross-section of System 2 coating, irradiated to 10^9 rad, original magnification 30X

Coating System 2 Performance

Aged System 2 specimens exhibited blistering after having been exposed to elevated temperature in air or in water (Figures 3-34 and 3-56). Similar blistering was observed during the testing of SRTC System 5 coatings. Numerous small blisters appeared in free-film specimens when they were heated in air to 200°F during tensile testing (Figure 3-34). The blisters were approximately 1mm in diameter and remained intact. Much larger blisters appeared when coated concrete specimens were heated to 200°F in tap water (Figure 3-35). The blisters which were formed are quite thin compared to the nominal 12 mil coating thickness, and are quite fragile when dry. The thickness of the coating layer forming the blister is only about 0.001 inch (1 mil). The thickness of the blisters indicates they are formed in the darkened, ostensibly oxygen affected, outer layer of the irradiated coating.

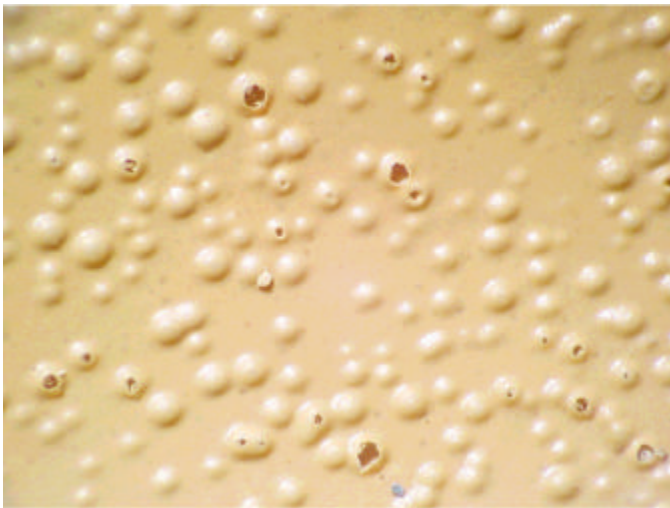


Figure 3-34 Micrograph of blistering formed on Phenoline[®] 305 free-film specimen following irradiation and heating to 200°F, dry; original magnification approximately 20x



Figure 3-35 Sloughing of surface of irradiated specimen following water soak at 200°F, original magnification 7X. Blister thickness is of the order of 1-2 mils. Note: The remaining coating is visible in the upper-right of the image

There is evidence of microvoid formation within the outermost layer of the irradiated coating (Figure 3-36). These voids may contain gases created during the irradiation of the coating.

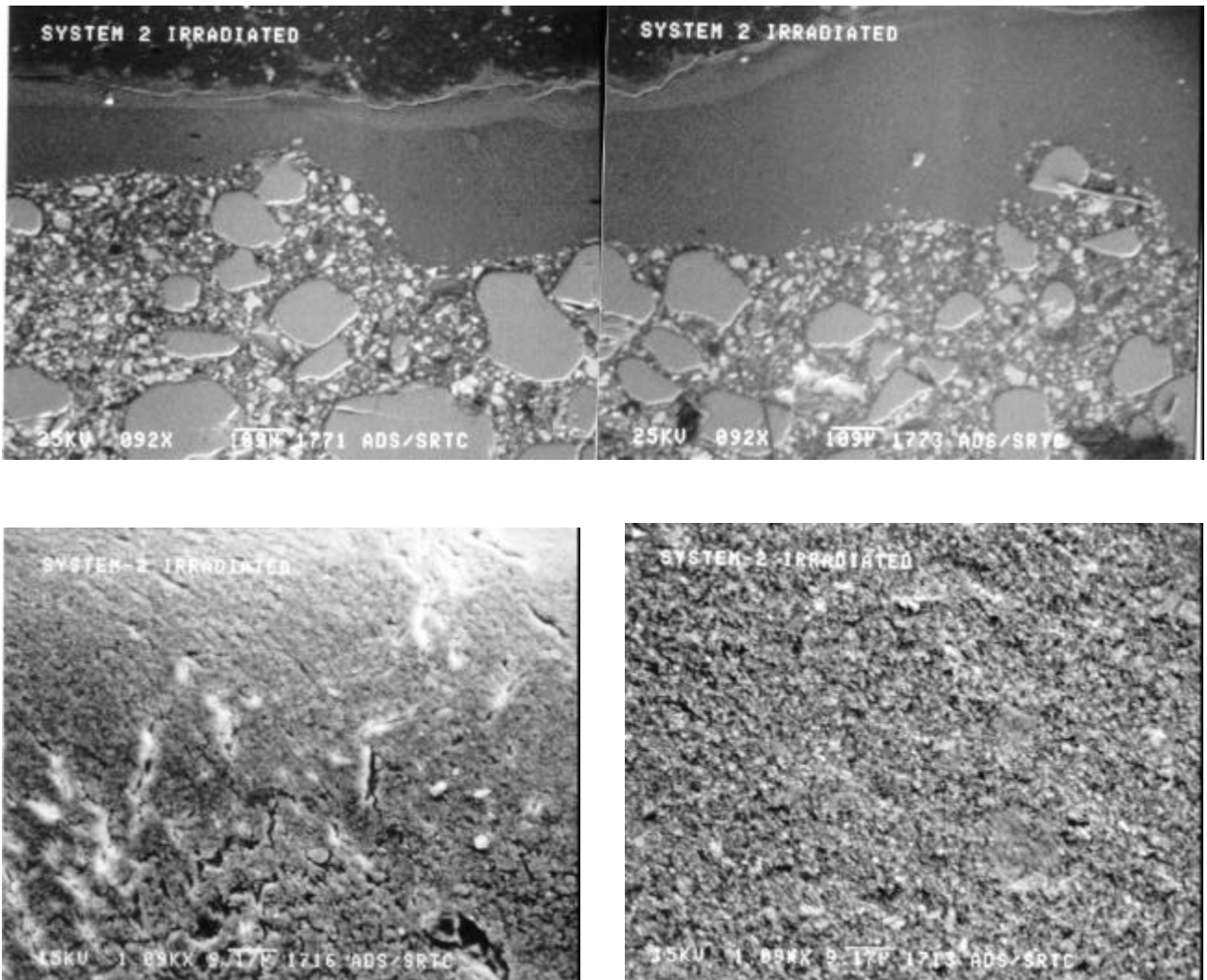


Figure 3-36. SEM micrographs illustrating the appearance of the outermost layer (left) and the bulk Phenoline[®] 305 coating (right) of irradiated System 2. This is the same specimen shown in Figure 3-33.

Coating System 2 Performance

As shown in Figure 3-1, the ductility of Phenoline® 305 increases significantly with increasing temperature; the effect is even more pronounced when the coating is wet as shown in Figure 3-2. Therefore, it is possible that gases which are formed within the coating agglomerate and expand with heating of the specimen, contributing to the formation of blisters.

Significant blistering was not observed in irradiated coating specimens during DBA-LOCA testing performed in accordance with ASTM D3911-95 (Figure 3-38). However, microscopic examination of the surface of the irradiated specimens following testing revealed the

presence of numerous pores in the coating (Figure 3-40). A cross-section of the irradiated coating made after DBA-LOCA testing (Figure 3-41) reveals the presence of extensive pores in the outermost layer of the topcoat. Therefore, it is possible any gases formed during irradiation were released from the coating during the high-temperature steam exposure, which occurs during the first 2.8 hours of the DBA test cycle. During this time, the specimen is heated with 75 psia steam to 307°F. At this temperature, the coating may become so soft, and the gases so mobile, that the gas pressure is relieved through the coating without forming blisters.

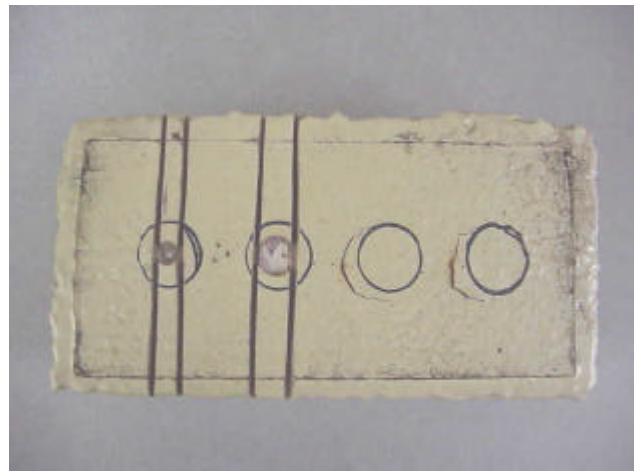
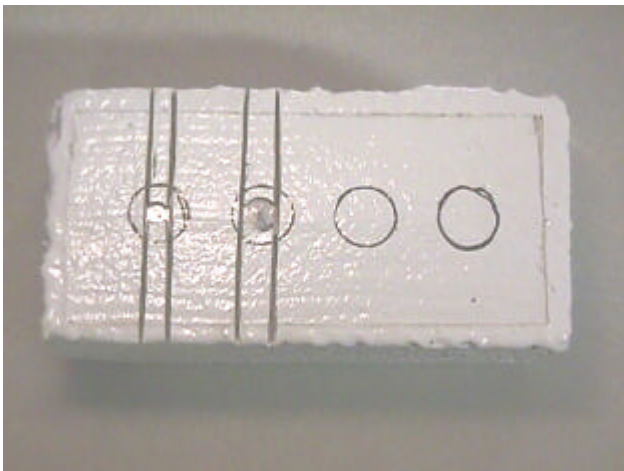


Figure 3-37. Overall views of nonaged System 2 specimens before (left) and after DBA testing. Note coating color change and circumferential cracks adjacent to Type 1 defects which are present following testing

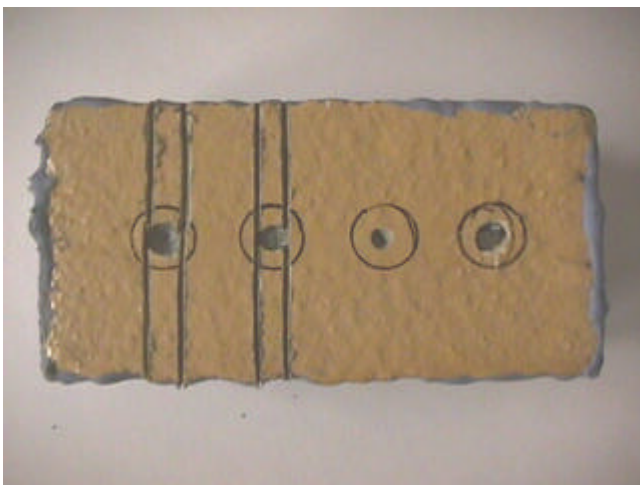


Figure 3-38. Overall views of irradiation-aged System 2 specimens before (left) and after DBA testing



Figure 3-39. Detail of the surface of the non-aged specimen after DBA testing. Note the presence of minor cracks in the coating, as discussed in Section 3.2.2. Original magnification 7X. A cross-section view of these cracks is shown in Figure 3-12.

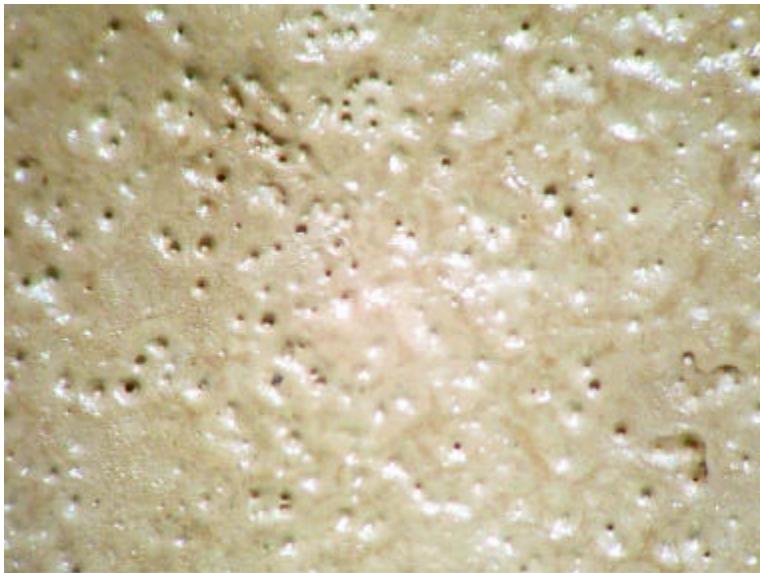


Figure 3-40. Detail of the surface of the irradiation aged specimen after DBA testing. Note the presence of pores in the coating. Original magnification 7X.

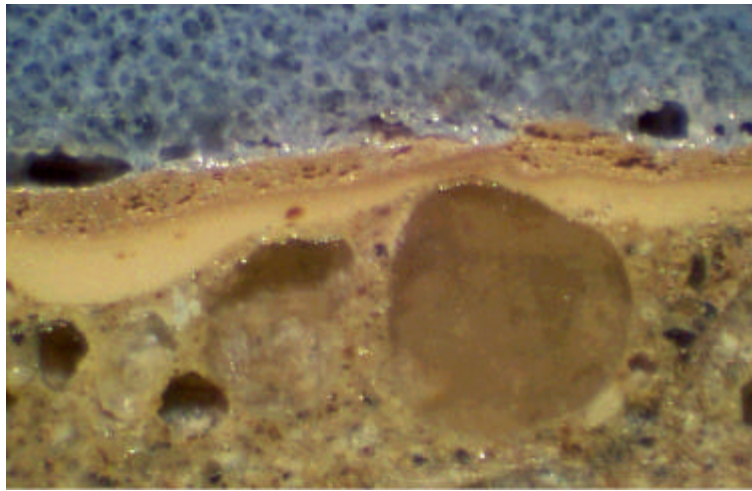


Figure 3-41. Cross-section of the surface of the irradiation aged specimen after DBA testing. Note the presence of pores in the coating. Original magnification 45X.

Blistering has been observed during DBA rapid pressure/temperature pulse testing (Figure 3-42). This could indicate that any gases present within the coating are not released through pores at high temperature (> 200°F), due to the rapidity of the temperature pulse. Rather, these gases remain to form blisters during the water spray portion of the test with extended exposure at a temperature of approximately 200°F. Formation of these blisters can be exaggerated by allowing a portion of the test specimen to become immersed during the water spray portion of the DBA pulse test.



Figure 3-43. Detail of irradiation-aged specimen in Figure 3-42, taken above the water immersion level, illustrating extensive blister formation. Original magnification 7X.

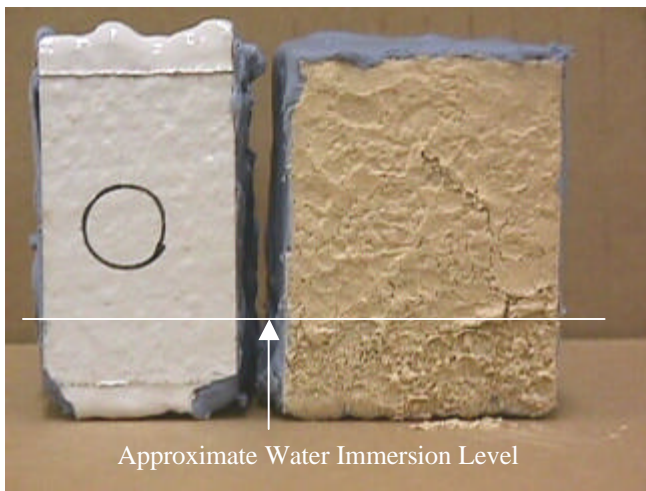


Figure 3-42. System 2 non-aged (left) and irradiation aged (right) specimens following DBA pulse-test. Note blister formation in the near-surface, oxidized layer of the irradiated specimen. Note also the presence of debris powder beneath the irradiated specimen. The bottom portions of both specimens were allowed to become immersed during the water spray portion of the pulse test.



Figure 3-44. Detail of irradiation-aged specimen in Figure 3-42 taken below the water immersion level. The blisters are of a larger size than those in Figure 3-43, and some of the blisters have ruptured and/or detached, revealing the underlying coating remnant. Original magnification 7X.

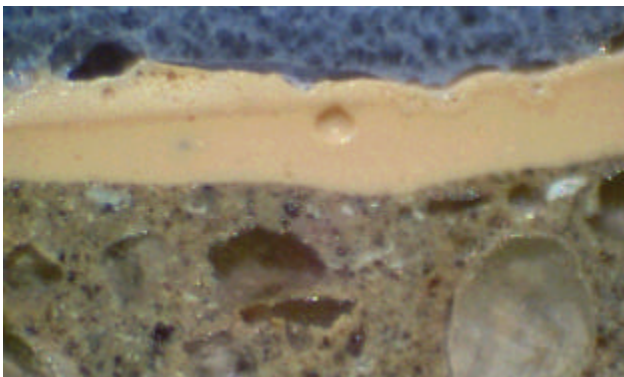


Figure 3-45. Cross-section of irradiation-aged specimen in Figure 3-42, taken from above the water immersion line. Note the presence of pores in the topcoat remnant. Original magnification 45X.

The blisters, which form in wet, irradiated coatings as shown above, can, in certain conditions, become a debris source term. This development is illustrated by Figures 3-46 through 3-52 below, which were made during a 200° F soak test of irradiation-aged and non-aged System 2 coating specimens.

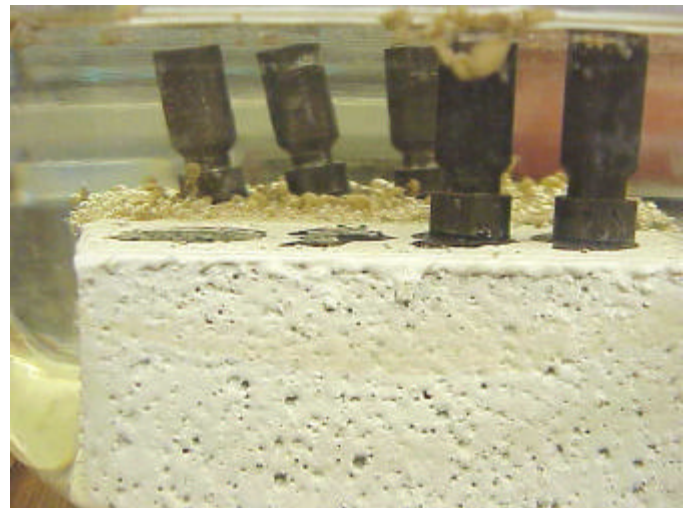


Figure 3-46. Overall view of non-irradiated System 2 specimen, submerged overnight in 200° F water.



Figure 3-47. Overall view of irradiated System 2 specimen, submerged overnight in 200° F water. Note: The irradiated specimen was coated on the top surface only.

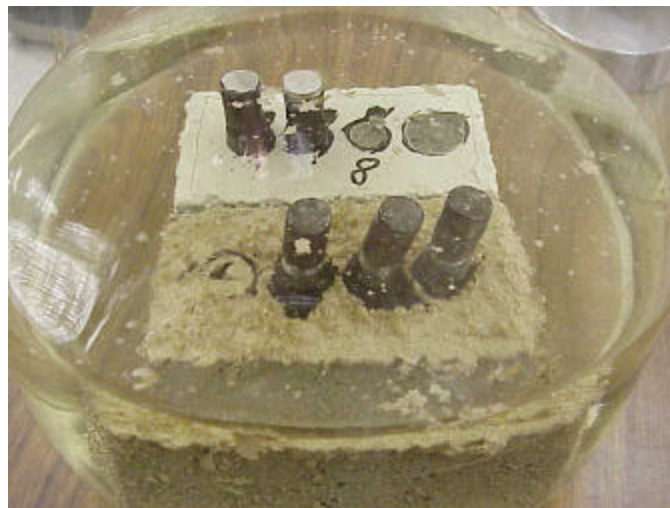


Figure 3-48. Irradiated and non-irradiated System 2 specimens, soaking in 200° F water. Note the presence of debris in the vessel

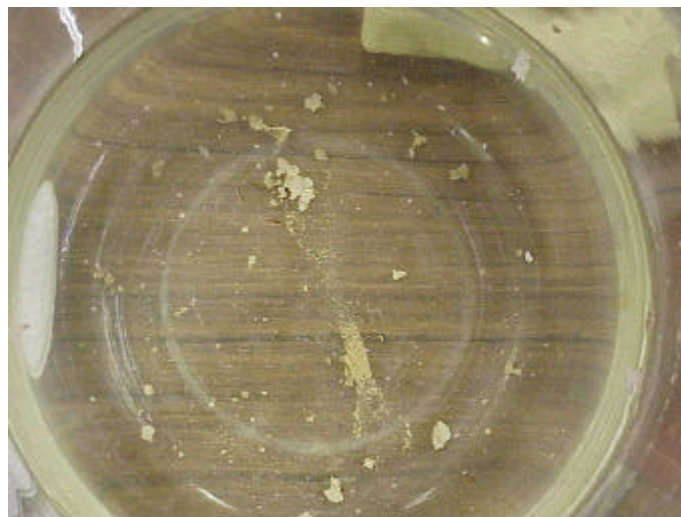


Figure 3-49. Coating debris remaining in the vessel following removal of the System 2 specimens



Figure 3-50. Overall view of some of the debris removed from the vessel used to soak the specimens



Figure 3-51. Detail of debris, 7X



Figure 3-52. Single debris blister, 20X

The debris which is formed during immersion of the irradiation-aged coating consists of thin blisters which form in the outermost layer of the topcoat (Figure 3-55), and then break free due to the buoyancy of the gas they contain. Therefore, the surface area of these blisters is significantly larger than the surface area of the coating from which they arise, due to the ductility of the wet coating (Figures 3-51 – 3-53).



Figure 3-53. Detail of the surface of the irradiation-aged immersion test specimen illustrating the extent of blister formation and detachment. Note the presence of pores in the topcoat remnant. Original magnification 7X.

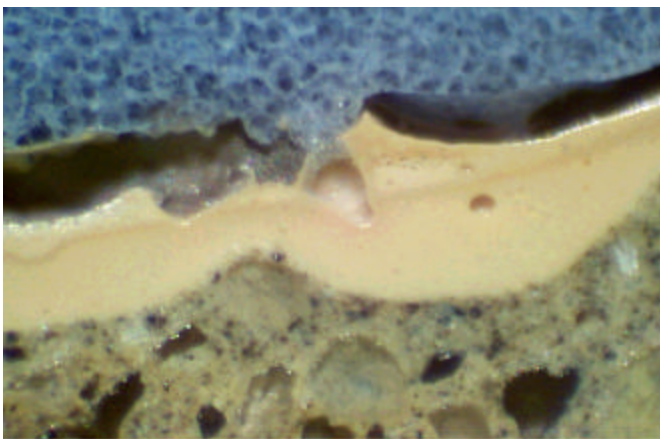


Figure 3-54. Cross-section of the surface of the irradiation-aged soak test specimen. Note the presence of pores in the topcoat remnant. Original magnification 45X.

The formation of blisters has been observed during immersion testing of coated specimens of both steel and concrete, and in every case, the blistering has been confined to the outermost layer of the topcoat. Therefore, water immersion testing was performed on free-film specimens of the topcoat and the underlying surfacer, in order to determine the origin of the gases responsible for the blistering. Observations made during free-film immersion testing (Figures 3-55 a – d) confirm that most or all of the gases which contribute to the formation of coating blisters, originate within the topcoat.



Figure 3-55a

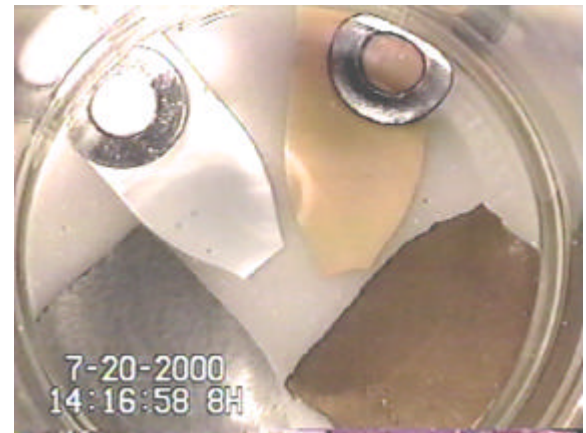


Figure 3-55b

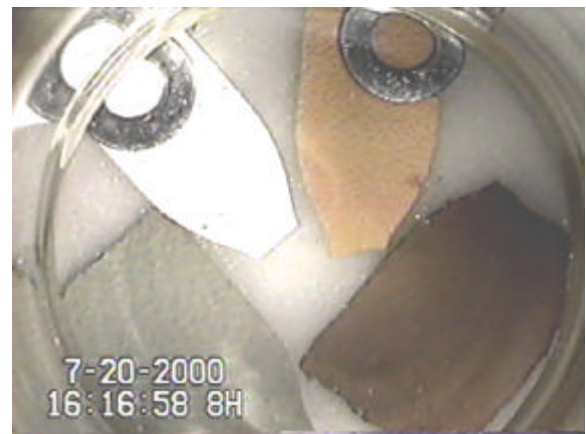


Figure 3-55c



Figure 3-55d

Figures 3-55 a-d. Effect of Temperature on Blister Development for Non-irradiated and Irradiated Phenoline[®] 305 and Starglaze[®] 2011S in Water Immersion. The top row in each photograph, left to right, is non-irradiated and irradiated Phenoline[®] 305. The bottom row, left to right, is non-irradiated and irradiated Starglaze[®] 2011S. The test was begun at room temperature. Figure 'a' shows the starting condition. Figure 'b' shows the results after a soak at 150°F for 2 hours. Figure 'c' shows the results after a soak at 175°F for an additional 2 hours. Figure 'd' shows the results minutes after the water temperature approached 200°F. (Note: Clock time is shown in the bottom-left of each photograph in the series.)

Debris Particle Size

Image analysis techniques may be used to characterize coating debris. Figures 3-50 through 3-52 show images of the System 2 coating debris at increasing magnification. Some of this debris was collected onto 20-micron filter paper for characterization of the larger particles. Particles smaller than approximately 0.1 cm in size were deliberately omitted in this analysis, due to limitations in optical imagery.

Medium magnification pictures were used to calculate the two-dimensional particle size (area) with the aid of Adobe Photoshop[®] software. Assuming circular particles, a diameter was calculated for each particle with a sample size of 100, using pixel count area. A frequency histogram of the resulting particle size diameters is shown in Figure 3-56. The most frequent particle diameter was 0.0099 cm (0.0039 in.) This frequency distribution was developed from a subjectively chosen subset of the available debris particles. Improved debris collection methods will be used in the future to provide the most representative sample of any debris developed.

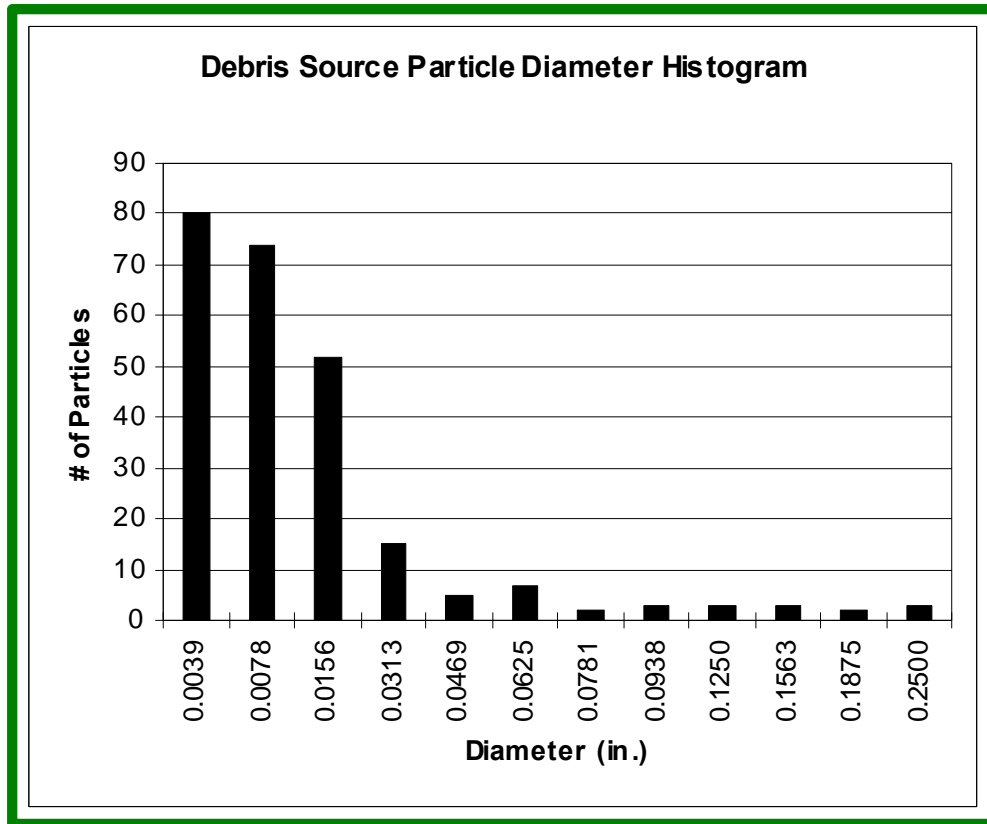


Figure 3-56. Frequency Histogram of Debris Size Distribution

It should be noted in interpretation and application of the results that extensive plasticity during the blistering process, before failure of the blisters, indicates a major surface area growth of the coating from the original size on the substrate, in conjunction with thinning of the coating as the blister disbonds from the substrate. This indicates that the debris source term analyzed will be calculated to be of greater area than the surface from which the coating was lost.

References for Table 3-1

1. Handbook of Chemistry and Physics, 64th Ed., p. E-5, CRC Press, 1983-1984.
2. ACI Manual of Concrete Practice, Part 3, p. 224.2R-3, ACI International, 1999.
3. T. Baumeister, et al., (Eds.), Mark’s Standard Handbook for Mechanical Engineers, 8th Ed., p. 4-63 (Table 3), McGraw Hill, 1978.
4. Concrete Manual – A water resources technical publication, 8th Ed. (revised), p. 18, 1981.
5. Concrete Manual – A water resources technical publication, 8th Ed. (revised), p. 27, 1981.
6. Concrete Manual – A water resources technical publication, 8th Ed. (revised), p. 30, 1981.
7. M. Fintel, Handbook of Concrete Engineering, 2nd Ed., p. 189, 1995.
8. H. Saechtling, International Plastics Handbook, p. 387, Hanser Publisher, 1983.

4.0 Summary and Significant Findings

4.1 Coating Research Program

The SRTC program consists of three major elements as shown in Figure 2-1 in Section 2 that are directed at determining performance of Service Level I coatings under DBA conditions. Measurements of coating mechanical and physical properties are made for input into analytical models in order to calculate coating deformations under environmental conditions. Predictions from analyses using the analytical models and the results from performance testing of coating specimens under simulated DBA conditions are used to arrive at insights into the potential for coating failure. This includes the degree of failure and the failed coating material characteristics (i.e., amount and size of coatings debris) for use in NRC's GSI-191, "PWR Sump Blockage" research program.

4.2 Performance of System 2 Coating

The results from the analyses and performance testing under DBA conditions of coating System 2 (Phenoline[®] 305 topcoat over Starglaze[®] 2011S surface on a concrete substrate), described in detail in section 3.2 and 3.3 of this report, are summarized below.

The results from the analyses and performance testing show that the performance of the System 2 coating depends upon:

- Aging Condition (Non-irradiated or irradiated)
- Defect Condition (Type, Size, Trapped Water)
- Temperature/Pressure Exposure Profile (Full DBA, Plant-Specific DBA, Water Immersion)

The performance of the System 2 coatings is discussed below using an outline format. The performance testing was laboratory tests using coated concrete block specimens, fabricated to include three conditions: non-defected; Type 1 defect that contains an intentional delamination or embedded non-bond area; and Type 2 defect that contains a hole through the coating to the substrate. These specimens, in non-aged and irradiation-aged conditions, were exposed to DBA profiles (ASTM D3911-95 or "full DBA", and other shortened DBA tests including a "plant-specific" DBA and water immersion) to determine their expected performance under the medium- to large-break loss-of-coolant accident.

I. Non-Aged Condition

The non-aged condition represents the properly applied and cured condition of the coating that has not been exposed to an aging environment that includes temperature, irradiation, and air with humidity for long exposure times. The non-aged condition of the properly applied and cured coating is the baseline condition.

A. Non-defected

Test results from the laboratory specimens exposed to either the ASTM D3911-95 DBA or the "plant-specific" DBA profile showed only minor cracking through the topcoat. A slight color change due to the DBA exposure was also observed. The results of the analysis using the computer model showed that tensile stresses were not sufficient to lead to major cracking of the topcoat, surfacer, or the concrete substrate as a result of mechanical stresses introduced in the coating. The observed minor cracking likely occurred at minor coating discontinuities and was beyond the scope of the analytical modeling. In addition, the non-defected specimen was exposed to a water immersion to temperatures up to 200°F for times up to 24+ hours. Neither color change nor physical damage was observed in the water immersion testing.

Summary: No cracking or delamination was predicted by analysis or observed by testing for the non-aged coating in the non-defected condition; therefore no coating debris is likely to form in a non-aged, non-defected System 2 coating under DBA exposure conditions.

B. Defect Type 1 (Embedded Non-Bond)

1. Without Trapped Water

No significant deformation to cause failure was predicted with analytical modeling of the "full DBA" test. Testing of laboratory specimens, however, showed cracking approximately half way around the circumference of 12 mm (0.47 inch) diameter Type 1 defects that did not have water deliberately injected into them. It is suggested that water may have entered the defect through the uncoated bottom of the concrete specimens and become trapped during the 2.8-hour phase in the DBA exposure, when the saturated steam is at 75 psia and prior to the cool-down. Trapped water in this size defect would cause cracking during the cool-down phase as predicted by the model (see paragraph I.B.2 below).

Summary and Significant Findings

2. With Trapped Water

The analysis results showed that a 12 mm diameter Type 1 defect would be subject to growth by cracking during the first cool-down from 307°F to 250°F in the ASTM D3911-95 DBA. Both cracking and delamination are predicted; however cracking precedes the delamination event. The DBA test results of a 12 mm Type 1 defect showed cracking at the predicted location. Although the coating cracked, no debris was created.

Analysis of a 0.125 inch diameter defect in an ASTM D3911-95 exposure showed that no cracking or delamination would occur. Testing of a specimen with a 0.125 diameter defect was not performed.

Summary: A non-aged System 2 coating containing Type 1 defects > 0.125 inch in diameter is subject to cracking under DBA exposure conditions; however it is not likely to form a debris.

C. Defect Type 2 (Hole in Coating)

No significant deformation leading to peel-back of the coating was predicted with analytical modeling in the DBA exposure. Testing of coated specimens in the ASTM D3911-95 DBA, the plant-specific DBA, and the water immersion showed no evidence of coating delamination or peel-back damage.

Summary: No coating debris is likely to form in a non-aged System 2 coating containing Type 2 defects under DBA exposure conditions.

II. Aged Condition

An “aged” coating is defined as a coating which has been properly applied and cured, and has been exposed to an aging environment that includes temperature, irradiation, and air with humidity. The findings in this section are based on the results of specimens that have been irradiated to 10⁹ rads per ASTM D4082-95, that is, no additional thermal or simulated service aging treatment was applied to the test specimens.

The irradiation of System 2 test specimens to 10⁹ rads per ASTM D4082-95 caused a color change from the as-prepared condition. This marked color change occurred in the first 1-2 mils of the topcoat.

The findings for aged coatings are based on the measured performance tests only.

A. Non-defected

The test results from the “plant-specific” DBA, a plant-specific rapid transient pressure/temperature exposure (with the temperature of the saturated steam approximately 200°F), and from water immersion (with the water temperature of approximately 200°F), showed the entire near-surface region (1-2 mil depth) of the topcoat will severely blister. Failure (disbondment) of the near-surface region did occur and a debris source term was formed. In the full DBA test, however, neither significant blistering nor a debris source was observed.

B. Defect Type 1 (Embedded Non-bond)

Disbondment of the near-surface layer of the topcoat, as described in A above, was observed during plant-specific LOCA and immersion testing of coatings with intentional defects. The following describes the performance of the aged coatings as a consequence of the presence of these intentional defects, only.

1. Without Trapped Water

No significant deformation to cause failure was predicted with analytical modeling of the “full DBA” test, or observed during DBA-LOCA testing.

2. With Trapped Water

The analysis results showed that a 12 mm diameter Type 1 defect would be subject to growth by cracking during the first cool-down from 307°F to 250°F in the ASTM D3911-95 DBA, similar to the prediction for the non-aged coating. Analysis of a 0.125 inch diameter defect in an ASTM D3911-95 exposure showed that no cracking or delamination would occur. No DBA-LOCA testing with trapped water was performed to confirm the model predictions.

C. Defect Type 2 (Hole in Coating)

Testing of coated block specimens showed no evidence of coating delamination or peel-back damage.

4.3 Summary of Major Findings for System 2 Performance

1. No failure of a non-aged, non-defected System 2 coating, which would lead to the formation of a debris source term, is expected to occur under ASTM D3911-95 “full DBA” simulation.
2. The presence of a large (greater than 1/8”) diameter embedded coating defect may result in local cracking of the coating during the rapid cool-down portion of the DBA event (e.g., quench from 307°F to 250°F of ASTM D3911-95 PWR profile). The driving mechanism is the vapor pressure loading of the blister caused by a hot substrate and relatively cooler ambient conditions. No coating debris is likely to form as a result of this coating cracking.
3. System 2 coatings that have been aged (irradiated to 10^9 rad per ASTM D4082-95) have shown the formation of a debris source term in both “plant-specific” DBA conditions and high temperature water immersion conditions, at temperatures near 200°F. The debris forms as a result of blistering that tears away a near-surface region (< 2 mils) of the topcoat. Rapid heat-up and hold to temperatures near 300°F (per ASTM D3911-95) did not cause a debris source.

This page left blank intentionally.

5.0 Future Activities

Understanding the Potential for Debris Formation from Aged NPP Containment Coatings Exposed to Medium-to-Large Break LOCA Conditions

5.1 General Conclusions

The performance testing results in this report clearly show that debris can form in coating systems used in NPP containment under certain conditions. Debris formation is observed in coatings that are irradiated to the present ASTM standard for conditioning (i.e., ASTM D4082-95) and are subsequently exposed to either steam or water immersion temperature-time profiles that are estimated to be relevant to medium-to-large break LOCAs. The debris is caused by disbondment of a portion of the top layer of the coating system that is degraded as a result of irradiation in air. The debris formation is dependent on both the specific conditioning or aging treatment and the simulated LOCA exposure conditions.

Specifically, debris formation was observed in the near-surface (approximately top 2 mils) region of an epoxy-phenolic (Phenoline[®] 305) that was on a System 2 (Phenoline[®] 305 topcoat over Starglaze[®] 2011S surfacer on concrete) coating specimen irradiated to 1×10^9 rads at 1×10^6 rads/hour in air at 120°F. Under high temperature water immersion (at approximately 200°F) or “plant-specific” DBA-LOCA steam profiles (see Section 3 of this report), the near-surface region blistered and lifted off the topcoat. Video records show that the blistering was driven by gas evolution in the near-surface region.

Debris formation has also been observed in other coatings investigated in the program. Factors that would affect the potential for debris formation in a coating and debris characteristics that could potentially impact sump performance have been suggested following the NRC public meeting in September 2000. These have been categorized into five areas of investigation below.

5.2 Factors Affecting Potential for Debris Formation in NPP Containment Coating

The following sections contain factors that would affect the potential for debris formation. The results in the coating research program to-date suggest that the debris formation is caused by gas evolution in an

oxygen-affected region of the topcoat. The mechanism causing the blistering and liftoff of the near-surface layer of the irradiated topcoat material has not been fully explained. The mechanism appears to involve gas from the near-surface layer agglomerating and forming bubbles that load and deform the near-surface layer material. This occurs in a “temperature window” due to two basic processes. The first process is gas agglomeration with bubble development that is temperature dependent. The second process is the softening of the material that is both temperature and wetness dependent. Below approximately 150°F, the bubble formation is slow and the material is stiff. Above temperatures of approximately 200+°F, the material is softened to the extent that the gas bubbles will pop through the material leaving pores but not causing blisters. At temperatures around 200°F, the gas bubbles coalesce in the softened, oxygen-affected region of the topcoat, forming blisters, which may detach as debris.

The factors are categorized into areas of investigation. The specific activities, including tests and test matrices, have not been fully developed, as yet. Tests at several conditions have been initiated in the coatings research program. The ultimate objective is to predict, with confidence, the conditions under which debris would form and the resulting debris characteristics.

5.2.1 Coating Characteristics

The structure of the coating will affect its susceptibility to radiation damage and oxidation. Two general factors are in this category:

- Coating Type (e.g., epoxy, epoxy-phenolic)
- Coating Formulation (specific vendor formulation)

5.2.2 Combined Effects of Aging Conditions

Aging includes the effects of several degradation mechanisms, primarily radiation and oxidation, over time. These mechanisms can act synergistically to make a coating susceptible to debris formation. The factors related to these degradation mechanisms are the following:

- Irradiation Dose
- Irradiation Dose Rate (Irradiation History)
- Irradiation Type (α , β , γ)
- Energy Spectrum
- Oxidation Conditions (e.g., Moist Air)
- Temperature History

The first four factors would affect the radiation damage of a coating. The last two factors would affect the oxidation damage of the coating. It is envisioned that radiation and oxidation damage can act synergistically to promote susceptibility to debris formation.

5.2.3 Combined Effects of LOCA Exposure Conditions

The development of blisters, a precursor to the formation of debris, is dependent on the evolution of gases and the softening of the coating. There appears to be a “temperature window” in which blisters form—at low temperatures, the gases do not evolve and/or the coating is too stiff; at too high temperatures, the gas escapes by pore formation in the coating. Wetness further exacerbates the softening of the coating. The following two conditions in simulated LOCA events are therefore factors in promoting potential debris formation:

- Steam Temperature/Pressure – Time Profile
- Water Immersion Temperature – Time Profile

5.2.4 Debris Formation Mechanism

The blisters from which the debris is formed are driven by gas generation. The following factors need to be investigated to characterize this gas source and blister development leading to debris generation:

- Gas Sources in Aged Coatings
- Gas Generation in Coating Under Temperature and Wetness Conditions

- Blister Development- Kinetics of Pressurization and Blister Formation

5.2.5 Debris Characteristics

Debris that has left the surface of the coating is available for transport. Several factors are important to evaluate the transport of the debris:

- Total Amount of Debris per unit Initial Surface Area of Coating
- Size Distribution
- Degree of “Stickiness”
- Float Characteristics (Dependent on size, density, and shape of debris)

These areas of investigation will be further developed in the SRTC program. Several tests to provide additional information are in progress and will be completed in CY00.

5.3 Additional Consideration of Factors Affecting NPP Containment Coating Performance

All samples irradiated to date in this program have been irradiated per ASTM D4082-95. Some initial samples were exposed to slightly lower cumulative dose levels, due to the amount of time required to achieve a full 1×10^9 rad dose and to obtain early insights. In all cases, damage due to radiation has thus far been limited to color changes and slight checking, with most of the damage being observed in the immediate surface of the coating and not completely throughout the bulk of the material. This is as expected, and is attributed primarily to the limited diffusion depth and availability of oxygen into the coating that can react with free radicals formed from the radiation-induced structural changes. This is also typical of materials irradiated at high dose rates (1×10^6 rad/hr) in relatively short periods of time (compared to actual service life), especially for materials of relatively low oxygen permeability.

There are significant limitations of conventional accelerated-aging methodologies, particularly for radiation exposure at much higher dose rates than anticipated in actual service. These limitations include:

- Diffusion-limited oxidation
- Dose-rate effects (chain scission vs. cross-linking)
- Synergistic effects of long-term oxidation, temperature, moisture, chemicals, etc.
- Variation in thermal transitions

Such effects are known to cause significant variation in performance and properties of materials such as thermoplastics (particularly polyolefins) and elastomers, which are more permeable by oxygen and moisture. The time to reach a particular level of degradation or degree of property change (e.g., 50% reduction in elongation) can be significantly less for such materials irradiated at lower dose rates than for the same material exposed at higher dose rates to the same cumulative dose. In fact in some cases, the effect is also observed to be worse at lower temperatures than higher temperatures due to a “self-healing” effect which occurs. In some polyolefin-based electrical cable insulation materials, samples exposed to the same total dose at varying dose rates and at higher temperatures exhibited less reduction in properties because the temperature was high enough to induce cross-linking. This is believed to somewhat offset the amount of chain scission induced by the radiation. Because this is a well-known phenomenon for other polymers, and due to the fact that existing commercial nuclear power plants may be required to be qualified for life extension of up to 60 years, the effects of long-term oxidation and low-level radiation are of interest. In fact, the only true measure of a coating’s DBA performance and subsequent debris generation (if any) is to expose or “requalify” under

DBA conditions a coating that has been in service for 15, 20, even 25 years. Although such effects are not expected to be catastrophic, this aspect of protective coatings in nuclear power plants has not been investigated. Radiation exposure, DBA exposure, and characterization of recently-applied coatings, regardless of formulation, is of limited value in understanding and predicting actual long-term performance and DBA response of older, in-service coatings.

For this reason, SRTC, the industry PIRT panel, and the NRC customer have worked to obtain several samples of coated substrate (primarily steel) and/or coating debris from nuclear power plants for such investigation. Specifically, samples have been received from the San Onofre Nuclear Generating Station (SONGS, Unit 3), Oconee Nuclear, Trojan Nuclear, and Braidwood, Unit 2 power plants. Additional samples have been requested from Maine Yankee. Of these, the Trojan Nuclear samples are considered to best represent the coating formulations identified by the PIRT panel as generic coating Systems 1 and 2, the most dominant and widely-used Service Level 1 coating systems in PWR power plants. These samples will be fully characterized in both the as-received (service-aged) condition as well as following both radiation (at varying dose rates and possibly temperatures) and DBA exposure.

Characterization is expected to include: FT-IR analysis for structural/compositional changes, SEM for morphology and porosity changes, adhesion/G-value mechanical testing, optical microscopy, thermal property analysis such as TGA and DSC, as well as visual examination and image analysis of debris, if generated. As some if not most of these samples are considered to be radiologically contaminated or potentially contaminated, appropriate protocols and procedures will be followed for sample handling, analysis, and waste disposal as necessary.

This page left blank intentionally.

Appendix A Mechanical Testing Description

Mechanical properties are key inputs to the coatings failure model. The mechanical properties of interest in the coatings program are adhesion, adhesion G-value, tensile strength, elastic (Young's) modulus and cohesion. Adhesion is the measure of the load or strength (load divided by the load bearing area) to separate a coating from its underlying layer or substrate. The adhesion G-value is the designation given in the coating failure model for the resistance to the separation of the coating layer from an underlying layer or substrate. The adhesion G-value may be considered the fracture toughness of the interface at which separation occurs. The tensile strength is the standard material science property of the maximum load on a specimen divided by the area bearing the load. In the coatings program the tensile strength is measured in the so-called free-film coating specimen. The free film is simply the cured coating that has been removed from a very weakly adherent substrate, such as polyethylene sheet. The elastic or Young's modulus can be measured from the load-elongation curve of the free-film specimen. It is assumed that the coating material is isotropic in these properties.

Cohesion is used here to designate the resistance to tearing of the free film. The cohesion test specimen is similar to the tensile test specimen except that it contains a notch or slit in its edge to initiate the tearing. The tests to obtain these properties were performed on an Instron universal (i.e., capable of both compression and tensile testing) testing machine (model 4507) equipped with an oven for elevated temperature testing. This appendix describes the methods developed for performing the tests.

A.1 Adhesion and Adhesion G-value Tests

The adhesion and adhesion G-value tests were developed from two American Society for Testing and Materials standard test methods. These are D5179-98 "Standard Test Method for Measuring Adhesion of Organic Coatings to Plastic Substrates by Direct Tensile Testing" and D4541-95 "Standard Test Method for Pull-Off Strength of Coatings Using Portable Adhesion Testers." These methods use a stud or puller affixed to a coating by an adhesive that is then pulled normal to the surface by a tensile machine in the former method or a manually operated apparatus in the latter. Figure A-1 shows one puller affixed to a test specimen and three pullers as they appear after testing. The pullers are 1.4 in. high and 12 mm (0.472 in.) in diameter; their design was adapted from that given in D5179-98. The total displacement of the puller normal to the coating surface between initial loading and separation of the puller from the specimen is of the order of a few thousandths of an inch. Such small displacements are not accurately measurable with the simple recording of the displacement of the Instron's moving crosshead. This is so

because the movement in taking up slack in the linkages of the gripping system, such as in the universal couplings that ensure loading in a direction normal to the specimen, is of the same magnitude as the displacements encountered in pulling the thin coatings to failure.

In these tests the displacement of the puller was measured with a single-arm extensometer that was mounted to contact the top of the puller. The extensometer was a Materials Testing Systems model number 632-06B-20 with a full-scale range of ± 0.160 in. and capable of operating to 300°F.

The upper grip for the pullers (design adapted from ASTM D5179-98 also) was machined with a pocket to accommodate the extensometer arm (Figure A-2). The upper grip was rigidly attached to a pull rod that was connected through a universal joint to a 200-lb load cell mounted in the Instron's fixed, upper crosshead. The lower grip held the 2-in. by 2-in. by 4-in. blocks and was connected rigidly to the Instron's moving crosshead. Threaded couplings with backing nuts were used to make rigid the connections between the upper pull rod and the upper grip and between the lower pull rod and the lower grip (Figure A-3). Two flexible couplings remained in the load chain: the universal joint through which the upper pull rod is connected to the Instron's load cell and the connection between the upper grip and the stud. These allow necessary motion for alignment, yet they require little force (compared to the load supported by the coating) to "set" themselves. A plumb bob was used to position the puller on the load axis. These steps ensure that the puller is pulled normally to the coupon (Figure A-4). The lower grip was equipped with a rectangular metal pan that was filled with water to keep a test specimen wetted when experimental conditions demanded.



Figure A-1. Aluminum pullers as they appear affixed to a test coupon with epoxy adhesive, and after testing

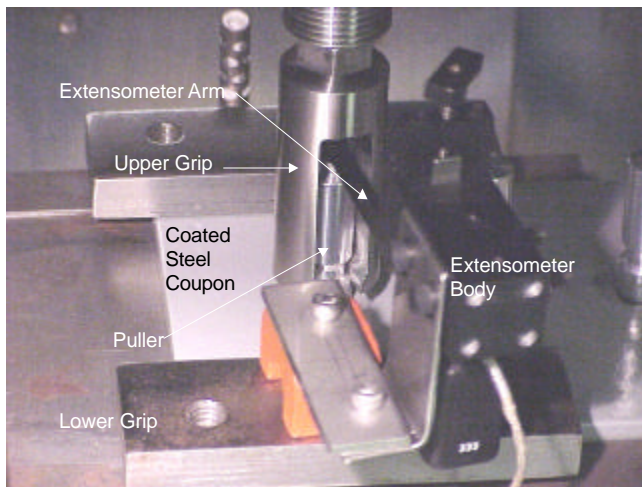


Figure A-2. Extensometer and grip for aluminum puller

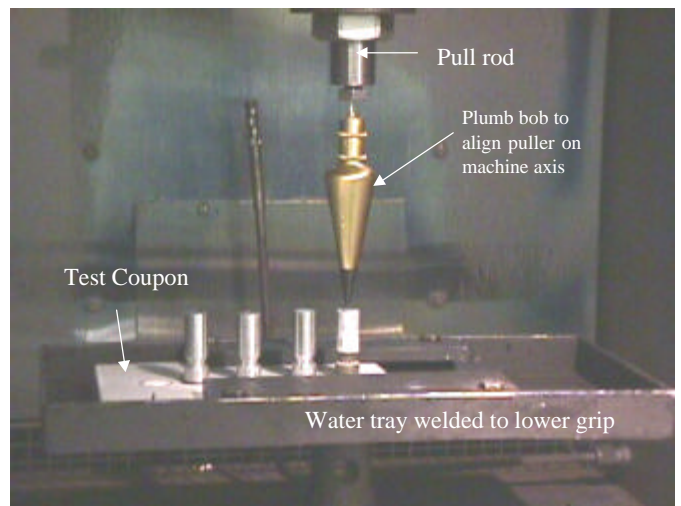


Figure A-4. Plumb bob arrangement to locate center of puller on Instron load axis

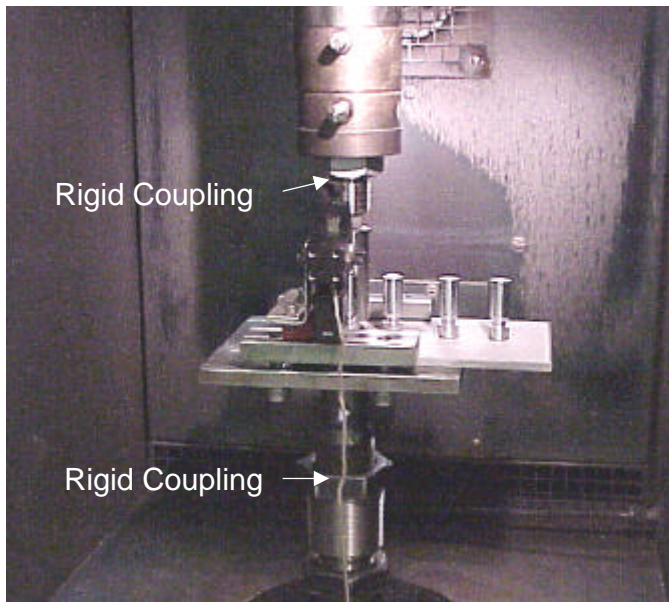


Figure A-3. Rigid coupling of upper and lower grips to Instron

Aluminum pullers, 12 mm in diameter, were used for both the adhesion test and the adhesion G-value test. They were affixed to the test specimens by Cotronics 4525 high-temperature (500°F) epoxy (Cotronics Corp., Brooklyn, New York). This epoxy cures at room temperature in 16 hours.

The concept of the adhesion G-value test is shown in Figure A-5. As the puller is displaced from the coupon surface the zero-adhesion (so-called type 1) defect propagates radially until failure. The zero adhesion defect is created by installing a glass disk on the substrate prior to the application of the coating(s). Half-inch diameter holes are cut in a stainless steel mask. The mask is placed in careful alignment on a clean, blasted concrete coupon, and used to position the glass disks. The prepared coupon is then coated with surfacer and topcoat. The same mask is used to guide the attachment of the pullers. Figures A-6 through A-8 illustrate the steps in the preparation of the concrete blocks.

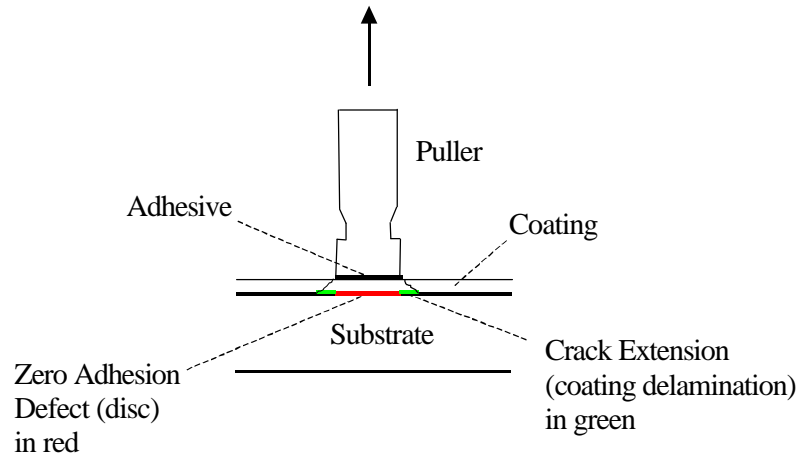


Figure A-5. Schematic diagram of the adhesion G-value test



Figure A-6. Light gritblasting of concrete blocks to prepare them for application of surfacer



Figure A-8. Mask used to position 12 mm diameter glass disks prior to application of surfacer



Figure A-7. Appearance of concrete blocks before (right) and after (left) preparation of surface

A.2 Tensile Test

The tensile test employed so-called dogbone-shaped flat specimens that were cut from cured coating applied to a polyethylene sheet or that were molded on the sheet by spraying coating through a mask.

The molded specimens were 4.5 inches in length overall with a 1.5-in.-long by 0.25-in.-wide gage section (Figure A-9). Specimens were pulled to failure at a crosshead speed of 0.02 in. per minute.

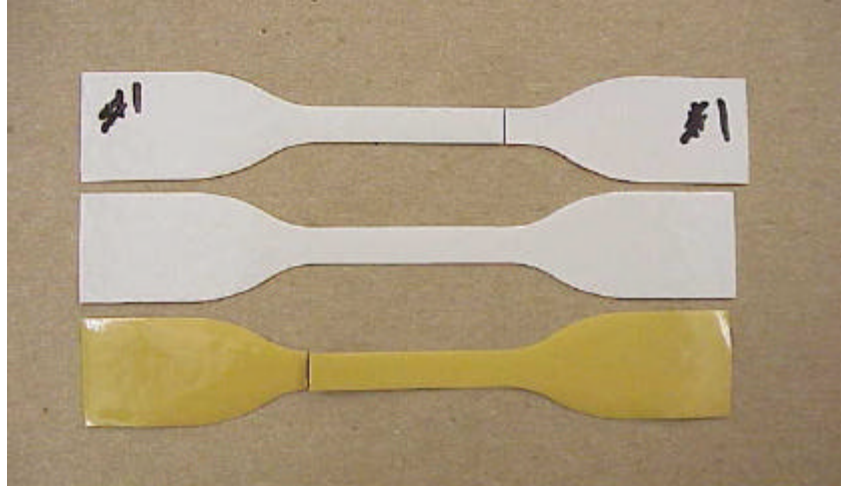


Figure A-9. Tensile specimens of Phenoline 3050, as cured (above) and irradiated and tested to failure (below). Note minor changes in specimen length observed as a consequence of test conditions.



Figure A-10. Starglaze 2011S surfacer tensile test specimens: as cured, top; irradiated, bottom

The specimens were securely held in knurled grips designed for relatively soft materials (Figure A-11).



Figure A-11. Tensile specimen fixed in knurled grips

This page left blank intentionally.

Appendix B Irradiation Aging of Protective Coatings

Many protective coatings based on thermosetting, highly cross-linked resins such as epoxies, epoxy-phenolics, and polyurethanes have been shown to be quite resistant to gamma radiation to this cumulative dose level. Although thermally very stable, straight, unmodified phenolic coatings have been shown to be somewhat less resistant to gamma radiation and show evidence of degradation at levels as low as 1×10^8 Rads for some materials. For this reason as well as to improve toughness and durability, phenolic resins are typically either reinforced or modified with other resins (mostly epoxies).

Due to the range of variation in polymer processing, compound additives, specific formulations, curing agents, etc., radiation exposure testing is often necessary in order to evaluate the radiation resistance of a particular material or specific compound. In addition, it is often desirable to irradiate an intact component as would be installed in the actual application, rather than simply exposing a test sample.

Although there are limitations to the applicability of short-term, high dose-rate radiation exposure methods to predicting long-term performance, this is often the only rapid and cost-effective way to evaluate radiation effects upon critical properties. In some cases, exposure to a range of dose levels and rates can be used to develop an accelerated aging profile for a particular material to predict longer-term performance. This principle is known as superposition and has been applied to many materials qualified for long-term service in high radiation environments such as gaskets and electrical cable insulation.

The actual absorbed dose of a material depends upon its density and basic elemental composition, as well as mass absorption coefficients and other energy absorption

properties. For most polymeric materials, including thermosetting polymers and protective coatings based thereon, the absorbed dose in Rads is assumed to be comparable to the energy of the radiation field applied. As the majority of polymers consist mainly of hydrogen and carbon, the mass absorption is generally comparable to that of water unless specifically measured.

There are two sources available for irradiation exposure. One is a Gammacell 220 (Figure B-1) with a current dose rate of 2.32×10^4 R/hr. The second source is a J.L.Shepherd Model 109 Irradiator, with a current dose rate of 1.27×10^6 R/hr. Both of these are gamma irradiators with Co-60 as the isotope. The chamber size of both sources is 6" diameter by 7.5" high. Auxiliary systems to raise or lower ambient temp and to introduce air or gas or chemicals to the system can be added.

Accelerated-aging of protective coatings has historically been performed per ASTM D4082, "Standard Test Method for Effects of Gamma Radiation on Coatings for Use in Light-Water Nuclear Power Plants". The technical basis for this test method is that the cumulative exposure dose shall be 1×10^9 Rads, and the dose rate shall be controlled at 1×10^6 R/hr or higher. The field shall be uniform to within 10% between any two locations in the sample. The 1×10^9 Rad total dose is historically based on a projected 40-year service life and includes the radiation exposure during a design basis accident (DBA). The high gamma dose was also intended to exceed plant life gamma dose to also account for possible beta exposure as well. In addition, the temperature shall not exceed 140°F (60°C) during sample irradiation due to known synergistic effects of temperature and radiation. Following exposure, samples are examined per other ASTM standards to evaluate coating performance and presence of defects such as chalking, checking, cracking, blistering, flaking, peeling, and/or delamination.



Figure B-1. GammaCell 220

Appendix C Application of Finite Element and Fracture Mechanics Analyses in Predicting Failure of NPP Coatings

C.1 Overview

The NPP protective coating systems in general consist of multiple layers with various thickness and different properties which may be functions of environmental variables such as the temperature and wetness. The coating systems may be subjected to wide range of time-dependent loading conditions under the LOCA events. Initial defects may be postulated to exist in the coating system as a standard fracture mechanics procedure to determine the failure mechanisms.

The finite element method is considered an efficient analysis tool when many variables and scenarios are involved. There are three fundamental categories of inputs to the models:

1. Configuration - includes initial defect size, location of defect in the coating system, number of coatings and coating thickness, and type of substrate onto which coating is applied
2. Material Property – includes mechanical (modulus of elasticity or Young’s modulus, adhesion energy, etc.) and physical (coefficient of thermal expansion, coefficient of thermal conductivity, etc.) properties or attributes of the coating layers and substrate materials
3. Loading – includes both direct loads (e.g., impingement of water) and environmental conditions that lead to coating stresses (e.g., thermal exposure leading to differential thermal expansion stresses)

The coating stress, strain, and the driving force leading to a defect growth will be calculated. With appropriate material failure criteria, the coating failure may be predicted and the conditions causing failure may be identified.

C.2 Finite Element Model Description

The finite element model used for most of the calculations contains 6210 rectangular elements and 6811 user-defined nodes. Heat transfer elements were used in the thermal transient analysis and continuum elements were used for the thermal stress analysis. The continuum elements can be either plane strain or axisymmetric, depending on the geometric characteristics of the problem. Only one-half of the analysis domain is modeled because of symmetry (with respect to the centerline or center-plane of the defect).

This model is capable of analyzing an intact three-layered coating system (topcoat, primer, and substrate), a defect at the topcoat-primer interface, a defect at the primer-substrate interface defect, or an intra-primer defect. There

are 10 elements through the topcoat thickness and 16 through the primer. Coarser mesh was used in the substrate region except for the area adjacent to the primer for better transition. The mesh is refined greatly for the defect driving force calculation in the region where the postulated defect edge is located. The width of the model is typically about 6 times the size of a postulated defect and is divided into 138 elements with various sizes. The ABAQUS [1] finite element program was used.

C.3 Solution Steps

The coating system under the LOCA experiences temperature excursions. Because the different materials are used for the topcoat, primer, and the substrate, the mechanical property and thermal expansion mismatch will cause stress to develop in and between the layers. No external forces acting on the coating surface were considered throughout the present analyses. The thermal transient and stress analyses are uncoupled.

To achieve the coating failure prediction, a fracture mechanics approach was adopted. Several defect sizes were separately postulated in the coating system and modeled by the finite element method. The defect may be subject to vapor pressure loading in some cases due to the entrapped moisture at elevated temperature. This procedure allows the failure condition be established as a function of the defect size. As a result, a threshold defect size or a critical condition to cause failure may be determined.

The calculation steps are listed below:

1. Thermal Analysis: Only conduction was considered in the current analysis. The temperature boundary condition was prescribed. Thermal transient analysis was performed based on the time-dependent ambient temperature profile, such as that given in ASTM D3911-95 DBA for PWRs. The physical properties input to the analysis are thermal conductivity, mass density, and specific heat. The properties may be temperature and radiation dependent. The temperature distribution was calculated in the finite element region.
2. Stress Analysis: A mesh identical to that of the thermal analysis was used. Only the finite elements were changed to the continuum type. The nodal temperatures obtained in Step 1 were directly input to the stress analysis model. Linear elastic analysis was performed in this preliminary assessment. The mechanical properties required for this calculation are the Young’s modulus (modulus of elasticity), Poisson’s ratio, and coefficient of thermal expansion. These properties also

may be temperature and radiation dependent. The nodal displacement, element stress and strain are calculated. The defect growth driving force, or the adhesion G-value, is calculated with the J-integral [2] method in the ABAQUS [1] program. The finite element mesh was designed to allow five contour integrals to be assessed near the edge of the defect. The first contour, at the tip of the defect, is normally ignored due to inaccuracy. When moisture is postulated to be trapped inside the defect, a vapor loading condition may occur when the temperature is above the boiling temperature. In this case, the moisture temperature is assumed to be the substrate temperature directly underneath the defect. The corresponding saturated vapor pressure was obtained from the thermodynamic properties of steam [3]. The pressure differential between the external environment and the vapor gives a net pressure acting on the defect. When the pressure in the external environment is greater than or equal to the vapor pressure generated inside the defect, the pressure loading is zero. This vapor pressure loading condition is also time dependent.

3. With the changing temperature profile in the coating system and the possible vapor pressure loading within the defect, stress will develop in the coating system. In general, the coefficient of thermal expansion of the coating materials is several times higher than the substrate (e.g., coefficients of thermal expansion for the steel substrate is about 1×10^{-5} m/m/°C and for the coating material is about 20×10^{-5} m/m/°C). This implies that the substrate temperature must be many times higher than that in the coating in order to negate the temperature-induced strain mismatch on the interface. This condition is very difficult to achieve because the coating materials normally are good thermal insulators (e.g., thermal conductivity for the steel is $43 \text{ W/m}\cdot\text{°C}$, while for the coating material is less than $1 \text{ W/m}\cdot\text{°C}$), unless the coating is subject to a cool-down and the substrate remains sufficiently hot. The resulting stresses and strains will be output for assessment against the failure criteria.
4. The G-value due to the applied load (in the present case, temperature variation and pressure loading), denoted by G_{applied} , will be calculated at the edge of the defect by the CONTOUR INTEGRAL option in the ABAQUS finite element code [1]. In traditional fracture mechanics, this quantity is named the energy release rate, the crack driving force, or the J-integral; in the rubber or polymeric industry, it is termed the tearing

energy of the material. Physically, it is the force to extend the defect by a unit length, or the energy available per unit width to extend the defect by a unit length. The G_{applied} obtained in the stress analysis is also time dependent. The value of G_{applied} can be compared to G_{material} (the material resistance to defect growth) obtained from testing of the coating materials, to determine if a defect grows in size.

C.4 Defect Modes and Failure Criteria

Two failure modes may be postulated, based on observations of irradiated and DBA tested coatings. These are termed Mode 1 and Mode 2.

I. Mode 1 Failure – Blistering followed by delamination and cracking

Figure C-1 shows an initial defect in the coating system. It can be an interfacial or intra-layer crack. Due to thermal expansion mismatch (leading to buckling) or vapor pressure loading, a blister may form. As the deformation progresses, the defect may grow in a self-similar manner, a delamination failure may occur but the blistering material remains adhered to the coating system. However, if the ultimate stress (σ_{ult}) or the failure strain (ϵ_f) is exceeded in the blistering/delaminating material, this defect will rupture, as depicted in Figure C-2. A local finite element mesh representing the deformation of a Mode 1 defect is shown in Figure C-3. Therefore, two competing failure mechanisms may exist:

1. If $G_{\text{applied}} \geq G_{\text{material}}$ is met but $\epsilon_{\text{applied}} \leq \epsilon_f$ and $\sigma_{\text{applied}} \leq \sigma_{\text{ult}}$, the defect delaminates to form a larger defect in a self-similar manner. The $\epsilon_{\text{applied}}$ and σ_{applied} represent the strain and stress due to the applied load, respectively.
2. If $\epsilon_{\text{applied}} \geq \epsilon_f$ or $\sigma_{\text{applied}} \geq \sigma_{\text{ult}}$, the defect should rupture at the location where the criterion is met.

When the Mode 1 defect is considered, axisymmetric finite elements are used in the calculation. Because the topcoat provides good thermal insulation, the temperature variation through the thickness of the coating system would be significant. Thermal transient analysis should be performed to obtain the temperature profile, which is then input to the subsequent stress analysis to determine the deformation and stress states of the defect.

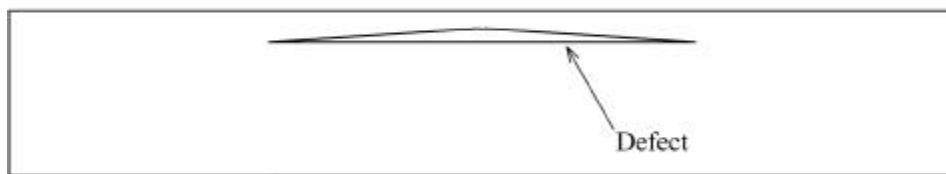


Figure C-1. Initial Mode 1 Defect

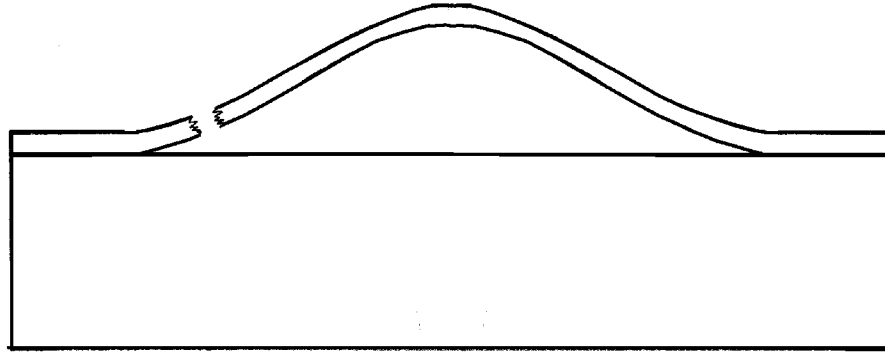


Figure C-2. Mode 1 Coating Failure

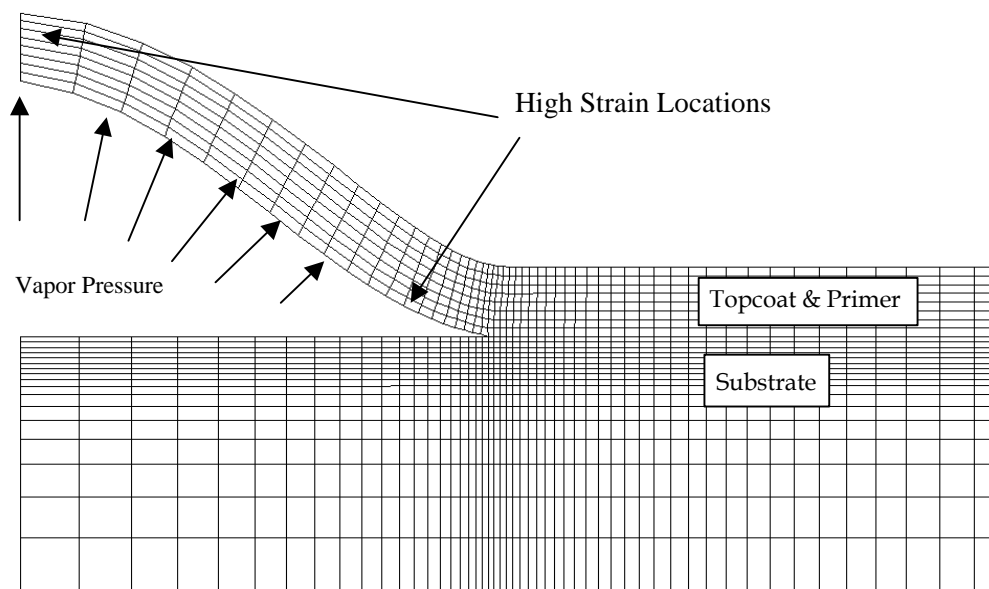


Figure C-3. Blistering due to buckling and/or vapor pressure loading

II. Mode 2 Failure – Cracking followed by delamination

A scratch-like crack penetrates through the topcoat to the primer or the substrate is assumed to exist. The main defect within the coating layer is perpendicular to this through-coating crack and is parallel to the coating layers (Figure C-4). Under the conditions of temperature

variation and thermal expansion mismatch, this defect may peel back and the defect may grow when $G_{\text{applied}} \geq G_{\text{material}}$. Eventually it will fall off the NPP containment wall when the condition $\epsilon_{\text{applied}} \geq \epsilon_f$ or $\sigma_{\text{applied}} \geq \sigma_{\text{ult}}$ is met. A deformed shape near the peel-back defect calculated by the finite element method is shown in Figure C-5.

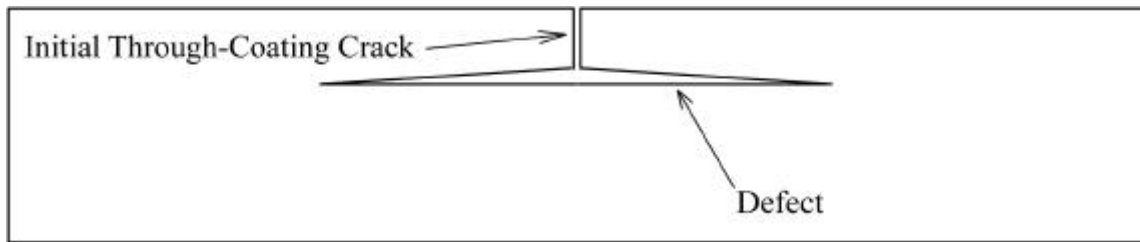


Figure C-4. Model for Mode 2 Coating Defect Analysis

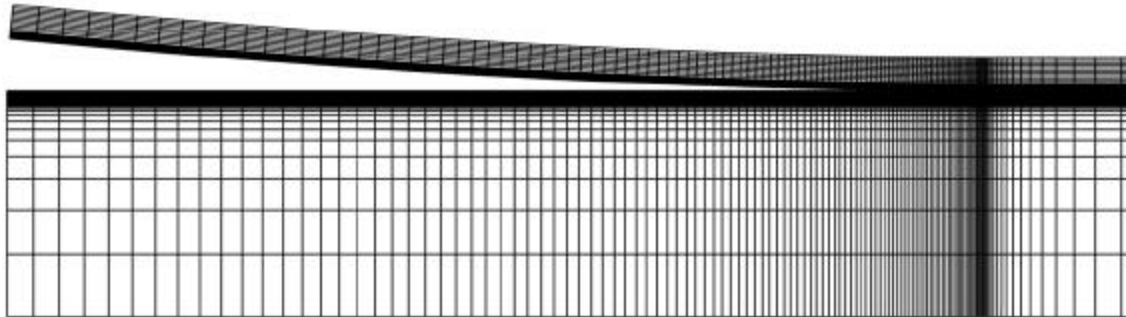


Figure C-5. Peel-Back due to thermal expansion mismatch ($\alpha_{\text{topcoat}} < \alpha_{\text{primer}}$)

Because of the initial, through-coating crack, the ambient temperature is short-circuited to the sublayer(s) which may have high thermal conductivity. This phenomenon is especially pronounced in the case of IOZ primer which is a zinc-rich layer and may have even higher thermal conductivity than that of the steel substrate. Therefore, a uniform temperature is quickly reached throughout the entire coating system. As a result, thermal transient analysis is not needed to establish the temperature distribution through the coating thickness. The deformation (peel-back) and stresses are caused by the temperature differential and thermal expansion mismatch. Two-dimensional plane strain elements were used for the Mode 2 defect analysis.

C.5 References

1. ABAQUS/STANDARD, Version 5.8, Hibbitt, Karlsson & Sorensen, Inc., Pawtucket, Rhode Island, 1999.
2. Rice, J. R., "A Path Independent Integral and the Approximate Analysis of Strain Concentration by Notches and Cracks," *Journal of Applied Mechanics*, Vol. 35, pp. 379-386, 1968.
3. Keenan, J. H. and Keyes, F. G., *THERMODYNAMIC PROPERTIES OF STEAM INCLUDING DATA FOR THE LIQUID AND SOLID PHASES*, First Edition, John Wiley & Sons, New York, 1936.

Appendix D Test Apparatus Descriptions

The SRTC coatings performance evaluation system (Figures D-1, 2, and 3) is used to examine the performance of NPP coatings in conditions simulating those expected to exist in a DBA LOCA. Figure D-3 shows a test specimen

being placed into the coatings performance evaluation system. It is currently being used to simulate DBA conditions specified in ASTM D3911-95 (Figure D-4).



Figure D-1. SRTC Coatings Performance Evaluation System. Insulated environmental test chamber is shown on the left, the 10 gallon steam generator is on the right.



Figure D-2. Overall view of the heater control console and the video monitoring and data acquisition systems for the SRTC Coatings Performance Evaluation System

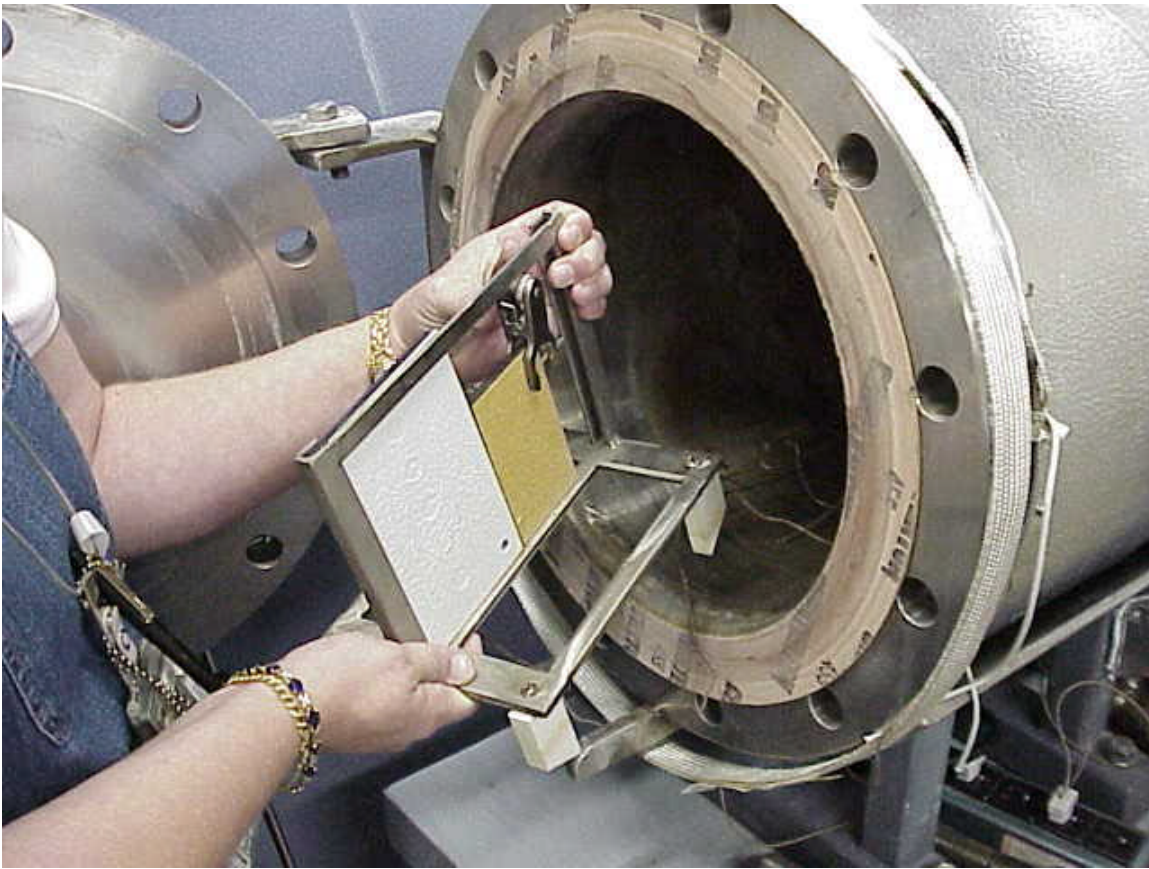


Figure D-3. Test Specimen being placed into the Coatings Performance Evaluation System

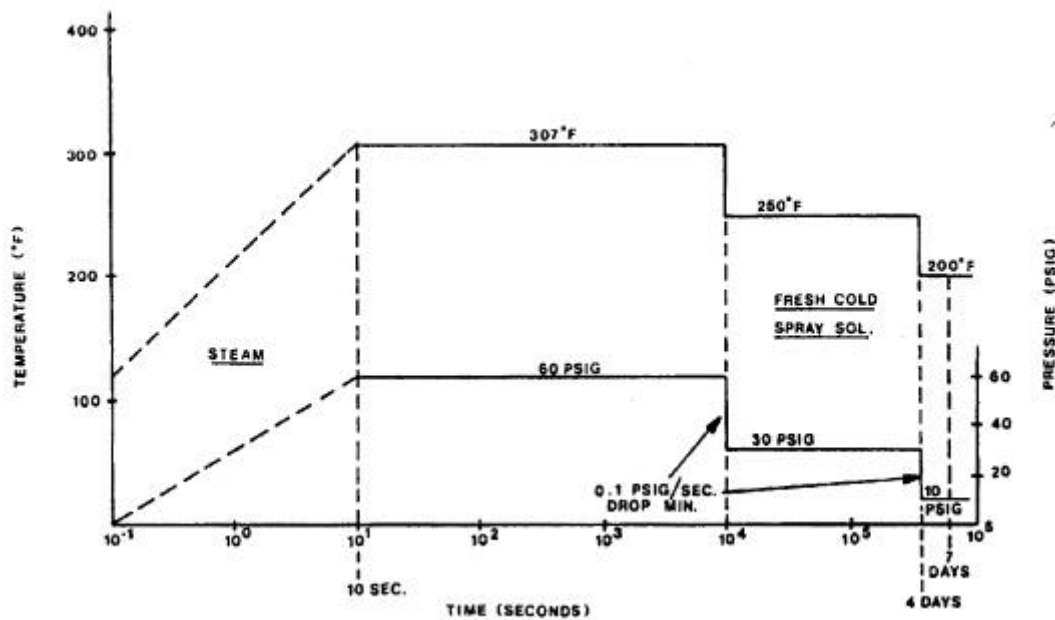


Figure D-4. Typical Pressurized Water Reactor Design Basis Accident (DBA) Testing Parameters (from ASTM D3911-95). (Note: The ASTM figure contains an error: 30 psig should be 15 psig, which is equivalent to 30 psia).

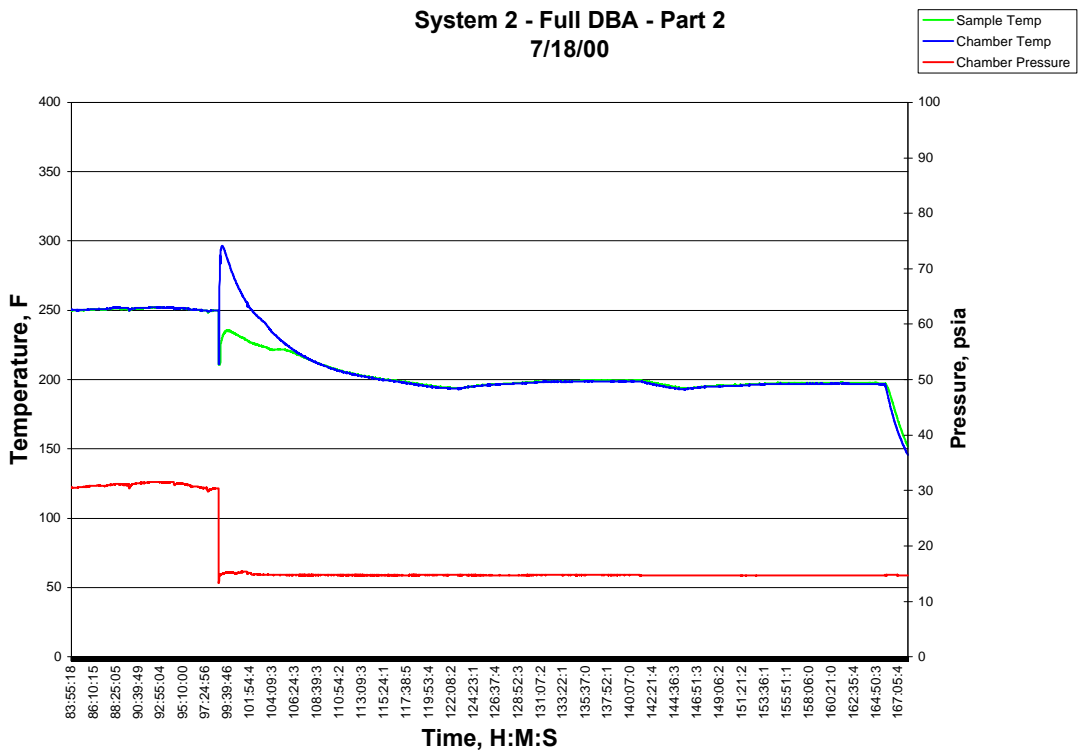
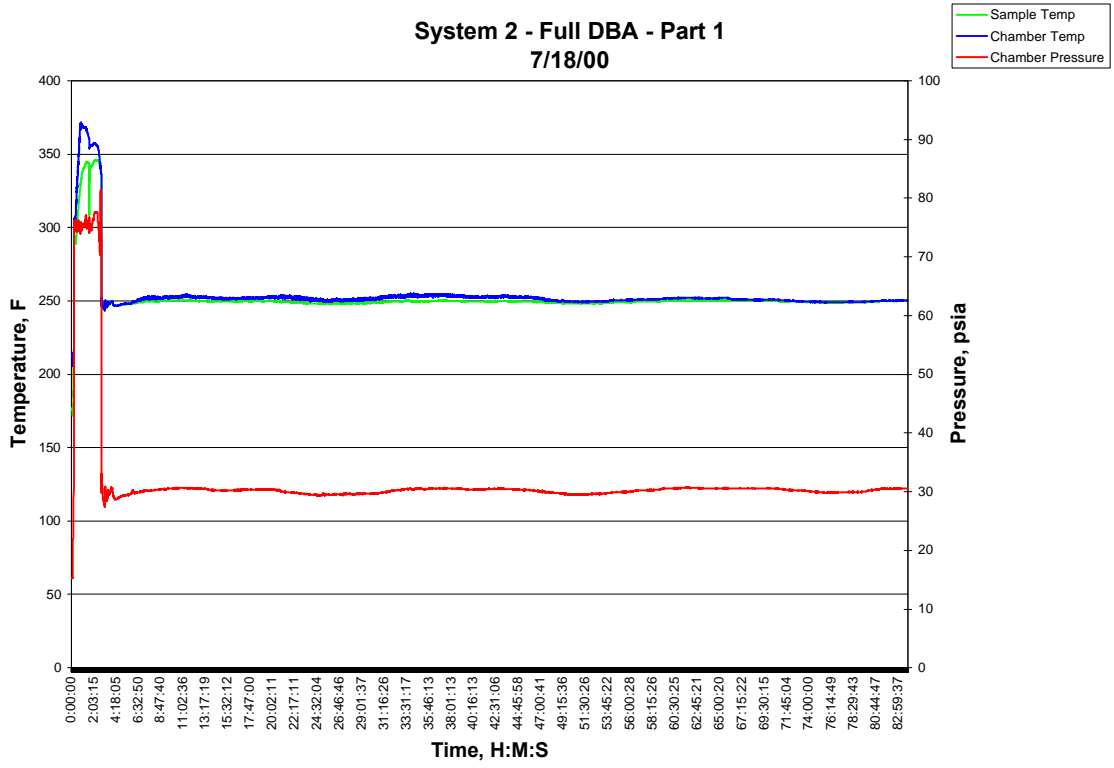


Figure D-5. Typical SRS DBA Test Cycle

The SRTC coating evaluation system is based on a monitored environmental test chamber (known as the METC) which can be supplied with live steam and/or cooling water spray (Figure D-6). The environmental test chamber is an insulated 12-inch diameter by 18-inch long pressure vessel, with flanged closures at each end. It is fabricated of Type 316 stainless steel. The ASTM code-stamped pressure vessel is protected with a 150 psi pressure relief valve. Strap and tape heaters are installed for supplemental control of temperature in the chamber (not shown in the schematic).

A 10-gallon stainless steel autoclave provides steam to the test chamber. A 500-psi rupture disk is installed on the autoclave.

Pressure transducers and thermocouples are installed on the autoclave and the test chamber, and a data acquisition system using Labview[®] software is utilized to document specimen test conditions. A video-borescope is installed in the test chamber and connected to a videotape recorder to document specimen performance during testing. An image from the video borescope is shown in Figure D-7.

The cool-down phase of the ASTM D3911-95 DBA cycle, which simulates activation of the emergency spray cooling headers in the NPP, is facilitated by a spray system installed in the test chamber. The system consists

of a 1000 psi Baldor pump, a heat exchanger to cool the spray solution that is recirculated from the bottom of the chamber, and a storage reservoir. Solution is supplied to the chamber through 0.25-inch diameter tubing. Two metering jet spray nozzles are installed in the chamber, each providing up to 0.030 gpm in a fine mist. Other spray configurations and rates are possible. All materials are Type 316 stainless steel to provide corrosion resistance to various spray solution compositions. To simulate the immersion of some NPP coatings during the early phases of emergency cooling system activation, a shallow reservoir was placed beneath some test specimens to allow the collection of spray coolant, with resultant immersion of a portion of the specimens.

The evaluation of the performance of coatings during immersion was performed in the METC, as stated above, and in an apparatus specifically designed to allow documentation at elevated temperatures, while at atmospheric pressure. This apparatus consisted of a custom-made glass container placed on a thermostatically controlled hot plate (Figure D-8). The container was designed to allow unrestricted observation of the specimens while at elevated temperature. A video camera connected to a time-lapse video recording system was used to document specimen performance (Figure D-9). An image of a specimen during testing is shown in Figure D-10.

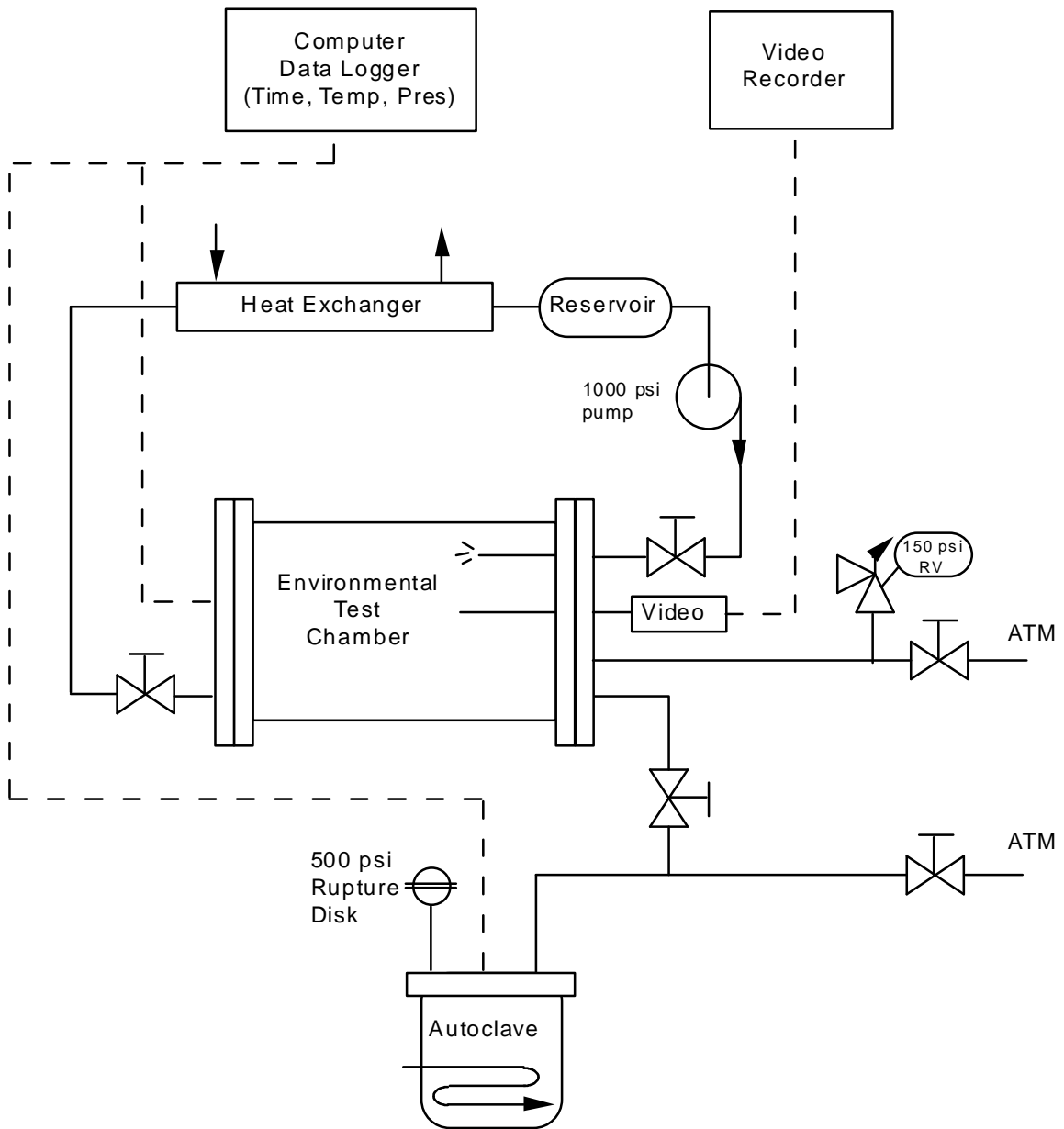


Figure D-6. Process schematic of coatings performance evaluation system

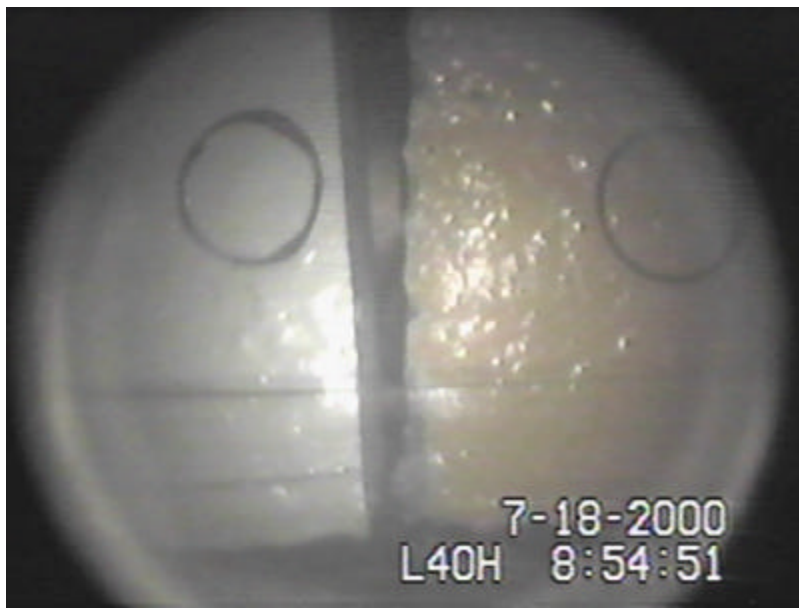


Figure D-7. Video Borescope Image of Non-Aged (left) and Aged (right) System 2 Specimens. The glass reservoir used to facilitate immersion of the bottom portion of the specimens is visible as a line across the specimens.

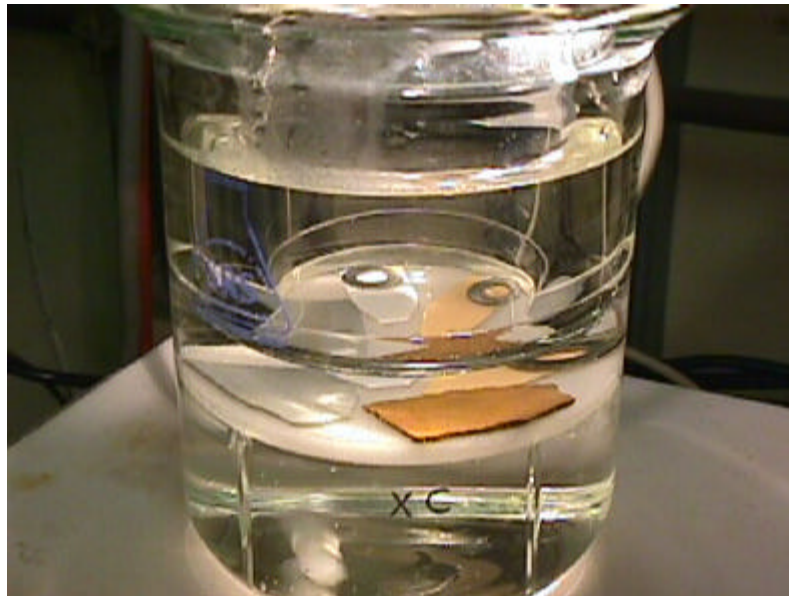


Figure D-8. Overall view of soak test vessel. The vessel is placed on a thermostatically controlled hotplate. Note coating specimens placed on permeable glass frit stage. A magnetic stirring bar is visible on the bottom of the vessel.



Figure D-9. Overall view of soak test system, illustrating video camera (on tripod), fiberoptic lighting system (orange box), time-lapse video recorder, and video monitor



Figure D-10. Video image of specimens at the beginning of testing, as recorded

Appendix E Performance Test Descriptions

DBA Testing

The SRTC coatings performance testing system is used to subject coating specimens to conditions simulating those which would be expected to exist in a NPP during a DBA LOCA. The system, described in Appendix D, has been used to simulate the temperature and pressure profiles found in ASTM D3911-95. A typical exposure test proceeds as follows:

1. Place specimen into specimen holder within environmental test chamber. Affix thermocouple to face of specimen. Confirm borescope view of specimen. Seal test chamber.
2. Prepare videotape recorder and computer data logger for collection of test data.
3. Preheat autoclave steam generator. Preheat test chamber with external strap/tape heaters.
4. Introduce steam into test chamber so that chamber pressure reaches 75 psia within 10 seconds. Maintain chamber pressure at 75 psia for 2.8 hours with supplemental strap/tape heaters. Judicious use of steam to maintain chamber pressure is permitted. Specimen temperature will be approximately 307°F.
5. After 2.8 hours, activate spray cooling system. Monitor chamber pressure and vent as necessary to achieve 30 psia within 5 minutes. Maintain chamber pressure with supplemental strap/tape heaters and by control of recirculation rate of spray coolant. Specimen temperature will be approximately 250°F.
6. After 4 days, stop application of spray coolant and vent chamber to atmospheric pressure. Reset external heaters to maintain sample temperature at approximately 200°F.
7. After 3 days, turn off electrical heaters and allow sample to return to room temperature.
8. Remove specimen and examine for blistering, delamination, peeling, and/or cracking of coating. Per ASTM D3911-95: Blistering is limited to intact blisters, completely surrounded by sound coating bonded to the surface. Delamination and peeling are not permitted. Cracking is not considered a failure unless accompanied by delamination or loss of adhesion.

Soak Testing

The SRTC soak test apparatus is used to subject coating specimens to immersion in water at elevated temperature. Immersion of coatings is expected to occur to some depth in NPP containment following activation of the emergency cooling spray systems. The soak test apparatus is described in Appendix D. A typical soak test would be conducted as follows:

1. Partially fill immersion test canister with distilled water. Tap water may be substituted if desired. Allow enough free space above liquid to allow insertion of top of canister.
2. If free-film specimens are to be tested, place glass frit stage into test canister to support free-film specimens. Use of glass frit stage will permit the use of a magnetic stirrer bar, if desired.
3. Place test canister onto thermostatically controlled hot plate. Set controller to desired temperature. Activate temperature controller, if pre-heating of water is required.
4. Position video camera above test canister ensuring entire test chamber is visible in video monitor.
5. Insert blank video tape into time lapse recorder and set recorder to desired recording period (i.e., 8, 24, or 40 hours). Confirm time and date are set correctly in video recorder.
6. Position fiber-optic light source for optimum illumination of test specimen.
7. Place specimen(s) into test canister. Adjust lighting as necessary.
8. Record coating performance test.

This page left blank intentionally.

Appendix F Characterization Facilities Description

SRTC maintains state-of-the-art testing and analytical capabilities to support the wide range of research and application programs related to nuclear applications. The materials and analytical research group totals over 100 engineers, scientists and technicians. They have a broad range of experience in nuclear materials and applications and form the core of all the materials technology programs

currently underway at SRTC. These range from materials applications involved in nuclear materials production, to reprocessing and waste storage and disposition.

A summary of the materials characterization facilities and available equipment and techniques is provided in Table F-1.



Figure F-1. SRTC Analytical Capabilities: Scanning Electron Microscope (top), Transmission Electron Microscope (middle), and X-ray Diffraction Unit (bottom)



Figure F-2. FT-IR Spectrophotometry Equipment

Appendix G Phenomena Identification and Ranking Table Process

G.1 PIRT Process Overview

The information obtained through the Phenomena Identification and Ranking Table (PIRT) process identifies phenomena derived requirements which are then integrated into experiments and/or analytical modeling to simulate accident scenarios or conditions of safety concern. Because importance ranking is a fundamental element of the PIRT process, judgments when prioritized with respect to their contribution to the accident scenario or safety concern, provide a structured approach to research program planning based on phenomena of highest importance. Since it is neither cost effective, nor required, to assess and examine all the parameters and models for arriving at a best-estimate code (or supporting experiments) in a uniform fashion, this methodology focuses on identifying those processes and phenomena that are expected to dominate the transient behavior, with the recognition that all plausible effects are considered in development of the PIRT. This screening of plausible phenomena, to determine those which dominate the plant response, ensures that a sufficient and efficient analysis of the problem has been performed. Since PIRTs are not computer code-specific, PIRTs are applicable to the accident scenario and plant design regardless of which code may be chosen to perform the subsequent safety analysis.

A typical application of the PIRT process is conceptually illustrated in Figure G-1 and is initiated by a definition of the problem and PIRT objectives. The PIRT process focuses on phenomena/processes that are important to the particular scenario, or class of transients in the specified nuclear power plant (NPP), i.e., those that drive events. Plausible physical phenomena and processes, and their associated system components are identified. From a modeling perspective, phenomena/processes important to a plant response to an accident scenario can be grouped in two separate-categories: 1) higher level system interactions (integral) between components/subsystems, and 2) those local to (within) a component/subsystem. Although the identification of plausible phenomena is focused toward component organization, experience gained has indicated it can be most helpful to relate the phenomena to higher level integral system processes. Time can often be saved when it can be demonstrated that a higher level integral system process is of low importance during a specific time phase. A subsequent and equally important step is the partitioning of the plant into components/subsystems. This latter step is a significant aid in organizing and ranking phenomena/processes. The phenomena/processes are then ranked with respect to their influence on the primary evaluation criteria, to establish PIRTs. Primary evaluation criteria (or criterion) are normally based on regulatory safety requirements such as those related to restrictions in fuel rods (peak clad temperature, hydrogen generation, etc.)

and/or containment operation (peak pressure, emergency core cooling system performance, etc.). The rank of a phenomenon or process is a measure of its relative influence on the primary criteria. The identification and ranking are justified and documented.

The relative importance of environmental conditions and phenomena present is time dependent as an accident progresses. Thus, it is convenient to partition accident scenarios into time phases in which the dominant phenomena/processes remain essentially constant, each time phase being separately investigated. The processes and phenomena associated with each component are examined, as are the inter-relations between the components. Cause and effect are differentiated. The processes and phenomena and their respective importance (rank) are judged by examination of experimental data, code simulations related to the plant and scenario, and the collective expertise and experience of the evaluation team. Independent techniques to accomplish the ranking include expert opinion, subjective decision making methods (such as the Analytical Hierarchy Process), and selected calculations. The final product of the application of the PIRT process is a set of tables (PIRTs) documenting the ranks (relative importance) of phenomena and processes, by transient phase and by system component. Supplemental products include descriptions of the ranking scales, phenomena and processes definitions, evaluation criteria, and the technical rationales for each rank. In the context of the PIRT process application to PWR containment coatings failures, the primary elements of interest are described in Section 2. The PIRTs resulting from this specific application are documented in Section G.7.

G.2 PIRT Objectives

The industry coatings PIRT panel is comprised of the following industry identified specialists:

Jon Cavallo, Chm.
Corrosion Control, Consultants and Labs, Inc.

Tim Andreycheck
Westinghouse Electric Corp, Pittsburgh, PA

Jan Bostelman
ITS Corporation

Dr. Brent Boyack
Los Alamos National Laboratory

Garth Dolderer
Florida Power and Light

David Long
Keeler and Long (now retired)

The PIRT objectives identified by the panelists were:

- a. To identify coatings systems applied to steel and concrete substrates in PWR containments to be considered for the PIRT process,
- b. To identify phenomena and processes applicable to coatings applied inside PWR containments, and,
- c. To rank those phenomena and processes with respect to their importance to coating failures.

G.3 Generic PWR Containment Coating Systems

The generic identification of protective coating materials applied to NPPs was derived from EPRI Report TR-106160, "Coatings Handbook for Nuclear Power Plants," plant responses to GL 98-04, June 1996, nuclear industry surveys and inputs from PWR Owners groups. EPRI TR-106160 lists data collected from 29 NPP respondents and represents over 200 commercial coating products applied to over 1000 different plant-specific areas or equipment. The industry coatings PIRT panel reviewed all available information, and based on their collective coatings knowledge identified following eight generic coatings systems for consideration in SRTC's coating research program.

- a. Steel substrate, inorganic zinc primer, epoxy phenolic topcoat,
- b. Steel substrate, epoxy phenolic primer, epoxy phenolic topcoat,
- c. Steel substrate, inorganic zinc primer, epoxy topcoat,
- d. Steel substrate, epoxy primer, epoxy topcoat, (SRTC System 5)
- e. Concrete substrate, surfacer, epoxy phenolic topcoat,
- f. Concrete substrate, surfacer, epoxy topcoat,
- g. Concrete substrate, epoxy phenolic primer, epoxy phenolic topcoat,
- h. Concrete substrate, epoxy primer, epoxy topcoat.

The PIRT for coating system (f) is reported in the Industry Coatings PIRT Report No. IC99-02, June 16, 2000, which is available through the NRC Public Document Room. PIRTs coating systems (a), (d), (f), (h) and non-topcoated inorganic zinc on steel have been submitted to the NRC. These systems were judged to be representative of coatings that were applied in the early to middle 1970s.

A cross-referencing of coating systems identified by the PIRT panel and coatings products selected by SRTC to represent those generic systems is provided in Section 2 of this report.

G.4 Coating System Components

To enable development of the individual PIRTs, the industry coatings PIRT panel partitioned each coating system into components as follows:

Steel Substrate

- a. Substrate
- b. Substrate/Primer Interface.
- c. Primer
- d. Primer/Topcoat Interface
- e. Topcoat

Concrete Substrate

- a. Substrate
- b. Substrate/Surfacer Interface
- c. Surfacer
- d. Surfacer/Topcoat Interface
- e. Topcoat

Figure G-2 illustrates the layering of coating materials on a steel substrate and postulated coating defects that was used in the PIRT process.

G.5 Accident Scenario

The industry coatings PIRT panel discussed a number of accident scenarios postulated for occurrence in PWR plants and their potential effects on containment systems, structures, and components (SSCs), coating systems, and the generation of coating debris which could transport to PWR containment sump(s). The following coating failure scenario was selected by the panel for use in its subsequent deliberations:

- a. Normal plant operation for 40 years (potentially longer due to plant life extension),
- b. Mechanical damage (see Figure G-1 for illustration of incipient and developed defects in coatings on concrete and steel substrates),
- c. Chemical damage (from plant process fluid leakage and over-spray/leakage of decontamination chemicals),

- d. Normal plant operation for 40 years (potentially longer due to plant life extension) followed by intermediate / large LOCA without jet impingement (note: small break LOCA was not considered because containment spray is not initiated and thus significant coating debris transport to the sump(s) is not probable).

Scenarios a, b, c, and d above may occur independently or synergistically to cause coating failure.

Jet impingement due to a LOCA was omitted from the panel's deliberations, since industry test experience indicates that none of the coating systems applied to PWR SSCs will survive direct steam impingement.

G.6 Scenario Phases

The coating failure accident scenario divided into the following phases (or time intervals).

PHASE 1: Normal Operation Followed by LOCA, No Jet Impingement

- (-) Time Coating System Installation
 - Surface Preparation
 - Coating Application
 - Curing
 - Integrated Leak Rate Testing (ILRT)

T=0 Start of Power Operations

T = 40 years Medium or Large Break LOCA
Occurs

(T could be 60 years in the case of plant life extension)

PHASE 2: 0 to 40 Seconds After Start of LOCA

PHASE 3: 40 Seconds to 30 Minutes After Start
of LOCA

PHASE 4: 30 Minutes to 2 Hours After Start of
LOCA

PHASE 5: Greater Than 2 Hours After Start of
LOCA

G.7 Primary Evaluation Criterion

The primary evaluation criterion, or parameter of interest, considered by the industry coatings PIRT panel concerning coatings on PWR containment SSCs is:

“Will the coating system detach from the surface to which it is applied?” or

“Will the paint fall off?”

The panel's focus was on the second question.

G.8 Phenomenon Ranking Scale

PIRTs utilizing complex hierarchical, multi-leveled scenarios (see Figure G-1) and the Analytical Hierarchy Process ranking methodology applied to NPPs have been time consuming and labor intensive. The PIRT panel instead selected a simplified ranking scale that drew on the knowledge of panelists who had extensive experience in NPP coating application as well as NPP accident analysis requirements and the PIRT process.

Basis for Ranking Selection:

High – Phenomena has a dominant impact on the primary parameter of interest (i.e. coating failure). Phenomena will be explicitly considered in the implementation of the Savannah River Technical Center (SRTC) Research Program

Medium – Phenomena has a moderate influence on the primary parameter of interest.

Phenomena will also be considered in the implementation of the SRTC Research Program

Low – Phenomena has a small effect on the primary parameter of interest. Phenomena will be considered in the SRTC research program to the extent possible.

The PIRT ranking for System 5 is summarized in Table G-1, which shows the variation of process or phenomena ranking as a function of time. Blistering and de-lamination were judged to be a HIGH concern throughout the accident scenario for the substrate/primer and primer/topcoat interface.

Tables G-2 through G-6 detail the process & phenomena rankings for the materials and material interfaces, rankings arrived at, and the definitions applied to those processes or phenomena to arrive at those rankings.

The integration of these PIRT panel findings with project activities is discussed in Section 2 of this report.

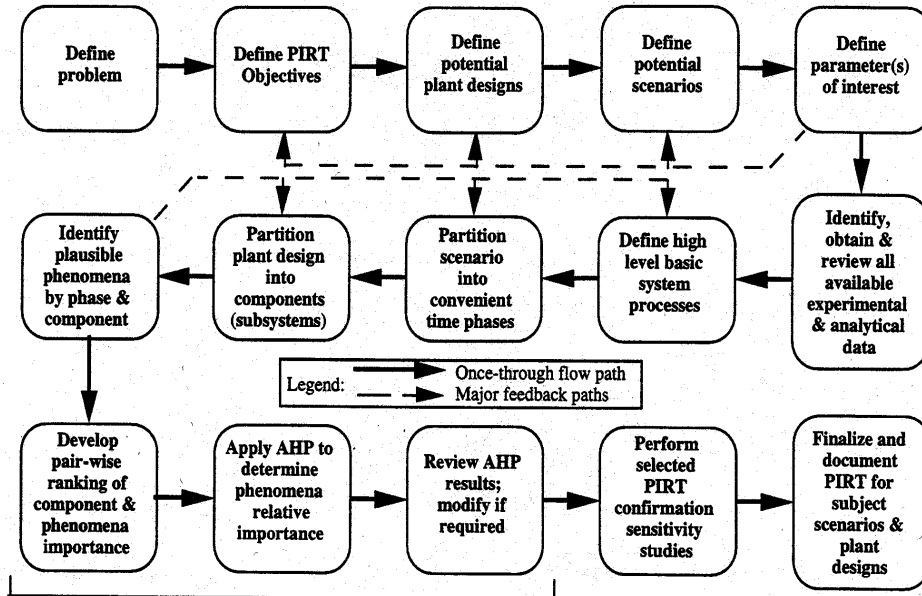


Figure G-1. PIRT Process

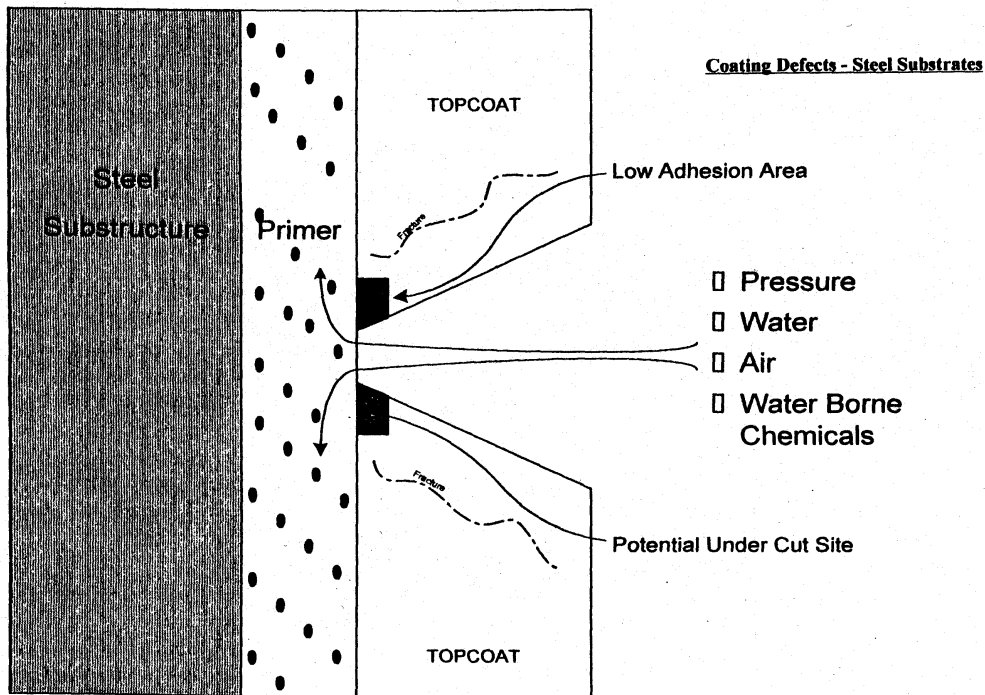


Figure G-2. Coating Defects and Phenomena of Importance

**Table G-1. PIRT Ranking Summary
Concrete Substrate - Surfacer -Phenolic Epoxy Topcoat
PIRT Coating System f, analog for SRTC System 2**

Phases - >		1	2	3	4	5
Process & Phenomena						
Substrate (Concrete)	Outgassing/Vapor Expansion	H	H	H	M	M
	Pressure Gradients from ILRTs	M	H	H		
Substrate /Surfacer Interface	Calcium Carbonate Build-up	M				M
	Blistering & De-lamination	H	H	H	H	
	Vapor Build-up	H	H	H	M	
Surfacer	Environmental Exposure	M				M
	Mechanical Damage					
	Minor coating anomalies	H	H	H	M	M
	Air/water & chemical intrusion					
	Above pool				M	
	Below pool				M	
Air/Water & Chemical Diffusion						
Surfacer/Topcoat Interface	Blistering & De-lamination	H	H	H	H	
	Vapor Build-up	H	H	H	M	M
Topcoat	Expansion and contraction					
	Environmental exposure	H				M
	Mechanical damage					
	Minor coating anomalies	H	H	H	M	M
	Air/water & chemical intrusion					
	Above pool					M
Chemical attack						

Processes/Phenomena ranked HIGH and MEDIUM

Blistering & De-lamination
Calcium Carbonate Build-up
Vapor Build-up
Environmental exposure
Minor coating anomalies
Air/water/chemical intrusion

Phase 1: Normal service from time of application and through 40 years operation.

Phase 2: 0 to 40 seconds into loss-of-coolant accident (LOCA).

Phase 3: 40 seconds to 30 minutes after a LOCA.

Phase 4: 30 minutes to 2 hours after a LOCA.

Phase 5: Beyond 2 hours after a LOCA.

Industry Coating Part Table G-1. Normal Operation

COATING DESCRIPTION: Concrete Substrate, Surfacer, Epoxy Topcoat						
Phase 1 Normal Operation	Component	Processes & Phenomena	Rank	Definition		
	Substrate (Concrete)		Outgassing / vapor expansion	High	Phase 1 vapor migration through concrete damage from ILRT Experience from Phase 1 ILRT shows coatings have come off from rapid depressurizations	
			Pressure gradients from ILRT's	Medium		
			Temperature gradients	Low		Temperature changes due to normal operations
			Compression / expansion	Low		Pressure changes due to normal operation
Increased radiation exposure	Low	Radiation damage due to normal operations				
Substrate/surfacer Interface		Calcium carbonate buildup	Medium	Potential pure vapor long term Differential growth due to changes in pressure, temperature		
		Differential expansion and contraction	Low			
		Blistering/delamination	High		Pressure and thermal loading	
		Vapor buildup	High		Vapor collection under surface	
Surfacer		Bulk movement	Low	Expansion of concrete due to temperature changes Exposure to heat over time Variations in coating due to application Not observed from experience; not considered likely Top coat protects the surfacer Not by bulk diffusion; can occur through pathways through top coat Damage from wear normal wear and tear Water migration through topcoat at mechanical damage and minor coating anomaly sites Small gradients during normal operation Through pathways through top coat Radiation damage associated with normal operations		
		Environmental exposure	Medium			
		Small coating anomalies	High			
		Cracking	Low			
		Chemical exposure	Low			
		Water diffusion (from concrete)	Low			
		Mechanical damage	Low			
		Water intrusion from pool	Na			
		Temperature gradient	Low			
		Water/air diffusion (from outside the topcoat above submerged level)	Low			
Increased radiation exposure	Low					

Industry Coating Pirt Table G-1. Normal Operation (cont'd)

	Surfacer/Topcoat Interface	Differential expansion and contraction Blistering/delamination Vapor buildup	Low High High	No difference in relative thermal expansion coefficients of the topcoat and surfacer Pressure and thermal loading Vapor collection under the top coat
	Topcoat (Epoxy)	Bulk movement Temperature gradient Increased radiation exposure Diffusion air/water Coating anomalies Environmental exposure Chemical attack Cracking Mechanical damage Condensation / cold wall Immersion in pool Washdown	Low Low Low Low High High Low Low Low Low NA NA	No movement; thermal expansion of concrete is small Does not have an effect on top coat Low; based on test data Small vapor transmissivity rate Pathways for air and water buildup Lots of exposure to heat over time Formulated to withstand chemicals Based on walkdowns of containments/drywells, etc. Does not affect bulk coating integrity; low priority Coating formulated to resist cold wall effects Soaking of coatings in coolant; not in this phase Water flow due to containment spray and condensation

Industry Coating Part Table G-2. 0-40 Seconds After Initiation of Loca

COATING DESCRIPTION: Concrete Substrate, Surfacer, Epoxy Topcoat				
Phase 2 0-40 Seconds (outside Zone of Influence)	Component	Processes & Phenomena	Rank	Definition
	Substrate (Concrete)	Outgassing / vapor expansion Pressure gradients Temperature gradients Compression / expansion Increased radiation exposure	High	Phase 2 vapor migration through concrete damage
			High	Loading due to rapid pressure changes
			Low	Would not degrade concrete
			Low	No evidence of significant impact
Low			Radiation damage due to increased radioactivity from event	
Substrate/surfacer Interface	Calcium carbonate buildup Differential expansion/contraction Blistering/delamination Vapor buildup	Low	Potential pure vapor long term	
		Low	Surfacer designed to withstand expansion/contraction	
		High	Pressure and thermal loading	
		High	Vapor collection between substrate and surfacer	
Surfacer	Bulk movement Environmental exposure Minor coating anomalies Cracking Chemical exposure Water diffusion (from concrete) Mechanical damage Water intrusion from pool Temperature gradient Water/air diffusion (from outside the topcoat above submerged level) Increased radiation exposure	Low	Movement of surfacer due to thermal expansion	
		Low	Exposure to heat over time	
		High	Perturbations in coating due to application process	
		Low	Not observed from experience; not considered likely	
		Low	Interaction of surfacer with chemicals in environment	
		Low	Bulk diffusion through pathways through top coat	
		Low	Damage due to impact loading	
		NA	Water migration through topcoat at mechanical damage and minor coating anomaly sites	
Low	Transient heat up of surfacer			
Low	Air and water migration through pathways through top coat			
Low	Radiation damage due to increased radioactivity from event			
Surfacer/topcoat Interface	Differential expansion/contraction Blistering/delamination Vapor buildup	Low	Difference in relative thermal expansion of the topcoat and surfacer	
		High	Pressure and thermal loading.	
		High	Vapor collection under the top coat	

Industry Coating Pirt Table G-2. 0-40 Seconds After Initiation of Loca (cont'd)

	Topcoat (Epoxy)	Bulk movement	Low	No movement; thermal expansion of concrete is small
		Temperature gradient	Low	Does not have an effect on top coat
		Increased radiation exposure	Low	Radiation damage due to increased radioactivity from event
		Diffusion air/water	Low	Small vapor transmissivity rate
		Coating anomalies	High	Pathways for air and water buildup
		Environmental exposure	Low	Lots of exposure to heat over time
		Chemical attack	Low	Formulated to withstand chemicals
		Cracking	Low	Based on walkdowns of containments/drywells, etc.
		Mechanical damage	Low	Does not affect bulk coating integrity; low priority
		Condensation / cold wall	Low	Coating formulated to resist cold wall effects
		Immersion in pool	NA	NA for this phase of event
		Washdown	Low	Water flow due to containment spray and condensation

Industry Coating Part Table G-3. 40 Seconds – 30 Minutes After Initiation of Loca

COATING DESCRIPTION: Concrete Substrate, Surfacer, Epoxy Topcoat				
Phase 3 40 Sec - 30 Min (outside Zone of Influence)	Component	Processes & Phenomena	Rank	Definition
	Substrate (concrete)	Outgassing / vapor expansion Pressure gradients Temperature gradients Compression / expansion Increased radiation exposure	High	Vapor migration through concrete damage
			High	Experience from Phase 1 ILRT shows coatings have come off from rapid depressurizations
			Low	Would not degrade concrete
			Low	No evidence of significant impact
	Substrate/Surfacer Interface	Calcium carbonate buildup Differential expansion/contraction Blistering/delamination Vapor buildup	Low	Potential pure vapor long term
			Low	Surfacer designed to withstand expansion/contraction
			High	Pressure and thermal loading changes
High			Vapor collection under surface	
Surfacer	Bulk movement Environmental exposure Coating anomalies Cracking Chemical exposure Water diffusion (from concrete) Mechanical damage Water intrusion from pool Temperature gradient Water/air diffusion (from outside the topcoat above submerged level) Increased radiation exposure	Low	Thermal expansion of concrete	
		Low	Lot of exposure over time to heat	
		High	Pathway for vapor transmission	
		Low	Not observed from experience; not considered likely	
		Low	Top coat protects the surfacer	
		Low	Migration of water through pathways in top coat	
		Low	Does not affect bulk coating integrity; low priority	
NA	Water migration through topcoat at mechanical damage and minor coating anomaly sites			
Low	Low, does not affect the surfacer			
Low	Low, only through pathways through top coat			
Surfacer/Topcoat interface	Differential expansion/contraction Blistering/delamination Vapor buildup	Low	No difference in relative thermal expansion coefficients of the topcoat and surfacer	
		High	Pressure and thermal loading.	
		High	Vapor collection under the top coat	

Industry Coating Pirt Table G-3. 40 Seconds – 30 Minutes After Initiation of Loca (cont'd)

	Topcoat (epoxy)	Bulk movement Temperature gradient Increased radiation exposure Diffusion air/water Coating anomalies Environmental exposure Chemical attack Cracking Mechanical damage Condensation / cold wall Immersion in pool Washdown	Low Low Low Low High Low Low Low Low Low Low NA Low	No movement; thermal expansion of concrete is small Does not have an effect on top coat Radiation damage due to increased radioactivity from event Small vapor transmissivity rate Pathways for air and water buildup Lots of exposure to heat over time Formulated to withstand chemicals Based on walkdowns of containments/drywells, etc. Does not affect bulk coating integrity; low priority Coating formulated to resist cold wall effects NA for this phase of event Water flow due to containment spray and condensation
--	--------------------	--	---	---

Industry Coating Part Table G-4. 30 Minutes – 2 Hours After Initiation of Loca

COATING DESCRIPTION: Concrete Substrate, Surfacer, Epoxy Topcoat				
Phase 4 30 min - 2 hrs (outside Zone of Influence)	Component	Processes & Phenomena	Rank	Definition
	Substrate (Concrete)	Outgassing / vapor expansion Pressure gradients Temperature gradients Compression / expansion Increased radiation exposure	Medium	Vapor migration through concrete
			Low	Delamination due to rapid pressure changes
			Low	Response to changes in containment environment temperature
			Low	No evidence of significant impact
Substrate/Surfacer Interface	Calcium carbonate buildup Differential expansion and contraction Blistering/delamination Vapor buildup	Low	Potential pure vapor long term	
		Low	Surfacer designed to withstand expansion/contraction	
		High	Pressure and thermal loading	
		Medium	Vapor collection under surface	
Surfacer	Bulk movement Environmental exposure Coating anomalies Cracking Chemical exposure Water diffusion (from concrete) Mechanical damage Water intrusion from pool Temperature gradient Water/air diffusion (from outside the topcoat above submerged level) Increased radiation exposure	Low	Movement of surfacer due to temperature changes	
		Low	Exposure over time to heat	
		Medium	Variation in finish due to application process	
		Low	Not observed from experience; not considered likely	
		Low	Top coat protects the surfacer	
		Low	Migration can occur through pathways through top coat	
		Low	Degradation of coating due to normal wear and tear	
Surfacer/Topcoat Interface	Differential expansion/contraction Blistering/delamination Vapor buildup	Low	Water migration through topcoat at mechanical damage and minor coating anomaly sites	
		Low	Low, does not affect the surfacer	
		Low	Low, only through pathways through top coat	
Surfacer/Topcoat Interface	Differential expansion/contraction Blistering/delamination Vapor buildup	Low	Radiation damage due to increased radioactivity from event	
		High Medium	No difference in relative thermal expansion coefficients of the topcoat and surfacer Vapor collection under the top coat	

Industry Coating Part Table G-4. 30 Minutes – 2 Hours After Initiation of Loca (cont'd)

		Bulk movement	Low	No movement; thermal expansion of concrete is small
		Temperature gradient	Low	Does not have an effect on top coat
		Increased radiation exposure	Low	Radiation damage due to increased radioactivity from event
		Diffusion air/water	Low	Small vapor transmissivity rate
		Coating anomalies	Medium	Pathways for air and water buildup
	Topcoat (epoxy)	Environmental exposure	Low	Lots of exposure to heat over time
		Chemical attack	Low	Formulated to withstand chemicals
		Cracking	Low	Break in coating surface due to tension in coating
		Mechanical damage	Low	Local coating failure due to impact loading
		Condensation / cold wall	Low	Liquid infusion into coating due to cold walls
		Immersion in pool	Low	Submergence of coatings in coolant in lower containment
		Washdown	Low	Water flow due to containment spray and condensation

Industry Coating Pirt Table G-5. >2 Hours After Initiation of Loca

COATING DESCRIPTION: Concrete Substrate, Surfacer, Epoxy Topcoat					
Phase 5 2 hrs - end (outside Zone of Influence)	Component	Processes & Phenomena	Rank	Definition	
	Substrate (concrete)		Outgassing / vapor expansion	Medium	Vapor migration through concrete damage from ILRT
			Pressure gradients from ILRT's	Low	Experience from Phase 1 ILRT shows coatings have come off from rapid depressurizations
			Temperature gradients	Low	Thermal response to containment transient
			Compression / expansion	Low	No evidence of significant impact
			Increased radiation exposure	Low	Radiation damage due to increased radioactivity from event
	Substrate/Surfacer Interface		Calcium carbonate buildup	Medium	Potential pure vapor long term
			Differential expansion/contraction	Low	Surfacer designed to withstand expansion/contraction
Blistering/delamination			High	Pressure and thermal loading	
Vapor buildup			Medium	Vapor collection under surface	
Surfacer		Bulk movement	Low	Thermal expansion of concrete	
		Environmental exposure	Medium	Lot of exposure over time to heat	
		Coating anomalies	Medium	Pathway for vapor transmission	
		Cracking	Low	Not observed from experience; not considered likely	
		Chemical exposure	Low	Top coat protects the surfacer	
		Water diffusion (from concrete)	Low	Not by bulk diffusion; can occur through pathways through top coat	
		Mechanical damage	Low	Does not affect bulk coating integrity; low priority	
		Water intrusion from pool	Medium	Water migration through topcoat at mechanical damage and minor coating anomaly sites	
Temperature gradient		Water/air diffusion (from outside the topcoat above submerged level)	Low	Low, does not affect the surfacer	
		Increased radiation exposure	Low	Low, only through pathways through top coat	
		Increased radiation exposure	Low	Low; based on test data	
Surfacer/Topcoat Interface		Differential expansion/contraction	Low	No difference in relative thermal expansion coefficients of the topcoat and surfacer	
		Blistering/delamination	High	Pressure and thermal loading	
		Vapor buildup	Medium	Vapor collection under the top coat	

Industry Coating Part Table G-5. >2 Hours After Initiation of Loca (cont'd)

	Topcoat (epoxy)	Bulk movement	Low	No movement; thermal expansion of concrete is small
		Temperature gradient	Low	Does not have an effect on top coat
		Increased radiation exposure	Low	Radiation damage due to increased radioactivity from event
		Diffusion air/water	Low	Small vapor transmissivity rate
		Coating anomalies	Medium	Pathways for air and water buildup
		Environmental exposure	Medium	Lots of exposure to heat over time
		Chemical attack	Low	Formulated to withstand chemicals
		Cracking	Low	Based on walkdowns of containments/drywells, etc.
		Mechanical damage	Low	Does not affect bulk coating integrity; low priority
		Condensation / cold wall	Low	Coating formulated to resist cold wall effects
		Immersion in pool	Medium	Increased importance due to time in this phase of event
		Washdown	Low	Water flow due to containment spray and condensation